Characterization of Chromosome 7q 21-32 Amplification in Hepatocellular Carcinoma

LEUNG, Kin Chung

A Thesis Submitted in Partial Fulfillment
of the Requirements for the Degree of
Doctor of Philosophy
in
Anatomical and Cellular Pathology

The Chinese University of Hong Kong
September 2011

ProQuest LLC.
789 East Eisenhower Parkway
P.O. Box 1346
Ann Arbor, MI 48106 - 1346

Abstract of thesis entitled:

Characterization of Chromosome 7q21-32 Amplification in Hepatocellular Carcinoma.

Submitted by: LEUNG Kin Chung

for the degree of Doctor of Philosophy in Anatomical and Cellular Pathology

at the Chinese University of Hong Kong

Abstract

Hepatocellular carcinoma (HCC) is a highly malignant tumor that is associated with high morbidity and mortality. Liver carcinogenesis, often arising from chronic liver cirrhosis, is a process characterized by step-wise accumulation of genetic aberrations that confer cell growth advantages, malignant transformation, vascular invasion and metastatic potentials. Genome-wide analyses have illustrated some commonly altered genomic events in association with HCC metastasis. Specifically, common genomic gain on 7q arm is largely suggestive of progression to advanced stage HCC progression. Despite the fact that chromosomal 7q gain is of pivotal significance, little has been known about its underlying candidate genes in the process of hepatic tumorigenesis.

Our earlier gene mapping analysis on 7q21-22 region identified a few candidate proto-oncogenes, including *PFTAIRE* protein kinase 1 (*PFTK1*) that possesses a Cdc2-related serine/threonine kinase signature. Although *PFTK1* protein has been shown to confer HCC cell migratory phenotypes, the prognostic value and mechanistic insight by which *PFTK1* enhances HCC motile properties remain largely elusive. In this thesis, tissue microarray analysis showed that increased *PFTK1* expression in human HCC is significantly associated with early age onset (≤40 years),

differentiation to advanced tumor staging and histologic presence of microvascular invasion. Coupling 2D-PAGE mass spectrometry with immunoprecipitation validation, β-actin (ACTB) and transgelin2 (TAGLN2) were confirmed as downstream substrates of *PFTK1* kinase. Nevertheless, the detection of serine-phosphorylated form of TAGLN2 would seem a downstream target of *PFTK1* kinase. Since the tumor suppressor role of TAGLN2 has been widely ascribed in the control of cancer metastasis, I attempted to define if TAGLN2 is an immediate phosphorylated target of *PFTK1* kinase. Knockdown experiments of *TAGLN2* in *PFTK1*-abrogated cells showed a recovery on cellular motile and invasive properties, as well as actin stress fiber formation, proposing a potential mechanism that halts the actin cytoskeleton dynamics. Residues S83 and S163 on TAGLN2 were identified as target sites for *PFTK1* protein in the control of the actin-binding property of TAGLN2 and thus HCC cell motility. The findings from this thesis highlighted a novel oncogene-tumor suppressor interplay where oncogenic *PFTK1* confers HCC cell motile phenotypes through phosphorylations on tumor suppressor TAGLN2. The phosphorylation of TAGLN2 would in turn promote cell migratory properties through the reduced actin-binding property of TAGLN2.

Given that *TAGLN2* suppression in *PFTK1*-knockdown cells could not completely revert the effects of *PFTK1*, this might suggest that other interacting partners are involved in the *PFTK1*-modulated biological path. Previous studies on Cdc2-related kinase substrates showed caldesmon (CaD), an actin-stabilizing protein, in the actin cytoskeletal modeling and cell migratory enhancement. In line with previous reports, I found CaD is a plausible phosphorylation target of *PFTK1* kinase in *PFTK1*-knockdown cells, there was loss of CaD phosphorylations and corresponding displacement from the F-actin fibers. Without the binding of CaD to

actin, actin stress fibers were evidently dispersed in *PFTK1*-abrogated cells, implicating reduced migratory capabilities. In addition to TAGLN2, CaD was underscored as another intermediate participant in the *PFTK1* biological cascade, suggesting the dynamics of actin organization by the kinase activity of *PFTK1*.

Recently, the concept of microRNA (miRNA) deregulations has been widely adopted as an essential regulatory event in cancer development, where their influence on multiple tumor suppressors and oncogenes has been well illustrated. Our group previously reported on the up-regulation of a miRNA cluster (miR-183/96/182) in HCC. This cluster located on 7q32 showed common overexpression in primary HCC tumors. In the present study, concomitant up-regulation of miR-183, -96 and -182 in primary HCC was shown to be significantly associated with poor prognosis of patients and clinical features of metastatic tumors including presence of microvascular invasion and advanced tumor differentiation. I also provided evidence that β-catenin transactivity could activate miR-183/96/182 overexpression, which could confer a migratory advantage in malignant hepatocytes through convergent targeting on Forkhead BoxO1.

In summary, this thesis highlighted the metastatic implications of 7q21-32 amplification in the progression of HCC. Overexpression of the target gene(s) or miRNA(s), including *PFTK1* and miR-183/96/182, was concordantly shown to confer HCC migratory phenotypes. Thus, detailed understanding of driver genes on the 7q21-32 region might provide key molecular informations underlying HCC metastasis, and hence aid development of more favourable therapeutic regimens for patients diagnosed with HCC.

摘要

肝細胞癌（HCC）是一種常見的高死亡率的惡性腫瘤。肝臟癌變通常源於慢性肝硬化，在這一逐步累積發展的過程中，包括了一系列可導致細胞生長紊亂、惡性轉化、血管侵襲乃至引起腫瘤轉移的基因異常改變。全基因分析揭示了一些與 HCC 轉移能力相關的常見基因異常事件。特別是在染色體 7q 上的拷貝數目增加提示著癌癥的晚期進展。事實上，7q21-31 區域上拷貝數目的增加與 HCC 晚期進展有關。儘管染色體 7q 上的拷貝數目增加有重要意義，但對於在此肝臟癌變過程中的相關基因我仍然知之甚少。

在早前對於 7q21-22 區域的基因圖譜分析中，我確定了一些候選的原癌基因，包括 PFTAIRE 蛋白激酶 1（PFTK1），其特點是有一個 Cdc2-相關的絲氨酸/蘇氨酸激酶。雖然 PFTK1 蛋白與 HCC 細胞的遷移能力表型有關，但是 PFTK1 對患者預後的影響以及其促進 HCC 遷移能力的機制仍然不清楚。在本文中，根組織微陣列實驗結果表明，人類 HCC 組織中 PFTK1 表達的增加與早期發病（≤40 歲），晚期腫瘤分期以及在組織學研究中發現的微血管侵襲等呈顯著相關性。通過使用 2D-PAGE 質譜分析法以及免疫沉澱技術，β-actin (ACTB) 和 transgelin2 (TAGLN2) 被證實是 PFTK1 激酶的下游作用底物，並且絲氨酸磷酸化形式的 TAGLN2 似乎更可能是 PFTK1 的下游作用目標。由於 TAGLN2 在抑制癌癥轉移中的作用已被廣泛描述，因此我嘗試去確定 TAGLN2 是否一個可被 PFTK1 直接磷酸化的目標底物。在去除 PFTK1 的細胞中，抑制 TAGLN2 的實驗結果顯示出細胞遷移能力以及侵襲能力的恢復，同時可見肌動蛋白應力纖維的形成，提示其可能具有抑止肌動蛋白細胞骨架運動的作用。我亦確定了 TAGLN2 上的 S83 和 S163 殘基是 PFTK1 的目標作用位點，PFTK1 通過作用于此目標位點，

可以控制 TAGLN2 與肌動蛋白的結合程度以及影響 HCC 細胞的遷移能力。因此，我的研究結果揭示了一個新的癌基因-抑癌基因間的相互作用：PFTK1 通過磷酸化抑癌基因 TAGLN2，從而改變 HCC 細胞的遷移能力。而 TAGLN2 的磷酸化反過來會通過減弱 TAGLN2 與細胞骨架的結合能力，從而促進細胞的遷移能力。

在去除 PFTK1 的細胞中，TAGLN2 的抑制并不能完全改變 PFTK1 的功能影響，這就提示了在 PFTK1 調節的通路中，可能存在其他有相互作用的蛋白。早前關於 Cdc2-相關激酶底物研究表明，鈣調素结合蛋白（CaD）是一種肌動蛋白固定蛋白，被證實參與肌動蛋白-細胞骨架重塑作用以及可以增強細胞的遷移能力。與此結果相符，我的實驗結果顯示 CaD 可能作爲一個 PFTK1 激酶的磷酸化目標，在 PFTK1 抑制的細胞中可見 CaD 磷酸化的缺失以及與纖維型肌動蛋白的脫離。在 PFTK1 缺失細胞中，CaD 沒有與肌動蛋白結合，肌動蛋白應力纖維明顯缺失，這可能提示細胞遷移能力的減弱。除 TAGLN2 外，我還發現了 CaD 是 PFTK1 相關的生物學事件中的另一個中介參與者，并影響著肌動蛋白的組織動態變化。

最近，關於 microRNA（miRNA）異常是癌癥發展中重要的調控事件這一概念被廣泛接受，其對於多個抑癌基因以及癌基因的影響已被確定。我的研究源自于之前的一個 miRNA 表達實驗，該實驗提示在染色體 7q32 區域上有一個被命名爲 miR-183/96/182 的 miRNA 簇表達有增加。在現在的研究中，我同時證實了在 HCC 病例中亦有 miR-183, -96 和-182 的表達增加，並且與患者的預後、腫瘤轉移的臨床特徵包括微血管侵襲和腫瘤分化程度顯著相關。我亦找到證據表明由 β-catenin 激活而引起的 miR-183/96/182 的過度表達可以通過其共同的目標 Forkhead BoxO1 導致細胞遷移能力的增強從而加劇細胞的惡性程度。

總的來說，本實驗揭示了 7q21-32 擴增子在 HCC 發展過程中的對轉

移能力的影響。該區域中的目標基因或者 miRNA 的過度表達 包括 PFTK1 和 miR-183/96/182，對 HCC 的細胞遷移能力有影響作用。因此，對於 7q21-32 區域的深入研究瞭解可以提供關於 HCC 轉移的關鍵分子機制，爲 HCC 患者提供更多更好的治療方法。

Acknowledgement

First of all, I would like to express my deepest gratitude to my thesis supervisor, Professor Nathalie Wong. She has given me much guidance and inspiration throughout my PhD training in addition to providing me the opportunity to be a PhD student in CUHK. Through the PhD training, I had some difficulties in doing this task, but she taught me patiently until I knew what to do. She tried and tried to teach me until I understand what I supposed to do with the project work. The skills I acquired not only enable me to establish the right attitude and responsibility in my daily work, but also enrich my scientific exposure. I truly thank for all the time and effort she spent on guiding me.

I am also obligated to the financial support from the Chinese University of Hong Kong during the period of study, without it I could not have finished my degree.

Besides, I would like to thank all the past and present lab members for making the working environment friendly and interactive. Many thanks to Dr Arthur KK Ching, Dr WK Ip, Dr Erwin TC Chan, Dr Queenie WL Wong, Dr Amy KY Chung, Dr JH Chu, Dr Ibis KC Cheng, Ms Priscilla TY Law, Mr CC Lau, Ms Emily PS Pang, Mr. Bruce CK Tsang, Mr Gary JW Chen, Ms PS Li, Ms Vanessa TI Fung, Ms He Mian, Mr Alfa HC Bai, Ms Navy LY Wong and Ms Joyce BS Yuen for their help and support during my study. Special thank is also given to Dr Anthony WH Chan for his help in collecting clinical information of patients in the Prince of Wales Hospital.

Last but not least, I would like to express my deepest gratitude to my beloved family members, Yin-Shan Yeung, and friends for all their spiritual support and encouragement especially during difficult times.

Publications related to thesis

Publications arising from thesis

1. Leung WK, Ching AK, Chan AW, Poon TC, He Mian, Wong AS, To KF, Wong N. (2011). A novel interplay between oncogenic *PFTK1* protein kinase and tumor suppressor *TAGLN2* in the control of liver cancer cell motility. *Oncogene*. in press.
2. Leung WK, Ching AK, Wong N. (2011). Phosphorylation of Caldesmon by PFTAIRE1 kinase promotes actin binding and formation of stress fibers. *Mol Cell Biochem.* 350(1-2): 201-6.
3. Leung WK, Wong N. (2011). Liang Q (ed). *Molecular Aspects of Hepatocellular carcinoma: MicroRNA in Human Hepatocellular Carcinoma (Chapter 6).* Bentham Science Publisher: Australia pp 56-66.
4. Leung WK, He Mian, Ching AK, Law PT, Chan AW, Wong N. β-catenin-mediated up-regulation of miR-183/96/182 confers hepatocellular carcinoma cell motile phenotypes through targeting Forkhead BoxO1. [Manuscript in preparation].

Technical publications related to thesis

1. Zhou Q, Ching AK, Leung WK, Szeto CY, Ho SM, Chan PK, Yuan YF, Lai PB, Yeo W, Wong N. (2011). Novel therapeutic potential in targeting the microtubules by nanoparticle albumin-bound Paclitaxel in hepatocellular carcinoma. *Int J Oncol.* 38(3): 721-31.

Table of content

List of figures

List of tables

Abbreviations

°C	Degree Celsius
%	Percentage
2D-PAGE	Two dimensional polyacrylamide gel electrophoresis
AFB_1	Aflatoxin B_1
AJCC	American Joint Committee on Cancer
AR	Androgen receptor
ATCC	American Type Culture Collection
bp	Basepair
cDNA	Complementary DNA
CGH	Comparative genomic hybridization
Chr.	Chromosome
ddH_2O	Double distilled water
DEN	N', N'-diethylnitrosamine
DNA	Deoxy- ribonucleic acid
dNTP	Deoxy-nucleotide Trisphosphate
EMT	Epithelial-to-Mesenchymal Transition
FITC	Fluorescein isothiocyanate
GAPDH	Glyceraldehyde-3-phosphate dehydrogenase
GFP	Green fluorescence protein
HBV	Hepatitis B virus
HBx	Hepatitis B virus x protein
HCC	Hepatocellular carcinoma
HCV	Hepatitis C virus
hr	Hour
HSC	Hepatic stellate cell
KEGG	Kyoto Encyclopedia of Genes and Genomes
kb	Kilobase
kDa	Kilo dalton
LOH	Loss of heterozygosity
M	Molar
mg	Milligram
min	Minute
miRNA	microRNA
ml	Milliliter
mM	Millimolar
mm	Millimetre

Abbreviations

mRNA	Messenger ribonucleic acid
NAFLD	Non-alcoholic fatty liver disease
NASH	Nonalcoholic steatohepatitis
ng	Nanogram
nM	Nanomolar
nm	Nanometre
ORF	Open reading frame
PCR	Polymerase chain reaction
PMF	Peptide mass fingerprinting approach
qRT-PCR	Quantitative reverse transcription polymerase chain reaction
RNA	Ribonucleic acid
rpm	Rotation per minute
rRNA	Ribosomal RNA
RT	Reverse transcription
SDS-PAGE	Sodium dodecyl sulfate polyacrylamide gel electrophoresis
sec	Second
shRNA	Small Hairpin RNA
siRNA	Small interfering RNA
U	Unit activity
UTR	Untranslated region
V	Voltage
µg	Microgram
µl	Microliter
µM	Micromolar

Chapter 1

Introduction

1. Introduction

Hepatocellular carcinoma (HCC) is a highly aggressive tumor that is rapidly fatal. It currently ranks the seventh most common cancer worldwide (5.9%) and the fourth leading cause of cancer-related deaths globally (9.2%) (Figure 1-1) (Ferlay *et al.,* 2010). Approximately 530,000 new HCC cases are diagnosed annually. The overall incidence of HCC is higher in males than females, where a male to female ratio of 2.3 to 1 has been illustrated.

HCC exhibits distinct geographic distribution, where more than 80% of HCC cases occur in sub-Saharan Africa and Southeast Asia, and China alone accounts for more than 50% of the world's cases (Figure 1-2). The geographical distribution of HCC is similar in both male and female population worldwide. In Hong Kong, HCC currently ranks the fourth most common cancer and the third common cause of cancer-related mortality (Figure 1-3) (HK Cancer registry 2010, Hospital Authority), where a male to female incidence ratio is suggested as 3.1 to 1.

Curative surgery and liver transplantation represent the only hope for long-term survival in individuals diagnosed with HCC, but is only applicable to a minority of patients. This is largely attributed to most patients being clinically diagnosed at advanced inoperable stages, often with concurrent intra- and extra-hepatic metastases. The 5-year survival rate of most HCC patients is consequently ~5% (Altekruse *et al.,* 2009; Bosetti *et al.,* 2008; Méndez-Sánchez *et al.,* 2008; Umemura *et al.,* 2009).

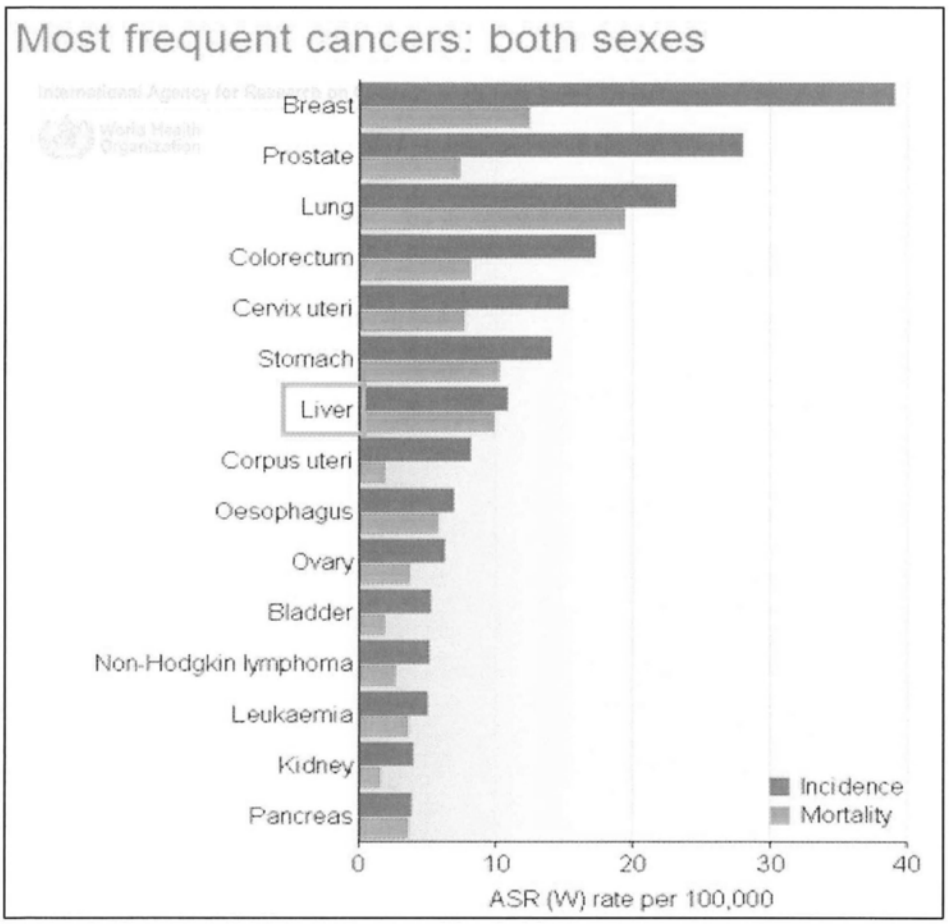

Figure 1-1 Worldwide liver cancer incidence and mortality in 2008.
(Figure adapted from Ferlay *et al.*, 2010)

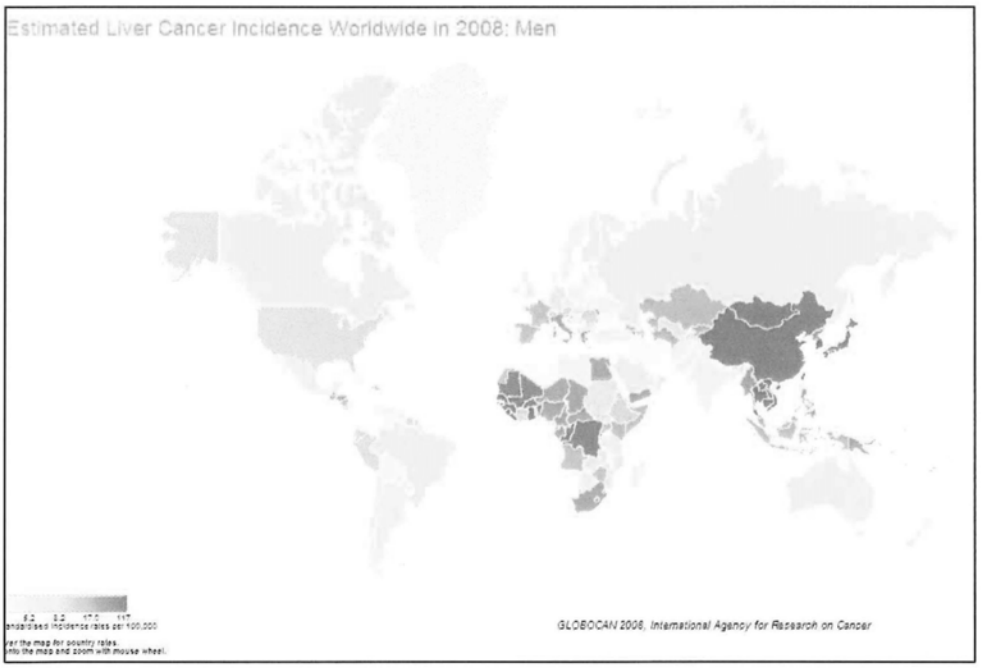

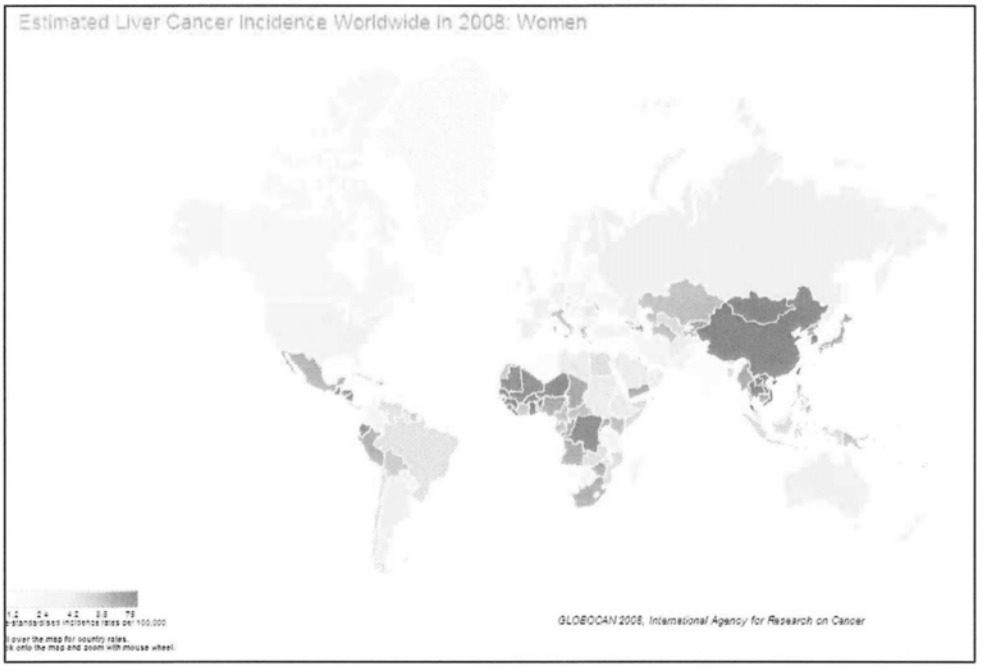

Figure 1-2 Geographic distribution of HCC incidence in Year 2008.
(Figure adapted from Ferlay *et al.*, 2010)

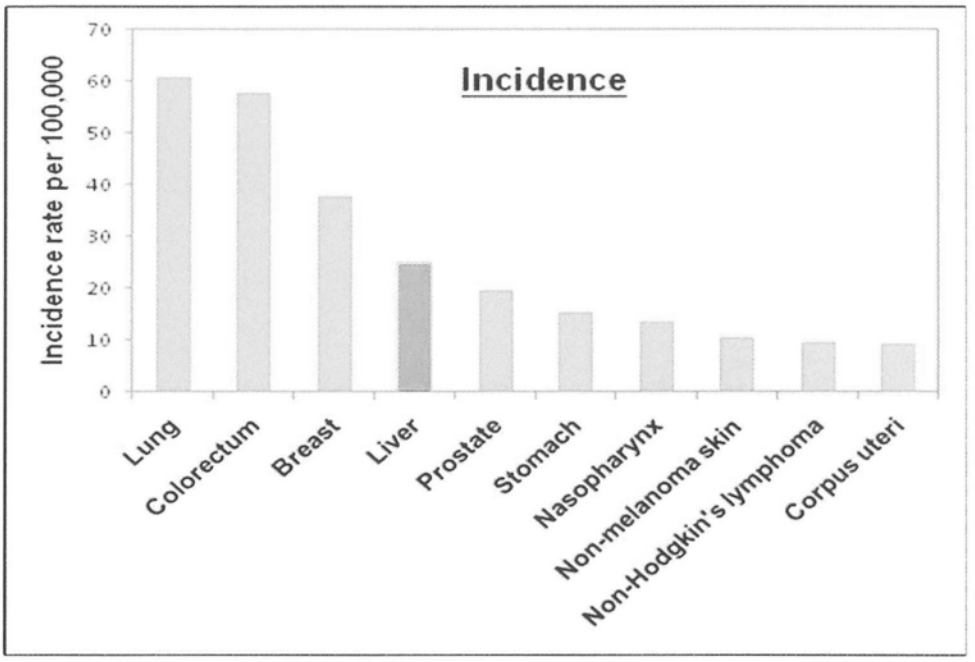

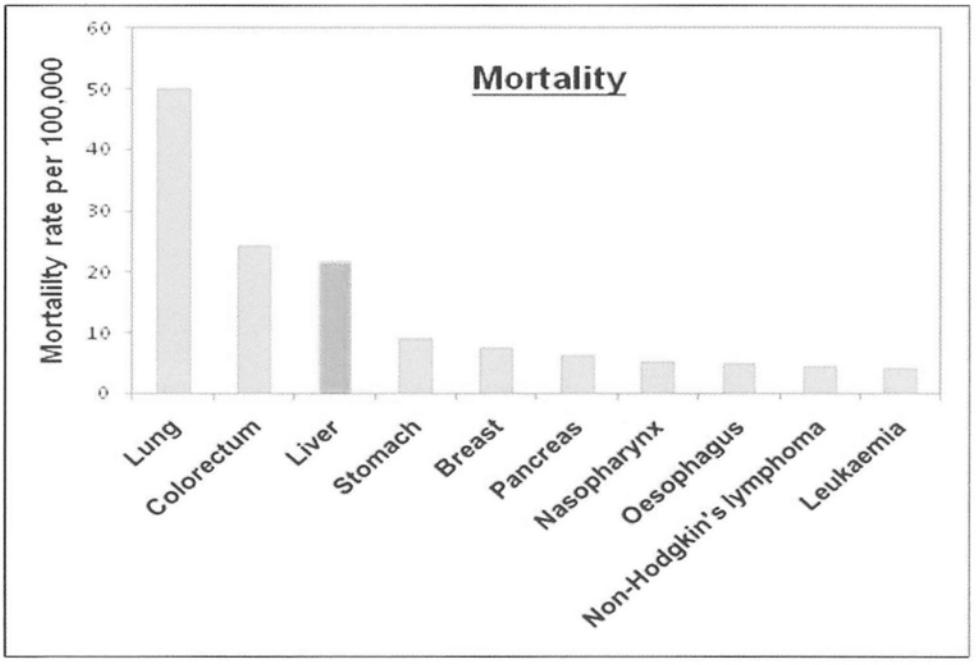

Figure 1-3 Leading cancer sites in Hong Kong in Year 2008.
Information obtained from The Hong Kong Cancer Registry, Hospital Authority.

1.1 Etiological factors of HCC

Epidemiologic studies have indicated a number of environmental factors contributing to HCC development including viral hepatitis types B (HBV) and C (HCV) infections, chronic liver diseases, the male gender, dietary aflatoxin-B1 consumption and alcohol abuse as important etiologic risks. The distinct geographical variations of HCC in countries such as China, Japan, Singapore, and parts of Europe and Africa have much attributed to the geographic prevalence of viral hepatitis and common dietary contaminant aflatoxin. In Hong Kong, viral Hepatitis B infection represents the most common risk factor.

1.1.1 Viral hepatitis infection

Hepatitis B virus (HBV) and Hepatitis C virus (HCV) are the major etiologic risks contributing to liver carcinogenesis. It was reported that approximately 80% HCC cases globally are associated with HBV and HCV infections (McGlynn and London, 2005). Patients suffered from acute viral infections often present symptoms such as jaundice, fever, liver enlargement and abdominal pain. More seriously, chronic hepatitis infection will lead to liver cirrhosis, and ultimately HCC.

1.1.1a Hepatitis B virus

Between 350 and 400 millions persons worldwide are chronically infected with HBV (Lavanchy, 2005). The major clinical outcomes of chronic infection are cirrhosis and HCC, either of which can cause liver-related death. It was estimated that chronic hepatitis B can lead to 320,000 deaths annually, where liver tumorigenesis accounts for 30 to 50% of HBV-related mortality.

The natural history of HBV-infected persons is highly complicated, and they usually move through a dynamic condition from a state of high viral load and no liver disease to one of active liver disease, followed by inactive disease, and then reverting back to active liver disease years later. Understanding the natural history of hepatitis B is particularly important because this can help clinicians decide on the need and optimal timing for antiviral therapy.

HBV is a small DNA virus which belongs to a prototype of the *Hepadnaviridae* family. Based on sequence analysis, HBV is classified into eight genotypes (A to H), either of each having a distinct geographic distribution (Norder *et al.,* 2004). Genotype A is commonly found in Northern Europe among Caucasians in the United States. Genotypes B and C are particularly common in Asian populations. Genotype D is found to be the most common genotype in Southern and Eastern Europe. Genotype F is frequently observed in native North and South Americans. However, the epidemiology of genotypes E, G, and H is not well understood.

The genome of HBV is a partially double-stranded circular DNA with approximately 3.2 kilobase (kb) in length surrounded by lipid bilayer envelope. The viral genome encodes four overlapping open reading frames (ORFs: *S*, *C*, *P*, and *X*) (Figure 1-4). The *S* ORF encodes the viral envelope proteins (HBsAg), whereas *C* ORF encodes either the viral nucleocapsid HBcAg or hepatitis B e antigen (HBeAg). The polymerase (pol) encoded by *P* ORF is functionally divided into three domains: the terminal protein domain, the reverse transcriptase domain, and the ribonuclease H domain. The HBV *X* ORF encodes a protein (HBxAg) with 154 amino acid in size, serving various functions including signal transduction, transcriptional activation, DNA repairing and inhibition of protein degradation (Cross *et al.,* 1993; Bouchard and Schneider, 2004; Hu *et al.,* 2006; Zhang *et al.,* 2001).

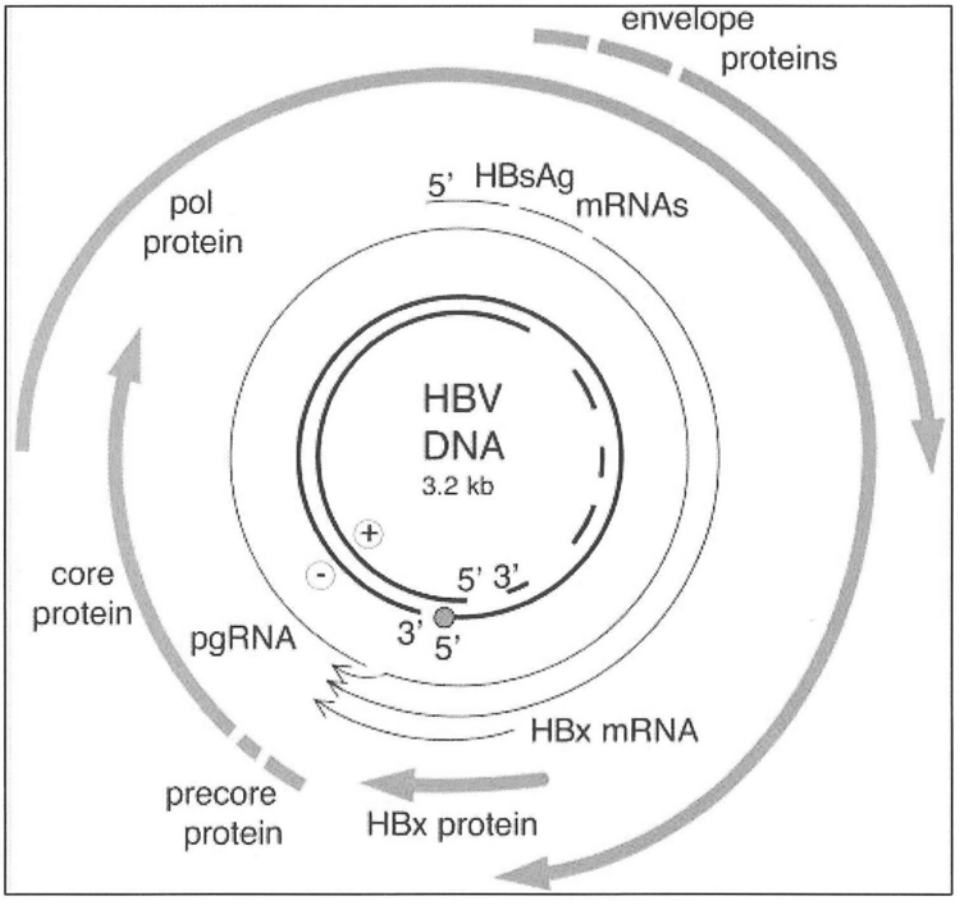

Figure 1-4 A schematic representation of the HBV genome.

Genomic DNA is indicated as the inner circle. The thick arrows represent the four open reading frames: core, envelope (surface antigen), polymerase (pol), and HBx proteins. HBV RNAs are represented as the thin lines. (Figure adapted from Bouchard and Schneider, 2004)

Extensive studies have addressed the importance of chronic hepatitis B and its DNA integration in liver cell carcinogenesis. Random DNA insertion was suggested to generate chromosomal instability, including chromosomal deletions at the HBV integration sites, and transpositions of the viral sequences together with the flanking cellular sequences from one chromosome to another (Wang *et al.,* 2004; Ziemer *et al.,* 1985). In addition, the insertion of viral DNA into a cellular gene and cis-activation of its expression are proposed as possible consequences of HBV DNA integration. It has been shown to occur in genes coding for proteins which are primarily significant in cell signaling, proliferation and viability (Ferber *et al.,* 2003; Horikawa and Barrett, 2001; Murakami *et al.,* 2005; Paterlini-Bréchot *et al.,* 2003; Tamori *et al.,* 1999). For instance, HBV DNA integration in intragenic regions of cell cycle gene (cyclin A) resulted in strong expression of hybrid HBV-cyclin A transcripts (Wang *et al.,* 1992). Recurrent HBV integrations into the human telomerase gene (hTERT) have also been reported (Ferber *et al.,* 2003; Paterlini-Bréchot *et al.,* 2003) for the maintenance of telomeric length and the escape of senescence. Besides, HBx has been suggested to interact with p53, therefore interfering its various antitumor actions such as cell cycle control and DNA repairing (Ahn *et al.,* 2002; Lee *et al.,* 2005; Mathonnet *et al.,* 2004). In terms of modulation of angiogenesis pathway, HBx expression was shown to induce up-regulation of the vascular endothelial growth factor (VEGF) transcription and stabilize hypoxia inducible factor HIF-1 (Han [1] *et al.,* 2007; Yoo *et al.,* 2008).

1.1.1b Hepatitis C virus

Chronic hepatitis C has been linked to liver carcinogenesis in various regions over the world. Approximately 22% (>100 000) of newly registered HCC patients possess HCV infection (World Health Organization). HCV-related HCC appears to be

prevalent in areas with an intermediate incidence rate of HCC such as Europe and Japan. Approximately 50 to 75% of HCC cases in Italy, Spain, and Japan are associated with HCV infection (Di Bisceglie, 1997). Prospective studies have indicated that nearly 80% of HCV-infected cases progress to chronic infection; 10 to 20% of them will develop complications of chronic liver disease, such as liver cirrhosis, and at least 1 to 5% will develop liver cancer (Lavanchy, 2011), provoking chronic hepatitis C as global health awareness.

HCV is an enveloped RNA virus which belongs to *flaviviridae* family. It possesses a positively single-stranded RNA molecule of approximately 9.6kb nucleotides in size. The HCV genome encodes both structural and nonstructural proteins. Figure 1-5 illustrated the HCV genomic structure with 4 structural proteins denoted as the core (C), envelope proteins (E1 and E2) and p7 for virion assembly, and 6 nonstructural proteins (NS2, 3, 4A, 4B, 5A, and 5B). The 5' untranslated region and the 3' X region are highly conserved, but parts of the E2 envelope protein are highly diverse so as to be denoted as hypervariable regions. The relatively conserved core, E1, and NS5B regions are employed for genotypes and subtypes determination. Amino acid sequences are found to be relatively conserved among different genotypes in the core and NS3 regions but are poorly conserved in other regions.

Although the precise mechanism(s) by which HCV infection causes HCC remains largely unknown, recent studies have proposed its potential carcinogenic effects on hepatic tumorigenesis. HCV proteins including core, NS3 and NS5A have been described in hepatocarcinogenesis through posttranscriptional repression of p21, which is known to be a cyclin dependent kinase inhibitor (Ghosh *et al.,* 1999; Kwun *et al.,* 2001; Lee *et al.,* 2002). HCV core proteins have also been suggested to exhibit transactivation activities on c-myc promoter (Ray *et al.,* 1995). Their oncogenic

properties were further substantiated by inducing the transformation of rat embryo fibroblasts to the malignant phenotype and the suppression of TNF-alpha mediated apoptotic cell death (Ghosh *et al.,* 2000; Ray *et al.,* 1996).

1.1.2 Liver cirrhosis

Cirrhosis is one of the consequences of chronic liver injury characterized by hepatic inflammation, vascular remodeling, and progressive fibrosis that lead to hepatic architectural distortion and liver dysfunction. Fibrosis is described as excessive deposition of extracellular matrix mediated by activated fibroblasts, and is in fact pre-requisite for liver cirrhosis. Recent molecular studies provoked the importance of epithelial-to-mesenchymal transition (EMT) from adult hepatic stellate cells (HSCs) into activated fibroblasts, which are key contributors to liver fibrosis and cirrhosis (Zeisberg *et al.,* 2007). Nearly 40% of the activated fibroblasts were originated from HSCs through EMT. Thus, understanding the underlying basis of fibrosis seems suggestive of the milestones of liver cirrhosis and carcinogenesis.

Liver cirrhosis occurs due to a variety of insights such as abused alcoholism, chronic hepatitis B and C, and fatty liver disease. Although the underlying basis by which cirrhotic liver is transformed into malignant lesions remains elusive, in fact between 60 to 90% HCC patients have underlying outcomes of liver cirrhosis (Craig, 1997), suggesting its significance in the role of HCC development. A resected cirrhotic liver containing a massive encapsulated HCC tumor is presented in Figure 1-6.

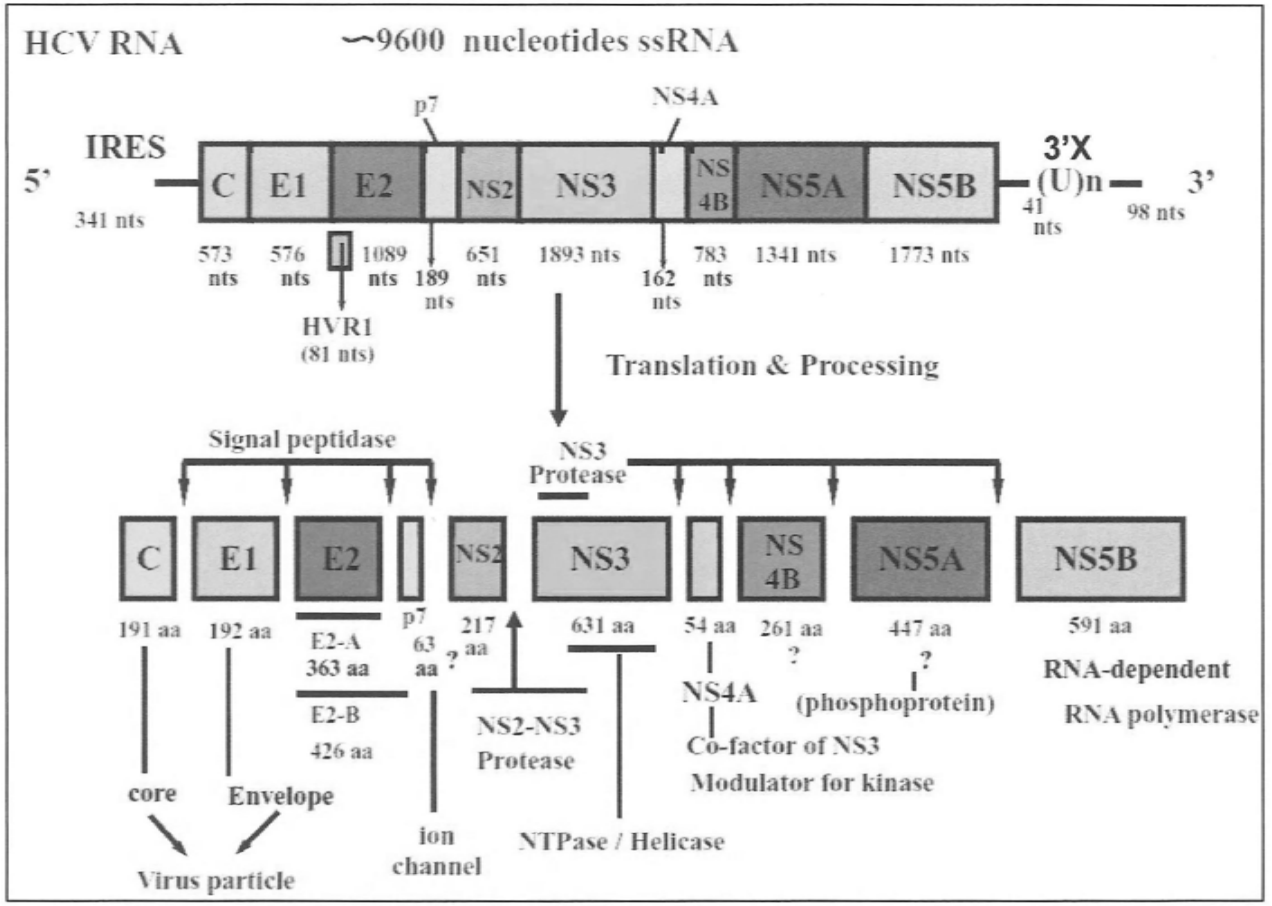

Figure 1-5 Structure and genome organization of hepatitis C virus.

The genome contains a single-stranded RNA, and both conserved and variable regions. There are two highly conserved regions at the 5′ and 3′ end of the viral genome (5′ untranslated region and 3′ X region, respectively).
(Figure adapted and modified from Chayama and Hayes, 2011.)

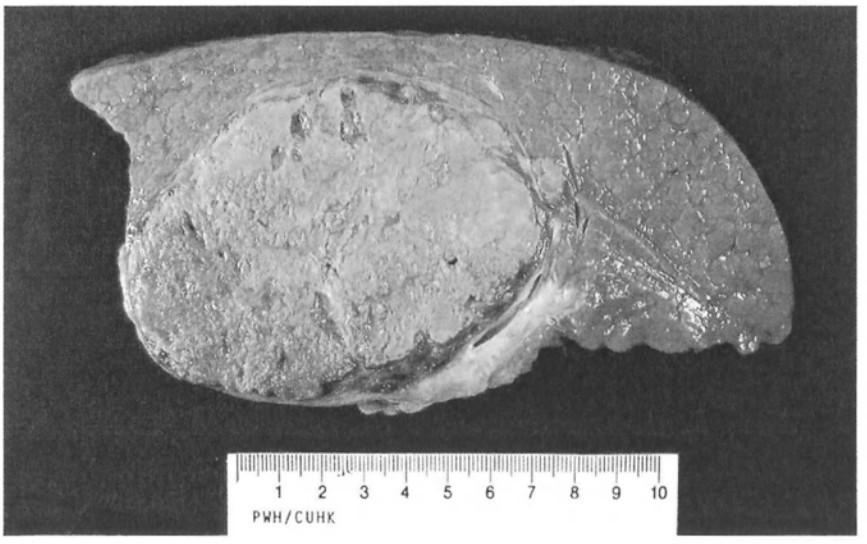

Figure 1-6 Macroscopic appearance of HCC.

A resected cirrhotic liver that contains a massive encapsulated tumor is shown.

1.1.3 Male gender

Epidemiology has suggested men have a higher HCC incidence than women (Ferlay *et al.,* 2010). Increasing studies therefore elevated the significance of carcinogenetic activities of androgen and protective actions of estrogen underlying the molecular mechanisms of HCC development.

For the androgen aspect, the male predominance of HCC has critical implications related to the androgen receptor (AR) activities. AR knockdown in hepatocytes was shown to postpone N',N'-diethylnitrosamine (DEN)-induced HCC formation and also reduced the number of resulting liver tumors, suggesting the active AR roles in augmenting the HCC risk (Ma *et al.,* 2008). Moreover, an intriguing interaction between the HBx viral protein and the androgen signaling pathway was recently established. The manifested carcinogenic effect of HBx-enhanced AR activation was further revealed by anchorage-independent colony-forming assay and the HBx transgenic mouse in an androgen concentration-dependent manner (Chiu *et al.,* 2007).

Besides the androgen perspective, estrogen was considered as a tumor-protective role with regard to the HCC gender disparity. Evidence derived from the DEN-induced mouse HCC model suggested the gender disparity of HCC occurrence with the tumor incidence higher in male than female mice (Maeda *et al.,* 2005). Reported studies on the antitumor effects of estrogen noted that DEN administration can enhance serum IL-6 level in male than in female mice, which can be abrogated by the administration of estradiol to the male mice (Naugler *et al.,* 2007).

1.1.4 Dietary aflatoxin B_1 exposure

Primary HCC is one of the most common malignancies worldwide. Aflatoxin B_1 (AFB_1) exposure is particularly important in favor of HCC carcinogenesis. People in Southern China and sub-Saharan Africa have the highest dietary AFB_1 exposure, along with chronic hepatitis B being the major causes of cancer mortality in these geographic areas.

AFB_1, which is a mycotoxin and derived from *Aspergillus flavus*, has been well classified as one of the hepatic carcinogens, which acts synergistically with HBV in the process of HCC development (Qian *et al.,* 1994). AFB_1 is commonly found in spoiled food stuffs, such as grains, corns, peanuts and soya beans, and metabolized in the liver to form an epoxide, which intercalates to the N7 position of specific guanines (Garner *et al.,* 1972). The formation of DNA adducts results in a transversion from AGG^{Arg} to AGT^{Ser} at the third position of codon 249 of *p53* (Bressac *et al.,* 1991; Hsu *et al.,* 1991). This hallmark mutation in the *p53* has been observed in 30-60% of HCC in aflatoxin-endemic areas (Bressac *et al*, 1991; Turner *et al*, 2002). Functional investigations suggested that transfection of a *p53* 249^{ser} mutant resulted in selective growth advantages of *p53*-null liver cancer cells (Ponchel *et al.,* 1994). The finding was further evident by the inhibitory effects of the 249^{ser} mutant on wild-type *p53*-mediated apoptosis (Wang *et al.,* 1995).

1.1.5 Alcohol abuse

Heavy alcohol consumption has been ascribed as important etiologic factors contributing to HCC development. This is documented with respect to heavy intake of >50-70g/day for prolonged period. Epidemiology has suggested frequent prevalence of alcohol-abused HCC in the United States and Italy, accounting for 32 to 45% of the cases (Morgan *et al.,* 2004). Chronic alcohol use of greater than 80 g/day for more than 10 years rises the risk for HCC by approximately 5-fold. It was also suggested a synergism between alcohol and hepatitis C in the development of HCC. Women seems more likely than men to liver injury from alcohol intake, and are more susceptible than men to develop cirrhosis at equivalent dosage of alcohol intakes because of sex disparity in alcohol metabolism (Frezza *et al.,* 1990). It was believed in terms of molecular veiws that chronic and excessive alcohol consumption could cause liver injury through oxidative stress and the activated release of chemokines and cytokines from Kupffer cells (Hoek and Pastorino, 2002), which were well-reported as pre-requisite for liver tumorigenesis.

1.1.6 Other risk factors for HCC development

1.1.6a Non-alcoholic fatty liver disease

HCC emerges as a common and lethal malignancy, while its incidence is substantially increasing in developed countries including Europe, Canada and the United States (Bosch *et al.,* 2004; El-Serag and Mason, 1999). Chronic liver disease including non-alcoholic fatty liver disease (NAFLD) has been found as one of the most common etiologies for hepatic carcinogenesis in these developed countries. Globally, the prevalence of NAFLD in the general populations is estimated ranging from 9 to 37% (Bedogni *et al.,* 2005; Ground, 1982; Hilden *et al.,* 1977; Lai *et al.,* 2002; Nonomura *et al.,* 1992; Nomura *et al.,* 1988; Omagari *et al.,* 2002; Shen *et al.,* 2003). Histopathology suggested a broad spectrum of NAFLD clinical outcomes ranging from isolated steatosis to a more aggressive way of chronic liver inflammation, namely nonalcoholic steatohepatitis (NASH). Approximately one-third of NAFLD patients progressively presented the clinical syndromes of NASH, ultimately leading to cirrhosis and even hepatic carcinoma (Williams *et al.,* 2011). Recent studies showed activation of Akt pathway plays a critical role in the proliferation of HCC originated from NASH (Martínez-López et al., 2010).

1.1.6b Obesity

Obesity has also been ascribed as an important risk factor for the development of various cancers, including liver carcinoma (Bugianesi *et al.,* 2002; Caldwell *et al.,* 2004; Lew and Garfinkel, 1979; Wolk *et al.,* 2001). The population showing body mass index (BMI) >30kg/ m^2 has been shown to associate with an increased risk of HCC development (Chen *et al.*, 2008; Polesel *et al.*, 2009), particularly for men

whose the relative risk of liver cancer mortality was approximately 5 times higher than those with a normal body mass index (Calle *et al*, 2003). The major explanation defining obesity as a definitely risk factor for HCC development is likely conferred by two factors: the increased risk for NALFD and subsequent progression to NASH.

1.2 Chromosomal aberrations

A consequence of stepwise genetic alterations has been accumulated and commonly detected during the process of cancer development. Molecular cytogenetic approaches such as comparative genomic hybridization (CGH) and loss of heterozygosity (LOH) have provided comprehensive information with respect to changes at genomic levels in HCC. Mapping of chromosomal gains and losses have recently resulted in identifying genomic amplification of oncogenes and inactivation of tumor suppressor genes. Therefore, better understanding on chromosomal aberrations could provide extensive knowledge on the process of hepatocarcinogenesis.

A number of studies mainly derived from the conventional CGH and LOH have reported various chromosomal aberrations associated with HCC development (Collonge-Rame *et al.,* 2001; Longerich *et al.,* 2011; Midorikawa *et al.,* 2006; Sy *et al.,* 2005; Yang *et al.,* 2003). These altered chromosomal events of HCC from at least three independent studies and ideogram representation on the summarized chromosomal aberrations were illustrated in Table 1.1 and Figure 1-7 respectively. In brief, gains on chromosomal arms of HCC were frequently observed on 1q (53 to 72%), 6p (26 to 37%), 7q (14 to 62%), 8q (43 to 61%), 17q (19 to 29%) and 20q (14 to 31%), and allelic losses were commonly detected on 4q (28 to 33%), 8p (31 to 56%), 13q (23 to 47%), 16q (29 to 36%) and 17p (26 to 67%).

Recently, our group has identified regional over-representations on chromosomes 1q, 3q and 7q in the progression of HBV-related HCC (Sy *et al.,* 2005). This study highlighted common genomic gains on 1q (66%), 6p (26%), 7q (32%), 8q (44%), 17q (29%) and 20q (25%) in a cohort of 100 cirrhotic HCC. Correlative

analysis on clinicopathologic features suggested recurring regional gains on 1q21-22, 3q22-28, 7q21-22 and 7q34-36 in association with advanced stage HCC. In line with these findings, bioinformatic analyses by SOTA on genome-wide chromosomal aberrations of 158 hepatitis B virus-associated HCC proposed copy gains on 7q21-31 and 3q22-24 regions as the late event of a stepwise tumor progression model for HCC, whereas gains on 8q regions appeared to be the earliest event for HCC development (Poon *et al.,* 2006) (Figure 1-8). Previous study using gene mapping analysis on 7q21-22 region highlighted *PFTAIRE* protein kinase 1 (*PFTK1*) as a candidate proto-oncogene in HCC (Pang *et al.,* 2007). Besides, positional mapping on amplified 8q24 region in HCC revealed that overexpression of Block of Proliferation 1 plays oncogenic positions in HCC eliciting epithelial-to-mesenchymal transition (Chung *et al.,* 2011). Therefore, mapping of candidate genes on these altered chromosomal regions seems particularly important in understanding the whole process of liver carcinogenesis.

Table 1.1 Chromosomal aberrations in HCC from at least 3 independent studies

Chromosomal Aberrations	Frequency occurred in HCC cases	References
+1q	53 to 72%	Collonge-Rame *et al.*, 2001; Longerich *et al.*, 2011; Midorikawa *et al.*, 2006; Sy *et al.*, 2005; Yang *et al.*, 2003
+6p	26 to 37%	Collonge-Rame *et al.*, 2001; Longerich *et al.*, 2011; Midorikawa *et al.*, 2006; Sy *et al.*, 2005
+7q	14 to 62%	Collonge-Rame *et al.*, 2001; Longerich *et al.*, 2011; Midorikawa *et al.*, 2006; Sy *et al.*, 2005; Yang *et al.*, 2003
+8q	43 to 61%	Collonge-Rame *et al.*, 2001; Longerich *et al.*, 2011; Midorikawa *et al.*, 2006; Sy *et al.*, 2005; Yang *et al.*, 2003
+17q	19 to 29%	Longerich *et al.*, 2011; Midorikawa *et al.*, 2006; Sy *et al.*, 2005
+20q	14 to 31%	Collonge-Rame *et al.*, 2001; Longerich *et al.*, 2011; Midorikawa *et al.*, 2006; Sy *et al.*, 2005
-4q	28 to 33%	Longerich *et al.*, 2011; Midorikawa *et al.*, 2006; Sy *et al.*, 2005
-8p	31 to 56%	Collonge-Rame *et al.*, 2001; Longerich *et al.*, 2011; Midorikawa *et al.*, 2006; Sy *et al.*, 2005; Yang *et al.*, 2003
-13q	23 to 47%	Longerich *et al.*, 2011; Midorikawa *et al.*, 2006; Sy *et al.*, 2005
-16q	29 to 36%	Longerich *et al.*, 2011; Midorikawa *et al.*, 2006; Sy *et al.*, 2005
-17p	26 to 67%	Collonge-Rame *et al.*, 2001; Longerich *et al.*, 2011; Midorikawa *et al.*, 2006; Sy *et al.*, 2005

Abbreviations: '+, -' chromosomal gains and losses respectively.

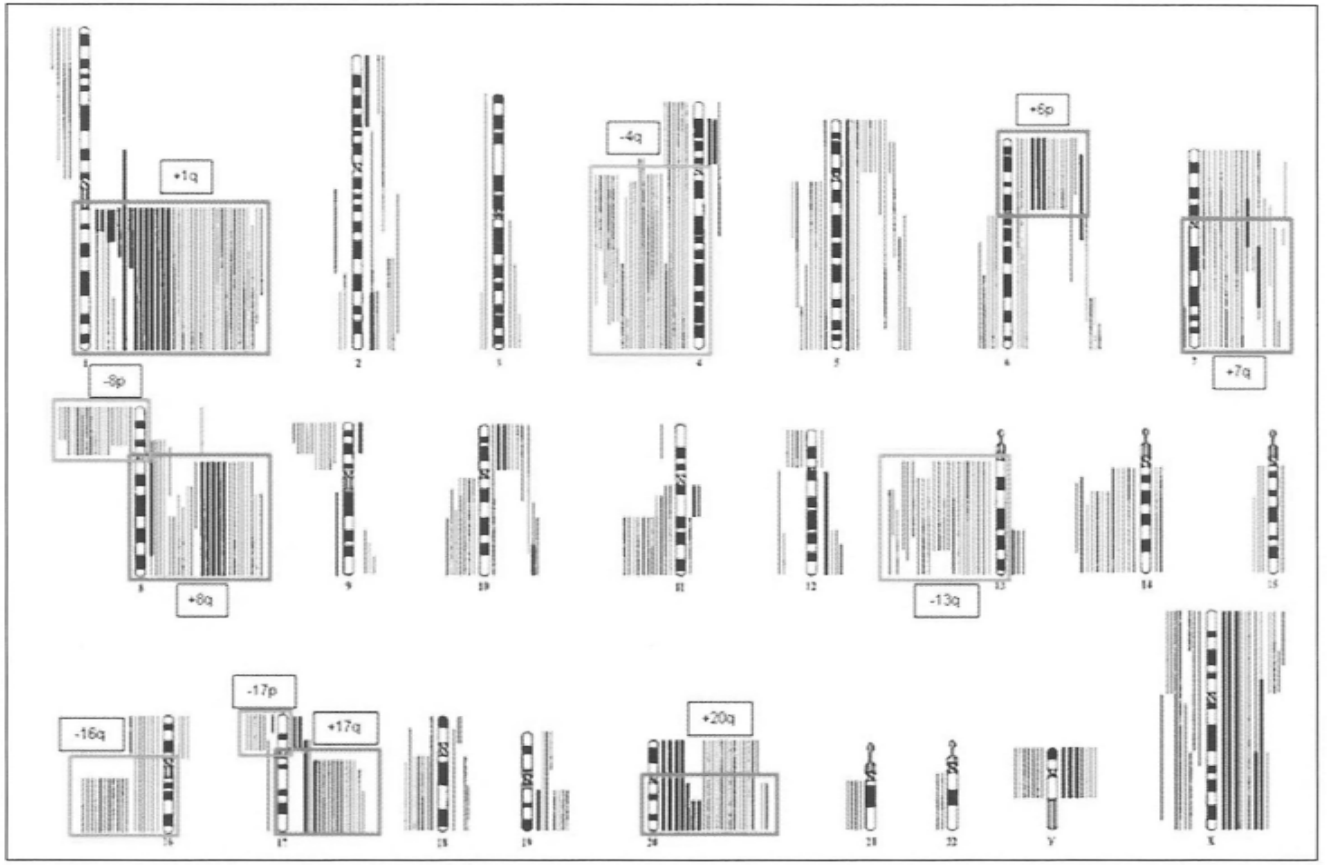

Figure 1-7 Summary of chromosomal imbalances detected by CGH in 47 HCC.

Frequent gains observed are labeled in green, and losses are labeled in red.

(Figure adapted from Wong *et al.,* 1999)

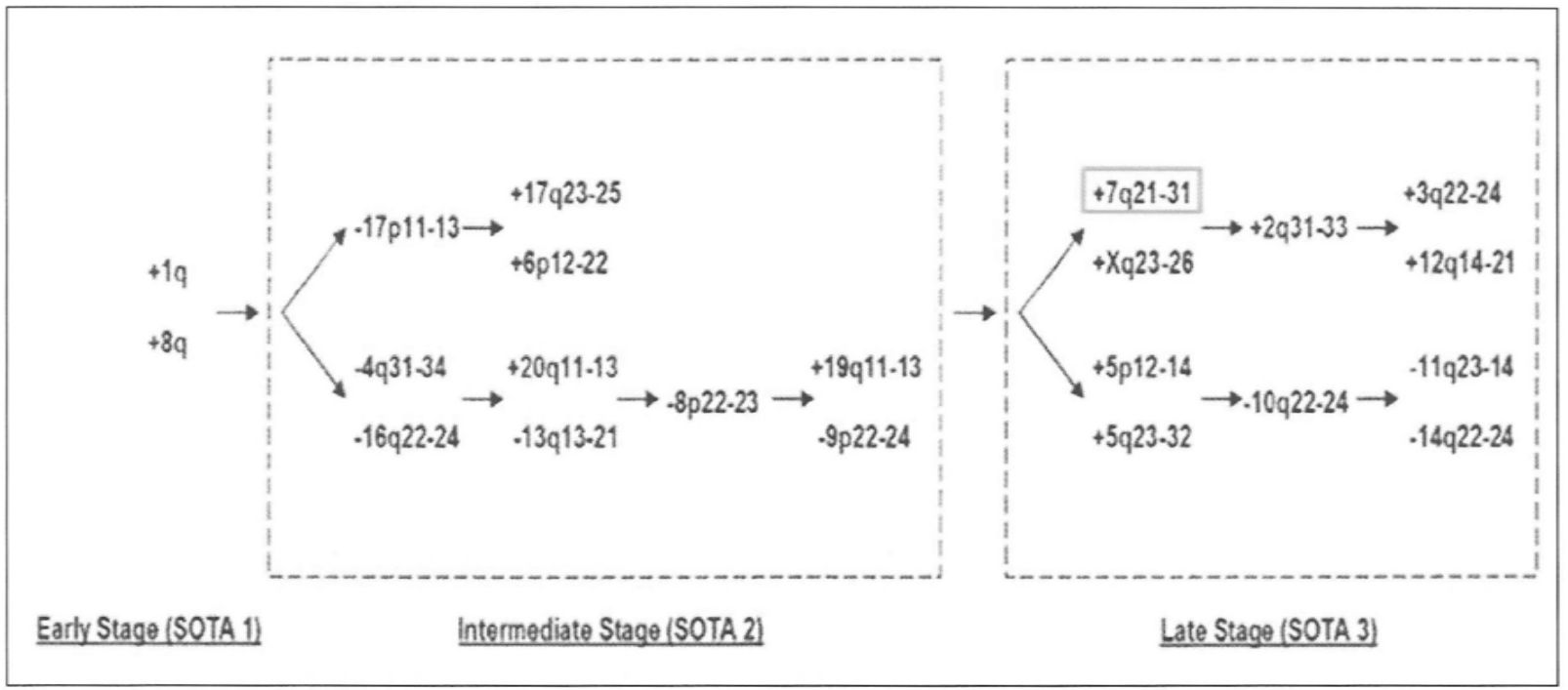

Figure 1-8 Proposed evolutionary changes in the HCC oncogenetic pathway.

Bioinformatic analysis by SOTA was used to construct an evolutionary tree of HCC based on changes in chromosomal information. For chromosomal imbalances in the intermediate and late tumor stage, the minimal overlapping regions are presented.

1.2.1 Gains of chromosomal 7q arm

Genomic amplification on 7q arm has been commonly ascribed in different types of cancers such as B-cell lymphoma, breast carcinoma, esophageal squamous cell carcinoma, lung adenocarcinoma and HCC (Chigrinova *et al.,* 2011; Collonge-Rame *et al.,* 2001; Hu *et al.,* 2009; Longerich *et al.,* 2011; Midorikawa *et al.,* 2006; Pinto *et al.,* 2006; Sy *et al.,* 2005; Yang *et al.,* 2003; Yen *et al.,* 2007). In HCC, approximately 14 to 62% cases demonstrated over-representation on 7q region (Collonge-Rame *et al.,* 2001; Longerich *et al.,* 2011; Midorikawa *et al.,* 2006; Sy *et al.,* 2005; Yang *et al.,* 2003). Recent fluorescent *in-situ* hybridization analysis on 7q amplicon in HCC revealed increased *CYP3A4* copy number, which was suggested to show reduced cytotoxic response to conventional chemotherapies (Lamba *et al.,* 2006). Our group has also illustrated frequent presence of 7q amplicon (32%), where regional gains on 7q21-22 and 7q34-36 are significantly associated with advanced tumor staging of HCC (Sy *et al.,* 2005). In addition, a tumor progression model further proposed the importance of amplified 7q region for the late stage development of HCC (Figure 1-8) (Poon *et al.,* 2006). In brief, copy number gain on 7q arm is of pivotal importance in the processs of hepatic carcinogenesis, especially advanced HCC development.

1.2.2 Identification of PFTK1 *within chromosomal 7q21 region*

The human *PFTK1* gene encodes *PFTAIRE* protein kinase 1, which shares 53% homology to Cdc2. The pivotal domains of *PFTK1* protein contain all subdomains that are highly conserved in the Cdc2 superfamily, including the serine/threonine kinase signature. The *PFTK1* transcript is highly expressed in brain, pancreas, kidney and ovary, but minimally observed in normal liver (Yang and Chen,

2001). Earlier array-based mapping examination for DNA copy gains in 5 HCC case that harbored gains o 7q21-22 highlighted a copy gain of 13 known genes (Pang *et al.,* 2007). Of the 13 known genes, seven were shown to be up-regulated in validative qRT-PCR (Figure 1-9). However, a significant up-regulation was suggested for only two genes, PFTK1 and ODAG, in association with advanced HCC tumors (40 stages I/II and 48 stages III/IV). Further correlative analysis suggested that only *PFTK1* up-regulation was significantly correlated with the presence of microvascular invasion. Subsequent functional investigations on knockdown and ectopic expression of *PFTK1* suggested its importance in promoting HCC cell motile properties. Based on these findings, further elucidation of *PFTK1* function, and its phosphorylated substrates, may offer a new avenue underlying the mechanisms of liver metastasis.

1.2.3 Identification of miR-183/96/182 within chromosomal 7q32 region

MicroRNA (miRNA) is a class of small, endogenous noncoding and regulatory RNA with a fundamental role in regulating gene expression (Ambros, 2001). As far, more than 1000 human miRNAs have been identified by cloning efforts and computational predictions. Despite the fact that the exact functions of many miRNAs remain unknown, recent bioinformatic algorithms predict that miRNA could regulate more than one-third of human genes (Krek *et al.,* 2005; Lewis *et al.,* 2005), underlying the potential significance of miRNAs in human cancers. Emerging evidence has begun to demonstrate that a number of miRNAs serve as crucial regulators in human cancers, including HCC (Asangani *et al.,* 2008; Fabbri *et al.,* 2007; Jiang *et al.,* 2008; Johnson *et al.,* 2005; Shiratori *et al.,* 1995; Ura *et al.,* 2009; Ma *et al.,* 2007; Wong *et al.,* 2010; Wong *et al.,* 2008). For instance, pioneering studies described let-7 miRNA as a negative regulator of the *RAS* guanosine

triphosphatases in human tumor cells (Johnson *et al.,* 2005). Specifically in HCC, evidences supported the roles of miRNA deregulations in terms of tumor progression, clinicopathlogic presentations as well as prognostic implications (Budhu *et al.,* 2008; Xiong *et al.,* 2010; Ura *et al.,* 2009). Taking advantage of compelling *in-vivo* studies on miRNAs, it was postulated that therapies targeting miRNAs, coupled with traditional approaches, could represent a novel curative treatment for HCC (Kota *et al.,* 2009). Based on these observations, understanding the biological basis of miRNAs in HCC becomes increasingly important. MiR-122, a liver-specific miRNA, is the most abundant miRNA accounting for 70% of the hepatic miRNA population, and is frequently down-regulated in approximately 60-95% human HCC (Leung and Wong, 2011). It functions in liver physiology (Girard *et al.,* 2008), and serves as a tumor-suppressor in the regulation of apoptotic process (Fornari *et al.,* 2009), control of intra-hepatic metastasis (Tsai *et al.,* 2009), and modulation of hepatitis C viral RNA replication (Jopling *et al.,* 2005). MiRNA-223 is also commonly repressed in HCC, where restoration of miR-223 in HCC cell lines negatively modulates cell viable capacity through targeting Stathmin1 (Wong *et al.,* 2008). On the other hand, frequent over-expression of miR-222 was suggested in HCC, while sequestration of miR-222 retarded HCC cell dissemination through enhancing AKT signaling (Wong *et al.,* 2010). Female-associated miR-18a was shown to target the *ESR1* gene encoding the estrogen receptor-α underlying the concept of gender disparity in HCC (Liu *et al.,* 2009).

Our group has previously defined a number of differentially expressed microRNAs (miRNAs) in HCC using miRNA expression profiling on a cohort of 20 HCC primary, 12 matching non-malignant liver and three HCC cell lines (Wong *et al.,* 2010) (Figure 1-10). From the study, I observed up-regulation of a miRNA cluster,

namely miR-183/96/182, where the gene loci are found within 7q32 region. MiR-183/96/182 up-regulation was commonly detected in breast, colorectal, endometrial, prostate, melanoma, and has been widely implicated in multitudes of biological processes including advantageous cell growth, anti-apoptotic effects and manifested cell invasiveness (Bandrés *et al.,* 2006; Guttilla *et al.,* 2009; Lin *et al.,* 2010; Myatt *et al.,* 2010; Schaefer *et al.,* 2010; Segura *et al.,* 2009). However, their biological role(s) in HCC remained largely undefined. Therefore, understanding the role of this cluster may hold promises for delineating the maze of liver carcinogenesis.

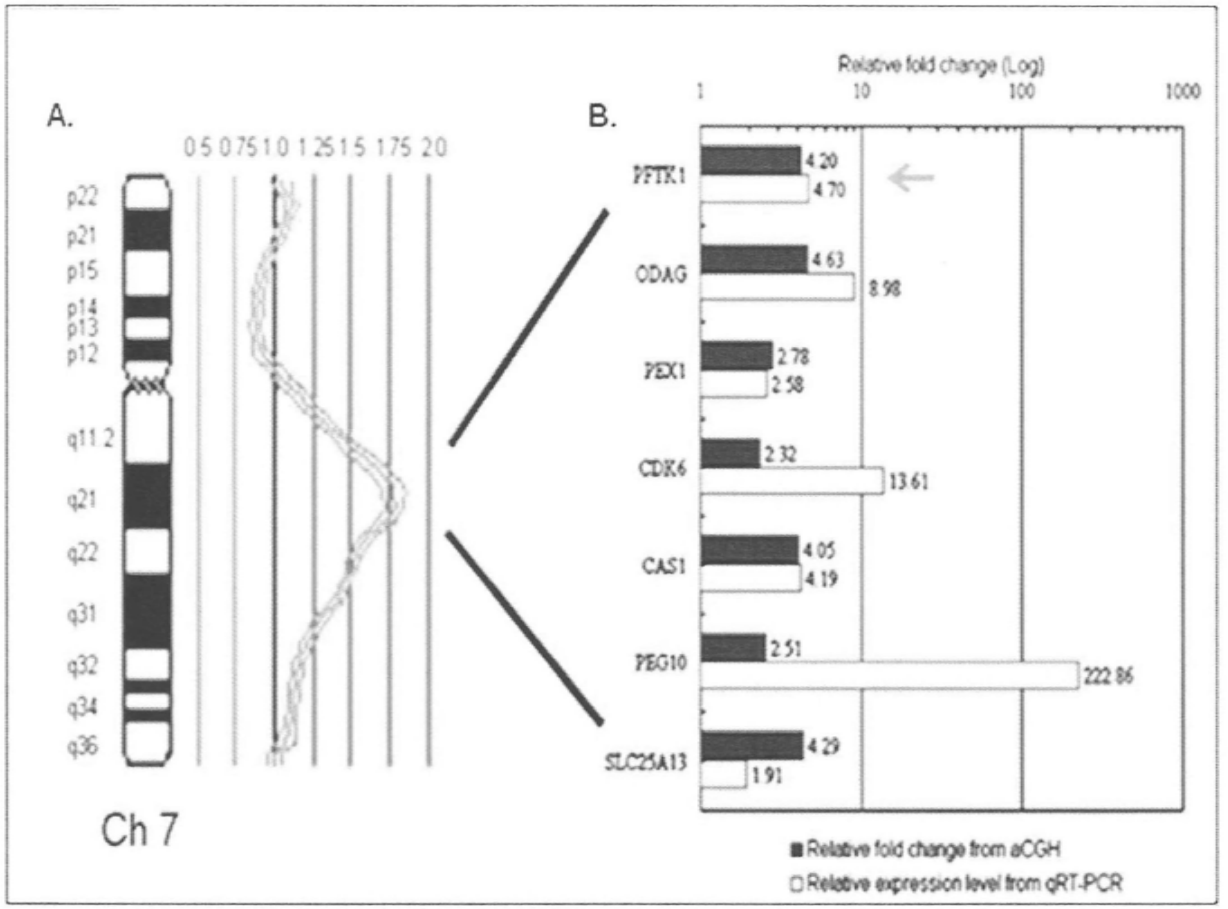

Figure 1-9 Up-regulated genes embedded in over-represented chr. 7q21-22 region.

(A) Chromosome-based CGH analysis on 5 HCC cases that displayed gains of the chr. 7q21-22. (B) An up-regulation of 7 genes validated by qRT-PCR, namely *PFTK1*, *ODAG*, *PEX1*, *CDK6*, *CAS1*, *PEG10*, and *SLC25A13*, was suggested.

(Figure adapted from Pang *et al.,* 2007)

A.

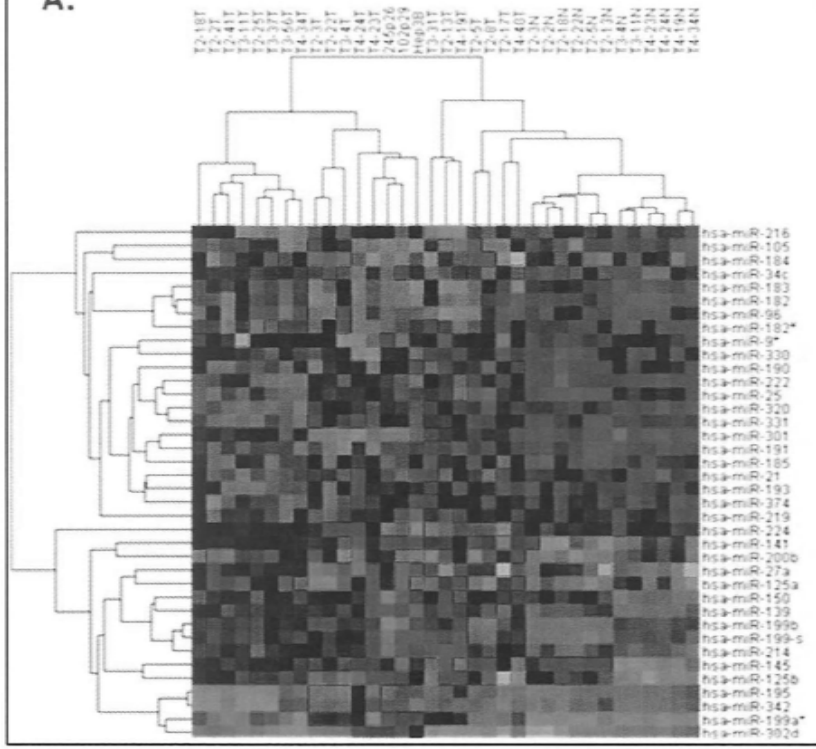

B. Up-regulated miRNAs

Rank	miRNA	Fold change (T/TN) (log_2)
1	hsa-miR-34c	7.05
2	hsa-miR-105	6.20
3	hsa-miR-183	4.89
4	hsa-miR-182	4.77
5	hsa-miR-96	4.00
6	hsa-miR-184	3.86
7	hsa-miR-190	3.50
8	hsa-miR-216	3.40
9	hsa-miR-182*	3.40
10	hsa-miR-224	3.37
11	hsa-miR-301	3.32
12	hsa-miR-9*	2.98
13	hsa-miR-222	2.54
14	hsa-miR-191	2.40
15	hsa-miR-25	2.39
16	hsa-miR-320	2.12
17	hsa-miR-21	1.90
18	hsa-miR-330	1.87
19	hsa-miR-219	1.68
20	hsa-miR-193	1.67
21	hsa-miR-185	1.55
22	hsa-miR-331	1.44
23	hsa-miR-374	1.42

Figure 1-10 Differential expressed miRNAs in HCC.

(A) Hierarchical clustering of 38 differentially expressed miRNAs based on fold change calculation.

(B) Twenty-three up-regulated miRNAs. A cluster of miRNAs, namely miR-183/96/182, were ranked top on the list.

(Figure adapted and modified from Wong *et al.,* 2010)

1.3 Aim of thesis

Recent genome-wide analyses of HCC have provided a wealth of information with respect to the association between genomic aberrations and metastatic implications (Poon *et al.*, 2006; Sy *et al.*, 2005). Chromosomal gains on 7q arm have been reported to be closely related to advanced stage HCC tumors. Bioinformatic analysis of genomic CGH data from >150 HCC patients further underpined gains of 7q21-31 in the progressive development of HCC (Poon *et al.*, 2006). These evidences underscore much importance for 7q gains in the liver tumorigenesis.

Earlier study from our group had reported on a candidate proto-oncogene *PFTK1* on 7q21 that conferred motile and invasive properties in HCC cells (Pang *et al.*, 2007). Given that *PFTK1* is a Cdc2 serine/threonine protein kinase, the **first objective** of this thesis was to characterize the phosphorylation target(s) of *PFTK1* kinase. Using 2D-PAGE mass spectrometry profiling on phospho-proteins of *PFTK1*-expressing and -nonexpressing Hep3B cells, a number of differential spots were identified. β-actin (ACTB) and transgelin2 (TAGLN2) were subsequently suggested to be two highest ranked phosphorylated substrates of *PFTK1* kinase. Further functional investigations led to the identification of a novel cascade of *PFTK1* phosphorylation on TAGLN2, leading to TAGLN2 inactivation and actin polymerization in favor of cell motility.

Since TAGLN2 could not completely revert the effect of *PFTK1*, other interacting protein(s) may be suspected to be involved in the *PFTK1*-modulated pathway. Reported literature has suggested caldesmon (CaD) as a downstream effector of Cdc2 protein, and a role for CaD in the control of cell migration (Juliano,

2003; Manes *et al.,* 2003). This led to the **second objective** that was to explore the role of CaD in *PFTK1*-modulated pathway.

Recently, altered miRNA expression has been recognized as an important event in the development of human cancers, where their influence on multiple tumor suppressors and oncogenes has been illustrated (Spizzo *et al.,* 2009). Previous miRNA expression profiling from our group has suggested a cluster of up-regulated miRNAs on 7q32, namely miR-183/96/182 (Wong *et al.,* 2010). This observation led to the **third objective** which was to elucidate the roles of miR-183/96/182 cluster in HCC. Functional investigations on miR-183/96/182 overexpression suggested a role for these miRNAs on HCC cell motility through targeting Forkhead box O1. The up-regulation of miR-183/96/182 was shown to be controlled by β-catenin transactivity.

Concordant with previous tumor progression model on the hepatocarcinogenesis (Poon *et al.,* 2006), my thesis on *PFTK1* and miR-183/96/182 underscored the importance of 7q21-32 amplification in the progression of HCC to advance metastatic tumors. Furthermore, findings suggested genomic amplicons are complex in nature, where one or more vital genes could be affected and simultaneously confer oncogenic effects.

Chapter 2

Materials and Methods

2.1 Materials

2.1.1 Chemicals and Reagents

Chemicals and Reagents	Company
Acetic acid	Merck & Co., Inc.
Acetonitrile	Thermo Fisher Scientific
40% Acrylamide/bis 29:1 Gel Solution	BioRad Laboratories
Agarose, regular	USB Corporation
Alumin, from bovine serum (BSA)	Sigma-Aldrich Company
Ammonium bicarbonate	Sigma-Aldrich Company
Ammonium persulfate (APS)	Sigma-Aldrich Company
Ampicillin Sodium Salt	USB Corporation
Betadine solution	Mundipharma Laboratories
Bio-Rad Protein Assay (Bradford)	Bio-Rad Laboratories
Bromophenol blue	Sigma-Aldrich Company
Calcium chloride (CaCl)	Sigma-Aldrich Company
Chloroform	Merck & Co., Inc.
Criterion XT Bis-Tris Gel	Bio-Rad Laboratories
Crystal violet	Sigma-Aldrich Company
α-cyano-4-hydroxycinnamic acid (CHCA)	Sigma-Aldrich Company
4',6-Diamidino-2-phenylindole (DAPI)	Sigma-Aldrich Company
Diethyl pyrocarbonate (DEPC)	Sigma-Aldrich Company
Dimethyl sulfoxide (DMSO)	Sigma-Aldrich Company
Dithiothreitol (DTT)	Sigma-Aldrich Company
Ethylenediaminetetraacetic acid (EDTA)	Sigma-Aldrich Company
Ethylene glycol-bis(2-aminoethylether)-N,N,N',N'-tetraacetic acid (EGTA)	Sigma-Aldrich Company
Ethanol	Merck & Co., Inc.
Ethidium bromide	Sigma-Aldrich Company
Formaldehyde	Sigma-Aldrich Company
Formic acid	Sigma-Aldrich Company
Glycerol	Sigma-Aldrich Company
Glycine	Sigma-Aldrich Company
Hematoxylin Solution, Harris Modified	Sigma-Aldrich Company
Hydrochloric acid	Merck & Co., Inc.

2.1.1 Chemicals and Reagents (con't)

Chemicals and Reagents	Company
Hi-Di™ Formamide	Applied Biosystems
Iodoacetamide	Calbiochem, Merck & Co., Inc.
Isopropanol	Merck & Co., Inc.
LB agar	USB Corporation
LB Broth	USB Corporation
Lipofectamine™ 2000	Invitrogen Corporation
2-Mercaptoethanol	Sigma-Aldrich Company
Mineral oil	Bio-Rad Laboratories
Mountant for histology	Sigma-Aldrich Company
Paraformaldehyde	Sigma-Aldrich Company
Phenyl methyl sulfonyl fluoride (PMSF)	GE Healthcare
PhosStop	Roche Diagnostics
Potassium ferricyanide	Sigma-Aldrich Company
Precision Plus Protein™ Standards (Dual Color)	Bio-Rad Laboratories
Protease Inhibitor Cocktail Tablets	Roche Diagnostics
ReadyStrip IPG Strips	Bio-Rad Laboratories
rec-Protein G-Sepharose® 4B	Invitrogen Corporation
RNase ZAP®	Ambion Inc.
Sephadex G-50 Fine	GE Healthcare
Sigma water	Sigma-Aldrich Company
Skimmed milk powder	Nestlé USA
S.O.C. medium	Invitrogen Corporation
Sodium Citrate	Sigma-Aldrich Company
Sodium chloride (NaCl)	Sigma-Aldrich Company
Sodium deoxycholate	Sigma-Aldrich Company
Sodium dodecyl sulfate (SDS)	Sigma-Aldrich Company
Sodium thiosulfate	Sigma-Aldrich Company
Tetramethyrhodamine B isothiocyanate (TRITC)-labeled Phalloidin	Sigma-Aldrich Company
Thiazolyl blue tetrazolium bromide (MTT)	Sigma-Aldrich Company
Triton X-100	Sigma-Aldrich Company
Trizma base	Sigma-Aldrich Company
TRIzol® reagent	Invitrogen Corporation
Trypan blue	Invitrogen Corporation
Tween 20	Sigma-Aldrich Company

2.1.1 Chemicals and Reagents (con't)

Chemicals and Reagents	Company
Urea	Sigma-Aldrich Company
N,N,N',N'-tetramethylethylenediamine (TEMED)	Sigma-Aldrich Company
Vectorshield anti-fade reagent	Vector Laboratories

2.1.2 Buffers

Buffers	Company
SSC solution (20X)	Ambion, Applied Biosystems
siRNA buffer (5X)	Dharmacon, Thermo Fisher Scientific
Tris acetate EDTA buffer (TAE), pH7.4	Sigma-Aldrich Company
Tris borate EDTA buffer (TBE), pH7.4	Sigma-Aldrich Company
XT MOPS Running Buffer (20X)	Bio-Rad Laboratories

Prepared Buffers	Constituents
Laemmli Sample Buffer	156.3mM Tris-HCl, 5% SDS, 62.5% glycerol, 0.1% bromophenol blue, 12.5% 2-Mercaptoethanol
Lower Running Buffer	1.5M Tris-HCl (pH 8.8)
Running Buffer (pH 8.8)	25mM Tris, 200mM glycine, 1% SDS
Upper Stacking Buffer	1M Tris-HCl (pH 6.8)
RIPA Cell Lysis Buffer	20mM Tris-HCl (pH 7.4), 150mM NaCl, 1mM EDTA, 1mM EGTA, 0.1% SDS, 1% Triton X-100, 1% sodium deoxycholate
Transfer Buffer	25mM Tris (pH 8.3), 200mM glycine, 20% methanol
Tris Buffered Saline (TBS)	150mM NaCl, 10mM Tris (pH 7.5)
Tris Buffered Saline Tween (TBST)	150mM NaCl, 10mM Tris (pH 7.5), 0.1% Tween

2.1.3 Cell Culture

Reagents and culture flasks	**Company**
AIM-V	Gibco Invitrogen Corporation
DMEM	Gibco Invitrogen Corporation
RPMI	Gibco Invitrogen Corporation
Fetal Bovine Serum (FBS)	Gibco Invitrogen Corporation
Geneticin (G418)	Gibco Invitrogen Corporation
Penicillin-Streptomycin, liquid contains 10,000 units of penicillin and 10,000 µg of streptomycin	Gibco Invitrogen Corporation
L-Glutamine 200mM (100X)	Gibco Invitrogen Corporation
MEM Non-essential amino acids solution 10mM (100X)	Gibco Invitrogen Corporation
Cell dissociation buffer	Gibco Invitrogen Corporation
Opti-MEM®I Reduced Serum Medium	Gibco Invitrogen Corporation
Phosphate Buffer Saline (PBS), pH7.4	Sigma-Aldrich Company
Trypsin-EDTA	Gibco Invitrogen Corporation
Tissue culture flask (25, 75, 150 cm^2)	Nalge Nunc International
Tissue culture dish (60, 100, 150 mm)	Becton Dickinson
Tissue culture plate (96-, 24-, 12-, 6-well)	Becton Dickinson
Matrigel Invasion Chambers in two 24-well plates, 8.0µm	Becton Dickinson
6.5mm Transwell with 8.0µm Pore Polycarbonate Membrane Insert	Corning Incorporated

2.1.4 Nucleic Acids

Nucleic Acids	Company
All custom designed oligos	Tech Dragon Limited
BLOCK-iT Fluorecent Oligo	Invitrogen Corporation
Human normal total liver RNA	Ambion, Applied Biosystems
Human normal total liver RNA	Clontech Laboratories, Inc.
Human normal total liver RNA	Strategene, Agilent Technologies
1kb Plus DNA Ladder	Invitrogen Corporation
Green Fluorescence Protein Expression Vector (*pEGFP-C2*)	Clontech Laboratories, Inc.
N-Terminal FLAG Expression Vector (*pFLAG-CMV2*)	Sigma-Aldrich Company
ON-TARGET plus si*PFTK1*	Dharmacon, Thermo Fisher Scientific
ON-TARGET plus si*TAGLN2*	Dharmacon, Thermo Fisher Scientific
ON-TARGET plus siControl Non-targeting Pool	Dharmacon, Thermo Fisher Scientific
MIRIDIAN Hairpin Inhibitor, hsa-miR-183	Dharmacon, Thermo Fisher Scientific
MIRIDIAN Hairpin Inhibitor, hsa-miR-96	Dharmacon, Thermo Fisher Scientific
MIRIDIAN Hairpin Inhibitor, hsa-miR-182	Dharmacon, Thermo Fisher Scientific
MIRIDIAN microRNA Hairpin Inhibitor Negative Control #1	Dharmacon, Thermo Fisher Scientific
Pre-miR™ miRNA Precursor, hsa-miR-183	Ambion, Applied Biosystems
Pre-miR™ miRNA Precursor, hsa-miR-96	Ambion, Applied Biosystems
Pre-miR™ miRNA Precursor, hsa-miR-182	Ambion, Applied Biosystems
Pre-miR™ Negative Control #1	Ambion, Applied Biosystems
Pre-miR™ Negative Control #2	Ambion, Applied Biosystems
pMIR-REPORT vector	Ambion, Applied Biosystems
TaqMan probes (inventory)	Applied Biosystems

2.1.5 Enzymes

Enzymes	Company
AmpliTaq Gold DNA polymerase	Applied Biosystems
Pfu DNA polymerase	Stratagene, Agilent Technologies
RQ1 RNase-free DNase	Promega Biotech Co., Ltd
T4 DNA ligase	Invitrogen Corporation
*Bam*H1	New England Biolabs
*Eco*RI	New England Biolabs
*Sal*I	New England Biolabs
*Xbal*1	New England Biolabs

2.1.6 Equipment

Equipment	Company
ABI 4800 MALDI-TOF/TOF Analyzer	Applied Biosystems
ABI PRISM 3100XL Genetic Analyzer	Applied Biosystems
AROS 160 orbital shaker	Thermolyne, Thermo Fisher Scientific
Auto-radiograph	GE Healthcare
Centrifuge 541R	Eppendorf International
CM3000-Cryostat	Leica Corporation
FACSCalibur System	Becton Dickinson
Gene Amp PCR System 9700	Applied Biosystems
GenePix 4000B Array Scanner	Axon Instruments
GS-800 ^{TM} Calibrated Densitometer	Bio-Rad Laboratories
ICYCLER IQ real time detection system	Bio-Rad Laboratories
Leitz DM RB fluorescence microscope	Leica Corporation
LSM 5 PASCAL	Carl Zeiss
ND-1000 UV-VIS Spectrometer	NanoDrop Technologies
PowerPac ^{TM} HC	Bio-Rad Laboratories
Thermomixer 5435	Eppendorf International
Victor$_3$ ^{TM} multilabel counter	Perkin Elmer

2.1.7 Kits

Kits	Company
BigDye Terminator Cycle Sequencing Kit	Applied Biosystems
Colloidal Blue Staining Kit	Invitrogen Corporation
Dual-Luciferase Assay Kit	Promega Biotech Co., Ltd
ECL Western blotting detection reagents	GE Healthcare
ECL plus™ Western blotting detection reagents	GE Healthcare
High Capacity cDNA Archive Kit	Applied Biosystems
One Shot® TOP10 Chemically Competent *E.coli*	Invitrogen Corporation
PhosphoProtein Purification Kit	Qiagen
PlusOne Silver Staining Kit	GE Healthcare
QIAamp DNA Mini Kit	Qiagen
QIAGEN® Plasmid Maxi Kit	Qiagen
QIAGEN® Plasmid Mini Kit	Qiagen
QIAquick Gel purification Kit	Qiagen
QIAquick PCR Purification Kit	Qiagen
QuikChange™ Site-Directed Mutagenesis Kit	Stratagene, Agilent Technologies
ReadyPrep 2-D Cleanup Kit	Bio-Rad Laboratories
ReadyPrep 2-D Starter Kit Rehydration/Sample Buffer	Bio-Rad Laboratories
SYBR Green PCR Reagents	Applied Biosystems
TaqMan® Universal PCR master mix	Applied Biosystems
TaqMan Universal PCR master mix, No Amperase® UNG	Applied Biosystems
TaqMan® Reverse Transcription Reagents	Applied Biosystems

2.1.8 Antibodies

Antibodies	Company
β-actin Mouse monoclonal	Sigma-Aldrich Company
β-catenin (active) Mouse monoclonal	Upstate, Millipore Corporation
β-catenin (total) Mouse monoclonal	BD Biosciences
Caldesmon Mouse monoclonal	Neomarkers, Thermo Fisher Scientific
FLAG Mouse monoclonal	Sigma-Aldrich Company
Forkhead Box1 Rabbit monoclonal	Cell Signaling Technology, Inc.
GAPDH Mouse monclonal	Chemicon, Millipore Corporation
PFTK1 Purified Rabbit Pab	Abnova Incorporation
Phosphoserine Rabbit polyclonal	Chemicon, Millipore Corporation
Phosphothreonine Mouse monoclonal	Sigma-Aldrich Company
Phosphotyrosine Rabbit polyclonal	Invitrogen Corporation
Transgelin-2 Goat polyclonal	Santa Cruz Biotechnology
β -tubulin Mouse monoclonal	Invitrogen Corporation
Vimentin Mouse monoclonal (Western)	Santa Cruz Biotechnology (sc-51721)
Vimentin Mouse monoclonal (Immunofluorescence)	Santa Cruz Biotechnology (sc-6260)
Anti-**goat** conjugated HRP IgG	Santa Cruz Biotechnology
Anti-**mouse** conjugated HRP IgG	Santa Cruz Biotechnology
Anti-**rabbit** conjugated HRP IgG	Santa Cruz Biotechnology
Mouse Alexa Fluor 488	Invitrogen Corporation
Mouse Alexa Fluor 594	Invitrogen Corporation
Polyconal mouse anti-**rabbit** immunoglobulins/biotinylated	DAKO

2.1.9 Softwares

Softwares	Company
ABI PRISM® 3130 Genetic Analyzer Data Collection Software v1.1	Applied Biosystems
Adobe Photoshop CS ver8.0	Adobe System Incorporation
AxioVision LE Rel 4.5	Carl Zeiss
CellQuest	Becton Dickinson
CodeLink Expression Analysis Software v.4	Amersham Biosciences
DNA sequencing analysis software v3.7	Applied Biosystems
GPS Explorer™ Workstation ver3.6	Applied Biosystems
GraphPad PRISM ver3.0	GraphPad Software Incorporation
LSM Image Browser	Carl Zeiss
LSM 5 PASCAL	Carl Zeiss
MedCalc® ver 11.0.1.0	MedCalc Software bvba
PDQuest 7.1.1	Bio-Rad Laboratories
Sequence Scanner v1.0	Applied Biosystems
SPSS 11.0 for Windows	IBM

2.1.10 Web Resources

Web Resources	URL
Mascot Search	http://www.matrix-science.com
miRBase	http://www.mirbase.org
National Center for Biotechnology Information (NCBI)	http://www.ncbi.nlm.nih.gov
NEBcutter V2.0	http://tools.neb.com/NEBcutter2/index.php
Primer3	http://frodo.wi.mit.edu/primer3
SwissProt	http://us.expasy.org/sprot
TargetScanHuman 5.1	http://www.targetscan.org
The Database for Annotation, Visualization and Integrated Discovery	http://david.abcc.ncifcrf.gov
Transcription Element Search System	http://www.cbil.upenn.edu/cgi-bin/tess/tess
UCSC Genome Bioinformatics	http://www.genome.ucsc.edu

2.2 Patients

2.2.1 Demographic information

Tumorous and adjacent non-malignant liver tissues were collected from HCC patients who underwent curative surgery at the Prince of Wales Hospital, Hong Kong. Informed consent was obtained from each patient. Chronic HBV infection was verified by serological analysis, and diagnoses of cirrhotic liver and HCC were confirmed by histological examination. The AJCC (6^{th} edition) was used in tumor staging and grading classifications.

A total of 180 paired HCC tumors and adjacent non-tumoral counterparts were recruited for tissue microarray analysis on the immunohistochemistry staining of *PFTK1* protein in Chapter 3. Histology confirmed a diagnosis of HCC in all 180 patients; the non-tumorous livers were cirrhotic in 72.1% of cases. Serological examination revealed chronic HBV in 91.2% of patients. The AJCC system classified 103 cases as stage I, 42 as stage II, and 26 as stage III, whereas recurrent cases were not included in the analysis.

In Chapter 4 with respect to the study on caldesmon phosphorylation, tumorous and non-malignant liver tissues were collected from 25 patients. Fifteen (60%) out of 25 cases were confirmed as cirrhotic, and 21 cases (84%) were revealed as HBV-positive carriers. Nineteen HCC cases (76%) were classified as stage I, 1 (4%) as stage II, and 5 (20%) as stage III according to the AJCC system.

Besides, 81 HCC patients were obtained for the correlative analysis of miR-183/96/182 in Chapter 5. The patients were also predominantly HBV-carriage (88.9%) with 69% of the cases underlying liver cirrhosis. The disease stages of the tumors were classified 51 cases as stage I, 15 as stage II, and 15 as stage III.

2.2.2 HCC tissue microarray

Formalin-fixed paraffin-embedded archive tissue of 180 paired HCC tumors and adjacent non-tumoral livers were arranged in tissue array blocks for the analysis of *PFTK1* protein in Chapter 3. Three tissue cores were taken from each case, and the paired tumors and adjacent non-tumoral tissues were printed sidewise in the same block. Five-μm sections were stained for *PFTK1* protein according to procedure described previously (Wong *et al.,* 2009). In brief, expression of *PFTK1* protein was detected by avidin-biotin-complex method using primary antibody (Abnova Incorporated, Taiwan) at a dilution of 1:250. After incubation with primary antibody, sections were treated with biotinylated mouse anti-rabbit immunoglobulins (at 1:200 dilution; Dako, Carpinteria, CA, USA) before the addition of streptavidin horseradish peroxidase conjugate (at 1:400 dilution; Invitrogen, Carlsbad, CA, USA). Chromogen signals were detected with diaminobenzidine-H_2O_2 substrate mixture. The immunohistochemistry grading of *PFTK1* was achieved by scoring the average percentage of positive cells from three cores of each HCC case and non-tumoral liver tissue. The overall grading defined nil to 10% staining as weak, 11-40% as moderate and $\geq$40% as high.

2.3 Cell culture

Eight HCC cell lines Hep3B, HepG2, PLC/5, SNU387, SNU398, SNU449, SNU475 and SK-HEP-1 were obtained from ATCC (Rockville, MD, USA). Twelve in-house HCC cell lines HKCI-1, -2, -3, -4, -6, -7, -8, -9, -10, -C1, -C2 and –C3 were previously established and reported (Wong *et al.,* 2008; Wong *et al.,* 2010). The HKCI cell lines with early passages (passages 25-35) were employed. An immortalized hepatocyte cell line L02 was kindly provided by Prof. Xin-Yuan Guan from the University of Hong Kong. The cell lines being employed in Chapters 3~5 were summarized in Table 2.1.

The ATCC cell lines were cultured in DMEM supplemented with 10% FBS, 1% MEM non-essential amino acids solution and 1% penicillin-streptomycin (Invitrogen). The HKCI series of in-house cell lines were cultured as previously described (Pang *et al.,* 2000). In brief, the cells were maintained in AIM-V medium supplemented with 10% FBS, 1% L-Glutamine and 1% penicillin-streptomycin (Invitrogen).

Table 2.1 Cell lines employed in different chapters

Chapters	Cell lines studied	
Chapter 3		
Characterization of *PFTK1* kinase in the role of liver cancer cell motility	In-house (HKCI):	HKCI-4
	ATCC:	Hep3B
	Prof. Xin-Yuan Guan:	L02
Chapter 4		
Phosphorylation on Caldesmon by *PFTK1* kinase promotes actin binding and formation of stress fibers	ATCC:	Hep3B
Chapter 5		
Role of miR-183/96/182 overexpression in HCC	In-house (HKCI):	HKCI-1, -2, -3, -4, -6, -7, -8, -9, -10, -C1, -C2 and –C3
	ATCC:	Hep3B, HepG2, PLC/5, SNU387, SNU398, SNU449, SNU475 and SK-HEP-1

2.4 Establishment of PFTK1-*suppressed stable clones*

Vector-based shRNA interference against *PFTK1* was constructed as previously reported (Pang *et al.,* 2007). Briefly, the annealed 29-mer shRNA against *PFTK1* was subcloned into pGE-1 vector (Stratagene, Santa Clara, CA, USA) predigested with *Bam*H1 and *Xba*I. The ligated products were introduced into TOP10 chemically competent cells (Invitrogen), and the transformed cells were plated on kanamycin (50μg/ml)-containing LB-agar plates. The plasmid for further investigations was verified by DNA sequencing.

The construct was then transfected into Hep3B cells by Lipofectamine^{TM} 2000 (Invitrogen). After 24 hr post-tranfection, the cell lines were selected under 1% G418 culture for at least 7 days, and five individual cell clones were selected for qRT-PCR analysis to ensure effective knockdown. Two stably *PFTK1*-suppressed cells, denoted as sh-*PFTK1*-c1 and sh-*PFTK1*-c2, were chosen for functional studies and downstream identification in Chapters 3 and 4. Cells transfected with shNEG RNA, abbreviated as sh-Mock, served as control cell lines.

2.5 Expression analysis by qRT-PCR

The expression of target genes or miRNAs in normal liver samples, HCC cell lines, HCC tumors and adjacent non-tumorous livers were performed using qRT-PCR analysis. In short, the RNA from liver samples were extracted and subsequently transcribed into cDNA by reverse transcription. The qRT-PCR analyses were performed using target-specific inventoried TaqMan Probes or primers designed by Primer3 (http://frodo.wi.mit.edu/primer3). All custom designed DNA oligos including primers were synthesized by TechDragon (Shatin, Hong Kong).

In HCC cell lines and primary tumors, all gene and miRNA expressions were determined relative to a reference pool of three normal livers (Ambion, Austin, TX, USA; Clontech Laboratory, Mountain View, CA, USA; Stratagene).

2.5.1 Total RNA extraction

Total RNA was extracted from both cell lines and HCC tumors using TRIzol® reagent (Invitrogen) according to manufacturer's instructions. In brief, after homogenizing the samples with TRIzol® reagent, chloroform was added leading to a separation into a clear upper aqueous layer containing RNA, an interphase and a red lower organic layer. RNA is precipitated from the aqueous phase with the addition of isopropanol. The RNA pellet was then washed by cold ethanol (75%) and air-dried for 15 min. Finally, it was resuspended into water for molecular usage (Sigma, St Louis, MO, USA). The quantity and quality of RNA extraction were measured by ND-1000 UV-VIS Spectrometer (NanoDrop Technologies, Wilmington, DE, USA) as reference to the ratio of absorbance at 260/280 nm. The integrity of RNA was determined by agarose gel electrophoresis. The RNA was stored at -80 °C until use.

2.5.2 qRT-PCR analyses

The RNA from each sample was treated with DNase to eliminate carryover of genomic DNA. One μg RNA was topped up to a total volume of 10 μl containing 1U/μL RNase-free DNase and 1μL of DNase reaction buffer (Promega, Madison, WI). The reaction proceeded at 37°C for 10 min. To ensure a complete elimination of DNA carryover, PCR reaction using primers targeting genomic β-globulin gene was performed. Absence of visualized banding in gel electrophoresis is suggestive of no genomic DNA contaminations. Primer sequences used for β-globulin were 5'-GAAGAGCCAAGGACAGGTAC-3' (sense) and 5'-CAACTTCATCCACGTTCACC-3' (anti-sense).

2.5.2a qRT-PCR for gene expression

Of total DNase-treated RNA, 1μg was subjected to RT reaction using the TaqMan® Reverse Transcription Reagents (Applied Biosystems, Foster City, CA, USA). A total volume of 50μl reaction mixture containing 12.5μl of 80ng/μl DNase-treated total RNA, 5μl of 10X TaqMan RT buffer, 11μl of 25mM $MgCl_2$, 10μl of 10mM dNTP mixture, 2.5μl of 50μM random hexamers, 1μl of 20U/μl RNases inhibitor, and 1.25μl of 50U/μl MultiScribe™ Reverse Transcriptase was prepared. The thermal cycling for the RT reaction was performed as follows: 10 min at 25°C, 60 min at 37°C and 5 min at 95°C. All first strand cDNA was stored at -80°C until use.

Based on the sequence information obtained from NCBI database (http://www.ncbi.nlm.nih.gov), I would design primers by Primer3

(http://frodo.wi.mit.edu/primer3) for gene expression analysis. To ensure primer specificity, further blast search was performed. The list of primers employed in different chapters was revealed in Table 2.2. PCR reaction was conducted on a 96-well optical tray with the addition of 25μl reaction mix containing 1μl of the cDNA template, 2.5μl of 10X SYBR Green PCR buffer, 1.5μl of $MgCl_2$, 0.5μl of 12.5mM dNTP, 0.25μl of 5U/μl TaqGold, 0.25μl of 1U/μl AmpErase UNG, 1μl of 10μM of individual primer set. The thermal cycles were as follows: 50°C for 2 min, followed by 40 cycles of 95°C for 15 sec and 60°C for 20 sec. Threshold cycles were calculated from the mean value of triplicate experiments. Reactions with no template were also included as negative control. All gene expressions were normalized with internal reference gene, *GAPDH* mRNA. The list of primer sets for qRT-PCR in Chapters 3~5 was demonstrated in Table 2.2.

2.5.2b qRT-PCR for miRNA expression

A total of 10ng DNase-treated RNA was subjected to RT reaction using the High Capacity cDNA Archive Kit (Applied Biosystems). A total of 15 μl reaction mixture (5ng/μl DNase-treated total RNA (2μl), DNase-treated total RNA (2μl), of 100mM dNTP (0.15μl), 5X miR specific RT-primer (3μl), 20unit/ μl RNase inhibitor (0.19μl), and 50U/ μl MultiScribe™ Reverse Transcriptase (1μl)) was prepared and subsequent to RT reaction. To enhance the binding of miR specific RT-primer to RNA template, RT mixture was chilled on ice for 5 min prior to RT reaction. The reaction was performed as follows: 30 min at 16°C, 30 min at 42°C and 5 min at 85°C. All first strand cDNA was stored at -80°C until use.

Three μl first strand cDNA were topped up to 17ul PCR reaction mix containing 10μl of Taqman® Universal PCR Master Mix, No AmpErase UNG and

1μl of 20X miRNA Taqman probe (Applied Biosystems). The reaction was performed in 96-well optical tray with thermal cycles as follows: 95°C for 10 min, followed by 50 cycles of 95°C for 15 sec and 60°C for 1 min. The emission intensity was detected by the ICYCLER IQ real time detection system using fluorophore FAM490 (Bio-Rad Laboratories). Threshold cycles were averaged from triplicate experiments. No-template reaction was included as negative control. All miRNA expressions were normalized with internal reference gene, *U6* snRNA. The list of inventoried TaqMan miRNA assays in various chapters was shown in Table 2.2.

Table 2.2 TaqMan assays or primers designed for gene/miRNA expression by qRT-PCR

Chapter 3	Genes	Primer Sequence (5' → 3')
	PFTK1	CTTGACATGTGGGGAGTAGGTT (forward)
		CCATGTGTCCTCATTTGGTG (reverse)
	GAPDH	ATGGGTGTGAACCATGAGAAG (forward)
	(Internal control)	AGTTGTCATGGATGACCTTGG (reverse)
Chapter 4		
	Caldesmon	TCACCTGCTCCCAAACCTTCT (forward)
		GAGGTTCCGCTTGCTGGAT (reverse)
	GAPDH	ATGGGTGTGAACCATGAGAAG (forward)
	(Internal control)	AGTTGTCATGGATGACCTTGG (reverse)
Chapter 5	**miRNAs**	**TaqMan® MicroRNA Assays**
	hsa-miR-183	002269 (Accession #: MIMAT0000261)
	hsa-miR-96	000186 (Accession #: MIMAT0000095)
	hsa-miR-182	002334 (Accession #: MIMAT0000259)
	U6 snRNA	001973 (Accession #: NR_004394)
	(Internal control)	

2.6 2D-PAGE comparative proteomics, image acquisition and data analysis

In Chapter 3, phosphoproteins from *PFTK1*-knockdown Hep3B cells and Mock control were enriched by PhosphoProtein Purification Kit (Qiagen, Hilden, Germany). In the first dimension isoelectric focusing, 12.5 μg enriched phosphoproteins were first mixed with rehydration buffer (Bio-Rad Laboratories), and immobilized on a nonlinear gradient IPG strip of pH 3-10 (Bio-Rad Laboratories) for 16 hr covered by mineral oil (Bio-Rad Laboratories). The program for isoelectrofocusing is shown in Table 2.3. Rinsed by milli-Q water, the strip was subsequent to the second dimension in 10% SDS-PAGE gel (Bio-Rad Laboratories) at a constant voltage of 135V for approximately 135 min. Fixed in 40% methanol and 10% acetic acid for at least 30 min, the gels were then stained with Colloidal Blue solution (Invitrogen) for at least 2 hr or overnight. Gels were later silver stained by PlusOne (GE Healthcare, Piscataway, NJ, USA). The stained gels scanned on calibrated densitometer GS-800 were quantified and analyzed by the PDQuest 2-D Analysis software ver7.1.1 (Bio-Rad Laboratories). The quantification of individual spots was normalized against the total valid spots of each image. Spots that showed >2-fold down-regulation following *PFTK1* knockdown were considered differentially expressed, and further processed for protein identification. The workflow of 2D-PAGE comparative proteomics is illustrated in Figure 2-1.

Table 2.3 Program set-up for isoelectrofocusing

Steps	Voltage (V)	Time (min)	Rapid/Linear
1	100	30	Rapid
2	200	60	Rapid
3	500	60	Rapid
4	1000	60	Rapid
5	8000	30	Linear
6	8000	150	Rapid
7	100	180	---

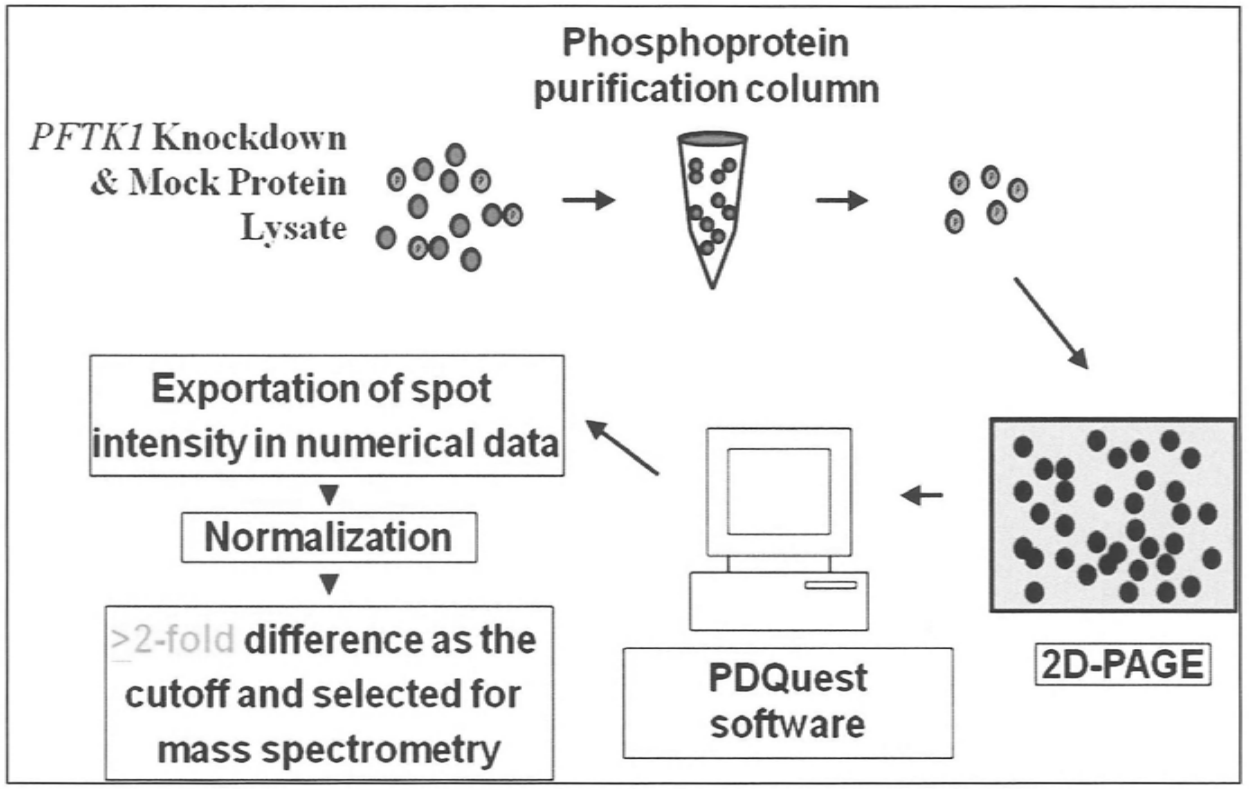

Figure 2-1 Identification of *PFTK1* phosphorylated targets by 2D-PAGE proteomics.
Phosphoproteins from *PFTK1*-knockdown Hep3B cells and Mock control were subsequent to 2D-PAGE analysis. Analyzed by PDQuest software, spots showing ≥2-fold difference were selected for mass spectrometry.

2.7 Protein identification by mass spectrometry peptide fingerprinting

In Chapter 3, all the differential protein spots were excised from the stained gels using punch and in-gel trypsin digestion according to gel image analysis. The gel pieces were destained, reduced with 1.75% DTT, alkylated with 350mM iodoacetamide, and digested with modified porcine trypsin overnight (Promega). Following trypsin digestion (12.5ng/ml), the peptides were harvested, cleaned up with C18 ZipTips (Millipore Corp., Billerica, MA), and subjected to mass spectrometric analysis (ABI 4800 MALDI-TOF/TOF Analyzer, Applied Biosystems) with CHCA (Sigma) as the matrix.

The acquired masses of tryptic peptide digests were submitted to Mascot search engine (http://www.matrix-science.com) to obtain the protein identities by PMF and the MS/MS ion search approach. The search parameters were adjusted and selected as follows: partial oxidation of methionine, phosphorylation of serine/threonine/tyrosine, and iodoacetamide modification of cysteine residues. The mass tolerance level of the parent peptides and the MS/MS ion masses were 100 ppm and 0.1 Da, respectively. The protein identity of each gel spot was considered as valid while the result of both PMF and MS/MS ion search represented the identical protein as the statistically significant hit ($P<0.05$) from the SwissProt database (http://us.expasy.org/sprot), and MS/MS ion search identified the sequences of two or more tryptic peptides identical to the same protein as the statistically significant hits achieved.

2.8 Expression microarray analysis

In Chapter 3, RNA extracted from si*PFTK1*-transfected Hep3B cells and Mock control was subjected to expression microarray analysis. The knockdown efficiency of *PFTK1* was confirmed by qRT-PCR analysis. The microarray experiment was conducted on the Codelink UniSet Human 20K I Bioarray. Each array chip contains 19,881 30-mer oligos, where each probe targets on a single human gene transcript. All arrays were scanned and quantified with the GenePix 4000B scanner, and normalized with the Codelink Expression Analysis software v.4. Differential expression was considered when gene expression showed $\geq$2-fold up-regulation or down-regulation. A pool of the differentially expressed genes was therefore subsequent to functional annotation analysis using DAVID (http://david.abcc.ncifcrf.gov). Molecular pathways were identified based on the information obtained from KEGG pathway database. The schematic workflow was represented in Figure 2-2.

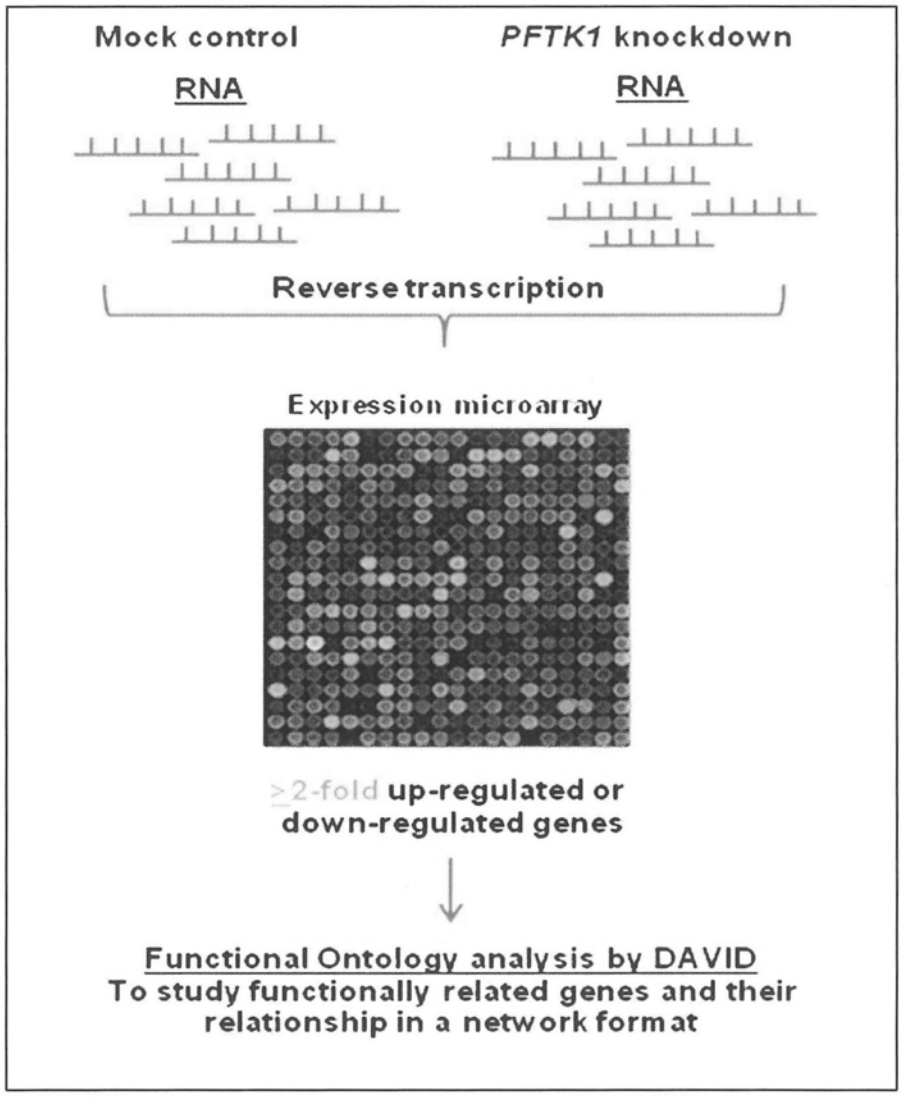

Figure 2-2 Expression microarray analysis.

RNA extracted from *PFTK1*-suppressed Hep3B cells was reversely transcribed and subject to microarray analysis. Differentially expressed gene was analyzed by functional ontology.

2.9 Flag-labeled TAGLN2 *expression vector and mutant constructs*

Full length cDNA clone encoding the human wild-type *TAGLN2* (KIAA0120) was amplified using primers 5'-AGGGTCGACGAGGATCTGGCG TGGCATCC-3' (sense) and 5'-AGAATTCAATGGCCAACAGGGGACCTGC-3' (antisense) by *Pfu* DNA polymerase (Stratagene). The *TAGLN2* cDNA and *pflag-CMV2* plasmid was digested with enzymes specific to *Eco*RI and *Sal*I sites (New England Biolabs, Ipswich, MA) at 37°C overnight. The digested DNAs were then purified using QIAquick PCR Purification Kit (Qiagen), and subsequently subcloned into *pflag-CMV2* with T4 DNA ligase (Invitrogen) at 16°C overnight. The ligated products were introduced into TOP10 chemically competent cells (Invitrogen) by heat shock transformation at 42°C for 30 sec. The transformed cells were recovered in S.O.C. medium (Invitrogen) at 37°C for 1 hr, and plated on ampicillin (100μg/ml)-containing LB-agar plates for colony selection. Eight colonies were inoculated into 2ml LB broth containing 100μg/ml ampicillin for 16 hr. Plasmids were then extracted using QIAGEN® Plasmid Mini Kit (Qiagen) and verified by DNA sequencing.

Phospho-defective (S11A, S83A, S94A, S145A, S155A, S163A and S185A) and phospho-mimetic (S83D and S163D) *TAGLN2* mutants were constructed by *in-vitro* site-directed mutagenesis (QuikChange site-directed mutagenesis kit; Strategene) using the wild-type *flag-TAGLN2* as template according to the manufacturer's instructions. In brief, primers containing the desired mutations were designed in length between 25 and 45 bases with melting temperature greater than or equal to 78°C. The mutations were placed in the middle of the primers with 10 to 15 bases on both sides with a total minimum GC content of 40%. One or more G or C

bases were desired to locate at terminations on both sides. Primers employed for cloning were listed in Table 2.4. A total volume of 25μl reaction mixture containing 2.5μl 10X reaction buffer, 50ng DNA template, 3.75μl of 2.5mM dNTP and 0.75μl of 10μM primers was prepared. The cycling parameters were outlined as: 95°C for 2 min, followed by 25 cycles of 95°C for 30 sec, 55°C for 1 min and 68°C for 6 min. The nonmutated parental DNA was subsequently digested with *Dpn*I at 37°C for 1 hr, followed by heat shock transformation. The authenticity of all constructs was confirmed by DNA sequencing. Approximately 1/4 to 1/8 colonies possessed the desired point-mutated sites for identifying *PFTK1*-phosphorylated serine residues in Chapter 3.

Table 2.4 Primers for *TAGLN2* cloning expression plasmids

Primer	Sequence (5'-3')
TAGLN2-wt-F	AGGGTCGACGAGGATCTGGCGTGGCATCC
TAGLN2-wt-R	AGAATTCAATGGCCAACAGGGGACCTGC
TAGLN2-S11A-F	GCATATGGCCTGGACCGGGAGGTGCAGC
TAGLN2-S11A-R	GCTGCACCTCCCGGTCCAGGCCATATGC
TAGLN2-S83A-F	AGAAGATCCAGGCCGCCACCATGGCCTTC
TAGLN2-S83A-R	GAAGGCCATGGTGGCGGCCTGGATCTTCT
TAGLN2-S94A-F	GCAGATGGAGCAGATCGATCAGTTCCTGCAAGC
TAGLN2-S94A-R	GCTTGCAGGAACTGATCGATCTGCTCCATCTGC
TAGLN2-S145A-F	GATGGGCTCTTCGATGGGGATCCCAAC
TAGLN2-S145A-R	GTTGGGATCCCCATCGAAGAGCCCATC
TAGLN2-S155A-F	GGTTCCCTAAGAAAGACAAGGAGAATCCTCGG
TAGLN2-S155A-R	CCGAGGATTCTCCTTGTCTTTCTTAGGGAACC
TAGLN2-S163A-F	CCTCGGAACTTCGACGATAACCAGCTGC
TAGLN2-S163A-R	GCAGCTGGTTATCGTCGAAGTTCCGAGG
TAGLN2-S185A-F	ACCGCGGGGCGGCTCAGGCAGGC
TAGLN2-S185A-R	GCCTGCCTGAGCCGCCCCGCGGT
TAGLN2-S83D-F	GAAGATCCAGGCCGACACCATGGCCTTC
TAGLN2-S83D-R	GAAGGCCATGGTGTCGGCCTGGATCTTC
TAGLN2-S163D-F	AGGAGAATCCTCGGAACTTCGATGATAACCAGCTGCAAGAGGG
TAGLN2-S163D-R	CCCTCTTGCAGCTGGTTATCATCGAAGTTCCGAGGATTCTCCT

2.10 DNA sequencing

The DNA sequencing was performed using the BigDye Terminator Cycle Sequencing Kit (Applied Biosystems). In 15µl of sequencing reaction, 2µl of plasmid was mixed with 3.22µM primer, 2.25µl Sequencing buffer and 1.5µl Big Dye. The thermal cycling conditions were as follows: 45 cycles of 1 min at 96°C, annealing at 50°C for 5 sec and extension at 60°C for 4 min. To remove unincorporated nucleotides, the PCR products were purified with Sephadex™ G-50 (GE Healthcare) fine column. Another 10µl of Hi-Di™ formamide (Applied Biosystems) was added to equal volume of purified product followed by denaturation at 95°C for 5 min. The denatured DNA was incubated on ice for 5 min prior to the sequencing reaction using ABI PRISM® 3100XL Genetic Analyzer (Applied Biosystems). The sequence information was obtained and analyzed by ABI PRISM® 3100 Genetic Analyzer Data Collection Software v1.1 and DNA sequencing analysis software v3.7 (Applied Biosystems). The NCBI Basic Local Alignment Search was utilized for sequence alignment.

2.11 Functional investigations

2.11.1 Transfection of HCC cell lines

Transfection efficiencies of cell lines were evaluated by the FITC-labeled double stranded RNA (Invitrogen) or GFP expression vector (*pEGFP-C2*) (Becton Dickinson, Franklin Lakes, NJ) tranfections. FITC or GFP signal from transfected cells were examined under fluorescence microscope at 24 hr post-transfection by Lipofectamine^{TM} 2000 (Invitrogen). The transfected cells were fixed in 70% ethanol and re-suspended in 1X PBS. The FITC or GFP fluorescence signals, which are reflective of cell transfecting efficiency, were measured by flow cytometry. Altogether 3 HCC cell lines (Hep3B, HKCI-4 and HKCI-1) and one immortalized hepatocyte L02 were transiently transfected with siRNAs or expression vector in Chapters 3~5.

In Chapter 3, two HCC cell lines, Hep3B and HKCI-4, and one immortalized hepatocyte cell line L02 were employed for characterization of *PFTK1* in the role of HCC. Compared with normal liver controls, both Hep3B and HKCI-4 exhibit up-regulation of *PFTK1*, whereas L02 elicits negligible *PFTK1* expression. L02 was transiently transfected with expression construct of GFP-fused *PFTK1* protein as previously described (Pang *et al.,* 2007). Transfection efficiency of GFP–tagged *PFTK1* protein was confirmed by Western blotting. The expression of *PFTK1* in Hep3B was stably suppressed by vector-based shRNA as described in section 2.4. In HKCI-4 cells, *PFTK1* expression was transiently suppressed using siRNA obtained from Dharmacon (Chicago, IL, USA). In rescue experiment, siRNA duplexes targeting *TAGLN2* were acquired from Dharmacon and transfected into *PFTK1*-abrogated cells. For immunoprecipitation assay, the three cell lines were

also ectopically expressed with *pflag-TAGLN2*. The protein expression of TAGLN2 was monitored by Western blot analysis to ensure efficient transfection. The above indicated *PFTK1*-suppressed Hep3B stable cells were also employed for the study of caldesmon phosphorylations in Chapter 4.

In Chapter 5, two HCC cell lines, Hep3B and HKCI-1, were recruited for the study of miR-183/96/182 cluster in the control of liver carcinogenesis. In short, both Hep3B and HKCI-1 cells, which showed concordant up-regulation of the three miRNAs, were transiently suppressed by RNA interference obtained from Dharmacon. The expressions of miR-183, -96 and -182 were monitored by qRT-PCR analysis to ensure efficient knockdown.

2.11.2 Cell viability assay

Cells were assessed every 24 hours for cell viability on at least 7 consecutive days by MTT solution (Sigma). The MTT assay is colorimetric assay for measuring the activity of enzymes (mitochondrial reductase) that reduce MTT to formazan dyes, giving a purple color (Figure 2-3). In short, cells with appropriate number (Table 2.5) were seeded in 96-well culture plate in quintuplicate. By the time of measurement, MTT at a concentration of 500μg/ml was added and incubated at 37°C for 2 hr. The synthesized purple crystals were then dissolved in 100 μl Dimethyl sulfoxide (DMSO) (Sigma). Measurements were made at 570nm relative to the basal absorbance 630nm using Victor$_3$™ multilabel counter (Perkin Elmer, Waltham, MA, USA). Two independent experiments were performed, and each measurement was expressed as a percentage of maximum absorbance.

2.11.3 Cell invasion and motility assays

The invasive capability of cells was determined using Matrigel invasion chamber (8-μm pores) (BD Biosciences, Sparks, MD, USA); cell migrating ability was measured by the Costar Transwell Inserts (8-μm pores) (Corning Incorporated, Cambridge, MA, USA).

The invasion and migration chambers were first incubated with pain DMEM or AIM-V medium at 37°C for 2 hr. Cells with appropriate number (Table 2.5) were seeded on the top chamber of each insert with complete medium added to the bottom chamber. By the time of measurement, the non-migrated and non-invaded cells on the membrane were wiped off with a cotton swab. Cells on the underside were fixed by absolute methanol for 5 min, followed by staining with hematoxylin (Sigma) for 30min. Subsequently, the inserts were rinsed with ddH2O, immersed in 80% ethanol twice for 2 min and 100% ethanol twice for 2 min. After the dehydration process overnight, the dried inserts were mounted on glass slide.

Cells on the underside of the membrane were counted from at least 10 microscopic fields (original magnification, X400). The mean number of invading or migrating cells was expressed as a percentage relative to control. Each experiment was performed in replicate inserts and the mean value expressed from three independent experiments.

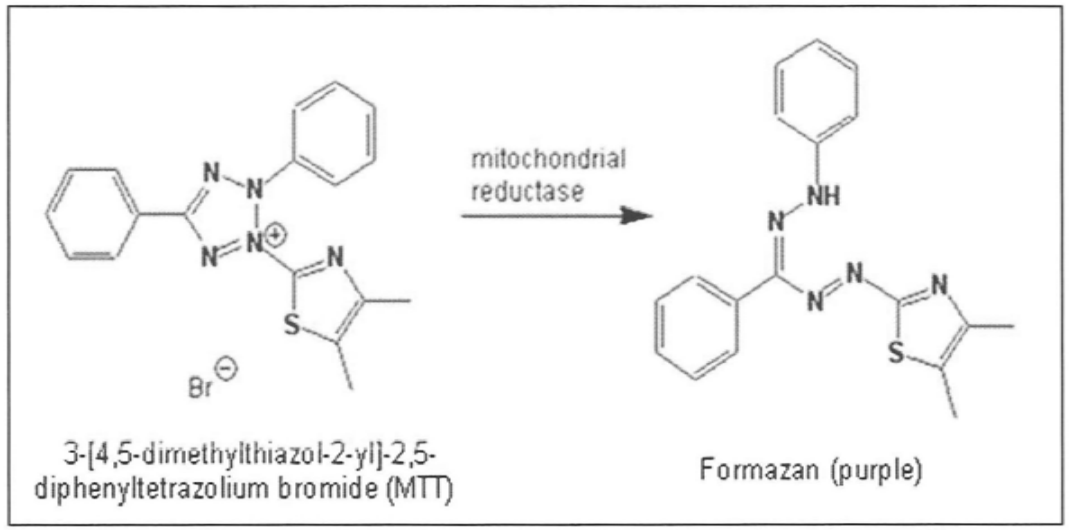

Figure 2-3 Cell viability assay.
MTT is reduced by mitochondrial reductase to form purple crystals (formazan).

Table 2.5 Cell number for functional investigations

Cells	MTT assay	Migration (time)	Invasion (time)
Chapter 3			
Hep3B	2×10^3	1×10^4 (24 hr)	5×10^4 (48 hr)
HKCI-4	2×10^3	1×10^4 (24 hr)	2×10^4 (24 hr)
Chapter 5			
Hep3B	2×10^3	1×10^4 (24 hr)	5×10^4 (48 hr)
HKCI-1	2×10^3	1×10^4 (24 hr)	3×10^4 (24 hr)

2.12 Immunofluorescence analysis

Cells were seeded at a density of 2 x 10^4 onto a sterilized coverslip (22 x 22mm) (MENZEL-GLÄSER, Braunschweig, Germany) located into a 6-well culture plate overnight. Rinsed with PBS for three times, the coverslips with cells were fixed with 4% paraformaldehyde (Sigma) for 15 min. The cells were then washed by PBS twice for 5 min, and permeabilized by 0.1% Triton X-100 (Sigma) for 5 min. The cells were gently washed with PBS twice for 5 min. The cells can be stored at 4°C for weeks or subsequent to further investigations.

Non-specific binding on the coverslips was blocked by 5% BSA (Sigma) or 5% goat serum (Invitrogen) for 1 hr. Cells were stained with TRITC-labeled phalloidin (Sigma) for filamentous actins or antibodies as indicated. The conditions of primary antibodies staining for Chapters 3 and 4 were summarized in Table 2.6. The indicated primary antibodies were added to the cells for 4 hr at room temperature. After PBS washing, secondary antibodies Alexa Fluor 488 and 594 (Invitrogen) were incubated in cells for 2 hr. Counterstained with DAPI (Sigma) in anti-fade solution (Vector Laboratories, Burlingame, CA), cells were examined by LSM5 PASCAL confocal microscopy (Carl Zeiss, Gottingen, Germany).

Table 2.6 Conditions of primary antibodies for confocal microscopy

Targets	Primary antibodies dilution	Secondary antibodies dilution	Company
Chapter 3			
β -tubulin	1:200	1:250	Invitrogen
FLAG	1:100	1:250	Invitrogen
Vimentin	1:250	1:250	Santa Cruz Biotechnology
TRITC-labeled Phalloidin	1:100000	---	Sigma
Chapter 4			
Caldesmon	1:200	1:250	Neomarkers, Thermo Fisher Scientific
TRITC-labeled Phalloidin	1:100000	---	Sigma

2.13 Western blotting

The cells (60 to 80% confluence) were washed with PBS and harvested with cell scrapper in RIPA lysis buffer supplemented with protease inhibitors including 1mM PMSF (GE Healthcare), 1X protease inhibitor cocktail (Sigma) and 1X to 5X PhosStop (Roche Diagnostics, Indianapolis, IN, USA) on the top of ice pack. The cell lysate was immediately incubated on ice for 15 min and centrifuged at 12,000rpm at 4°C for 10 min. The protein concentrations of cell supernatants were quantitated by the Bradford assays (Bio-Rad Laboratories) at an absorbance of 595nm.

Depending on the protein abundance, an amount of 10-20μg protein lysate was accordingly mixed with Laemmli sample buffer and heated at 95°C for 5 min. Based on the molecular sizes, proteins were resolved by 8-15% of sodium dodecyl sulfate polyacrylamide gel electrophoresis accordingly. All the blotting paper and nitrocellulose membranes (GE Healthcare) were pre-wetted in transfer buffer. The proteins on the gel were then transferred onto nitrocellulose membrane. Prior to the addition of primary antibody, non-specific bindings were minimized by 5% skimmed milk or BSA at room temperature for 1 hr. The blot was then incubated with primary antibody against target proteins at 4°C overnight with gentle shaking. After washing the blot with TBST three times for 10 min, corresponding secondary antibodies conjugated to horseradish peroxidase were incubated for 1 hr at room temperature. The blots were washed three times for 10 min by TBST, and finally visualized by an enhanced chemiluminescence detection kits (GE Healthcare). The protein levels of GAPDH were utilized as a loading control in each experiment. The ratios of antibody dilutions in Chapters 3~5 were highlighted in Table 2.7.

Table 2.7 Conditions of primary antibodies for Western blotting

Targets	Primary antibodies dilution	Secondary antibodies dilution	Company
Chapter 3			
β-actin	1:10000	1:5000	Sigma
β-tubulin	1:1000	1:5000	Invitrogen
FLAG	1:1000	1:5000	Sigma
Transgelin2	1:200	1:2000	Santa Cruz Biotechnology
Vimentin	1:250	1:2000	Santa Cruz Biotechnology
Phosphoserine	1:500	1:2000	Chemicon, Millipore Corporation
Phosphothreonine	1:1000	1:5000	Sigma
Phosphotyrosine	1:1000	1:2000	Invitrogen
Chapter 4			
Caldesmon	1:1000	1:5000	Neomarkers, Thermo Fisher Scientific
Chapter 5			
β-catenin (active)	1:1000	1:5000	Upstate, Millipore Corporation
β-catenin (total)	1:1000	1:5000	Becton Dickinson
Forkhead Box1	1:500	1:2000	Cell Signaling Technology, Inc.
Loading Control			
GAPDH	1:20000	1:5000	Chemicon, Millipore Corporation

2.14 Immunoprecipitation

Quantitated protein lysates were first incubated with 30μl of rec-Protein G-Sepharose (Invitrogen) for 3-4 hr at 4°C to eliminate non-specific protein bindings. The cleared lysate supernatants were incubated with 2μg specified antibody for 2 hr at 4°C with agitation. The immune complexes were precipitated by 50μl rec-Protein G-Sepharose beads at 4°C overnight with agitation. The beads were then washed with PBS three times for 5 min. Centrifuged at 1,2000 rpm for 2 min, the supernatants containing unincorporated proteins were removed completely. With the addition of 50μl of 2X Laemmli sample buffer, the target proteins were eluted following heating at 95°C for 5 min. Reactions without protein loading acted as negative control. Resolved on SDS-PAGE, the immune complexes were analyzed by Western blot. The technique of Western blot was performed as described in section 2.12. The experimental outlines of immunoprecipitation for Chapters 3 and 4 were highlighted in Figure 2-4.

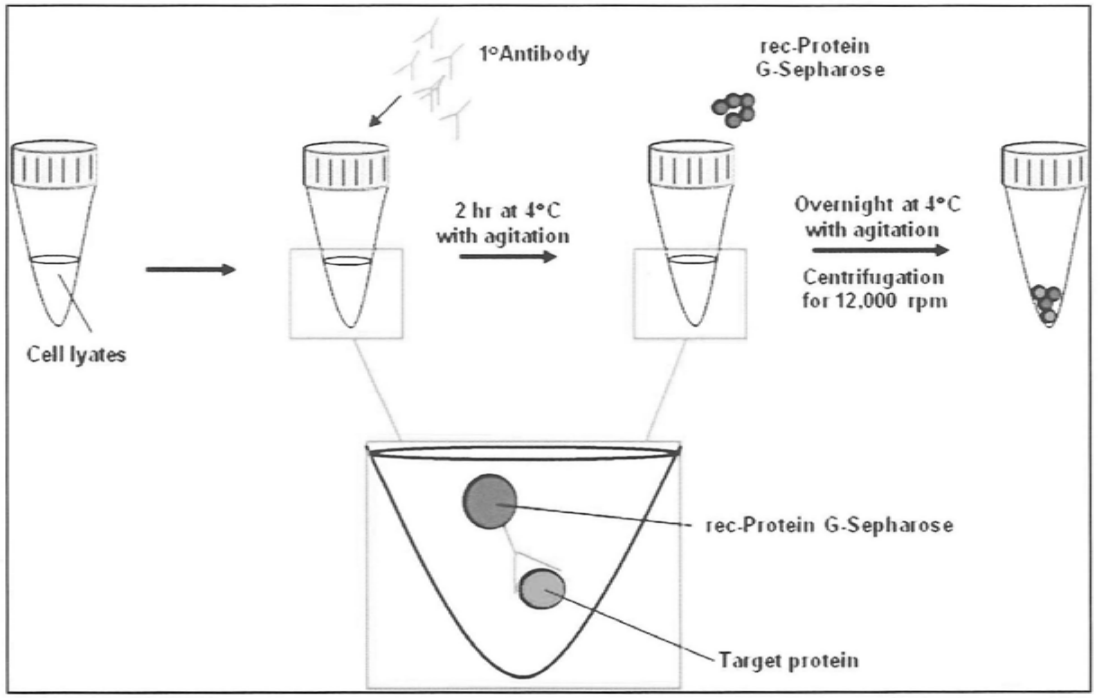

Figure 2-4 Immunoprecipitation assay.
Immunoprecipitated proteins were subsequent to Western blot analysis.

2.15 Luciferase reporter assay

In Chapter 5, the putative binding sites of miR-183, -96 and -182 on FOXO1 3'UTR were cloned downstream of CMV promoter-driven firefly luciferase cassette in a pMIR-REPORT vector. The mutant construct was generated by deletion of the complementary seed sequence to miR-183, -96 and -182 binding regions. The sequences of the wild-type (WT) and mutant (MUT) contructs were illustrated in Table 2.8. Firefly and Renilla luciferase signals were determined by Dual-Luciferase Assay Kit. Each experiment was performed in triplicate, and the average value was calculated from four independent experiments.

Table 2.8 Oligonucleotide sequences for cloning expression plasmids containing *FOXO1* 3' UTR

	Sequence (5'-3')
FOXO1 3'UTR-WT-sense	CTAGCAGGTTATGTGCTGCTGTAGATAAGGACTGTGCCATTGGAAATTTCATTACAA TGAAGTGCCAAACTCAC
FOXO1 3'UTR-WT-antisense	AGCTGTGAGTTTGGCACTTCATTGTAATGAAATTTCCAATGGCACAGTCCTTATCTA CAGCAGCACATAACCTG
FOXO1 3'UTR-MUT-sense	CTAGCAGGTTATGTGCTGCTGTAGATAAGGACTTGGAAATTTCATTACAATGAAGA CTCAC
FOXO1 3'UTR-MUT-antisense	AGCTGTGAGTCTTCATTGTAATGAAATTTCCAAGTCCTTATCTACAGCAGCACATAA CCTG

2.16 Statistical analysis

In Chapter 3, the Student *t*-test was employed to examine the immunohistochemical scorings on *PFTK1* protein from tissue microarray, mRNA expression of *PFTK1* in stable clones and the functional effects of *TAGLN2* knockdown in *PFTK1*-suppressed Hep3B and HKCI-4 cells. The test was also applied in the functional analyses of phospho-defective and phospho-mimetic mutants on Hep3B cells. Correlative analysis of *PFTK1* scores with clinicopathological features of HCC tumors was examined by Spearman's ρ test.

In Chapter 4, the Student *t*-test was used to assess the caldesmon gene expressions in human HCC as compared with adjacent non-tumoral lesions.

In Chapter 5, the Student *t*-test was applied in the correlative analysis of miR-183/96/182 expression with clinicopathological features of HCC tumors, the comparison of their expression between HCC cell lines and normal liver samples, their functional effects on HCC cells, the effects of CTNNB1 knockdown on miR-183/96/182 expressions and luciferase reporter assays. The chi-square test was used for comparison of patients' characteristics and miR-183/96/182 by vital status. The patient age by vital status was compared using t-test. The t-test was also employed in comparing the expressions of miR-183, -96 and -182 between HCC primary cases and their adjacent non-tumoral liver. Relative risks (RRs) of death in relation to miR-183/96/182 expression and other predictor variables were computed from univariate Cox proportional hazards model. Subsequent multivariate Cox regression models were constructed to estimate the RRs for miR-183/96/182 expression. Disease-free associated with the expression were evaluated by the Kaplan-Meier survival curve and the log-rank test.

A difference was considered significant when $P \leq 0.05$. All statistical analysis was performed using SPSS for Windows 10.0 and Graphpad Prism 3.0.

Chapter 3

Characterization of *PFTK1* kinase in the role of liver cancer cell motility

3.1 Introduction

Recent progress by genome-wide analysis on molecular biology has allowed the identification of causal genetic changes that underline the mechanistic basis of HCC development and progression (Katoh *et al.*, 2007; Herath *et al.*, 2006). Previously, our group has reported on the significance of frequent chr.7q21-22 amplicons in close association with HCC progression to advance tumors with metastatic properties (Poon *et al.*, 2006). Recurrent proximal gains on chr.7q are in fact common in a number of human cancers (Knuutila *et al.*, 1998), where it has been implicated in apparent metastatic properties of colorectal carcinoma (Nakao *et al.*, 2001), angiogenic potential in prostate cancers (Strohmeyer *et al.*, 2004) and subordinate survival of patients being diagnosed with sporadic Burkitt's lymphoma (García *et al.*, 2003). In HCC, *PFTK1* was previously highlighted as proto-oncogene within the chr.7q21-22 amplicon, where increased *PFTK1* expression was significantly correlated with advanced HCC development (Pang *et al.*, 2007). Our earlier investigations by ectopic expression and gene knockdown experiments confirmed an important role for *PFTK1* in the cellular invasiveness and motility of HCC cells. Nevertheless, little has been ascribed regarding the underlying basis of *PFTK1* in conferring HCC cell migratory properties.

PFTK1 protein, encoded by human *PFTAIRE* protein kinase 1 gene, has a sequence homology to the Cdc2 kinase in 53% identity of the catalytic motif. The pivotal domain of *PFTAIRE1* possesses all functional signatures that are highly conserved with the Cdc2 superfamily, including the serine/threonine kinase domains. The human *PFTK1* transcript with 6kb in length is commonly observed in brain, pancreas, kidney, heart, testis and ovary but negligibly found in other tissues such as

placenta, lung and liver (Yang and Chen, 2001). Since *PFTK1* is a novel Cdc2 family member, limited studies have been conducted to define its functional physiology or biological significance. Our earlier studies identified a role for *PFTK1* as a key regulatory contributor in HCC cell dissmination (Pang *et al.*, 2007). Although it has been well reported that Cdc2 family plays essential roles in cell cycle transition and cell proliferation in eukaryotic cells (Solomon, 1993; Kirschner, 1992; Pines, 1992) and would thereby be expected to have minimal effect on cell migratory phenotypes, concordant with our findings a previous report revealed that Cdc2 up-regulation could manifest cell invasiveness through partnering with cyclin B2 and caldesmon in enhancing actin contractile force (Manes *et al.*, 2003). The idea of cell cycle regulator being entailed in cell migration was substantiated by another study that cyclin D1 played a part in cell motility (Neumeister *et al.*, 2003).

In this chapter, the prognostic value of *PFTK1* as tumor biomarker in HCC by tissue microarray array analysis was examined, and in parallel attempts have been carried out to characterize the phosphorylation targets of *PFTK1*, specifically in promoting HCC cell motility. Coupling 2D-PAGE comparative proteomics with mass spectrometric protein identification, information on differentially expressed phosphoproteins in *PFTK1*-expressing cells was acquired. Subsequent investigations provide compelling evidence to support transgelin2 (TAGLN2*)*, a tumor suppressor gene, is a functional target of *PFTK1*. This study also highlights a novel oncogene-tumor suppressor interplay, where oncogenic *PFTK1* confers HCC cell motile properties through inhibiting the actin-binding ability of TAGLN2 by serine-phosphorylation. As concurrent extra- and intra-hepatic metastases are the major cause of morbidity and mortality in HCC patients, expanding knowledge on the biological basis of HCC cell motility holds much promise in gaining novel

informations into the process of tumor cell dissemination and predicting metastasis.

3.2 Results

3.2.1 Tissue microarray analysis on PFTK1 *expressions in HCC primary tumors*

To establish prognostic value of *PFTK1* in HCC, *PFTK1* protein was examined for its expression in a cohort of 180 primary HCC tumors and matched adjacent non-malignant liver. Immunohistochemical staining of *PFTK1* protein demonstrated various degrees of signal intensities that were categorized into low, moderate and high expressions. Representative images of *PFTK1* protein staining are illustrated in Figure 3-1A. Among the HCC cases studied, 73.9% of HCC tumors (133 of 180) revealed significant *PFTK1* up-regulations compared with their paired non-tumoral liver ($P<0.0001$; Figure 3-1B). Besides, correlative analysis on clinicopathologic features of HCC indicated enhanced *PFTK1* expressions in association with early age onset (≤40yr; $P=0.021$), advance tumor progression to poorly differentiated stage ($P<0.0001$) as well as the histologic presence of microvascular invasion ($P=0.05$; Table 3.1).

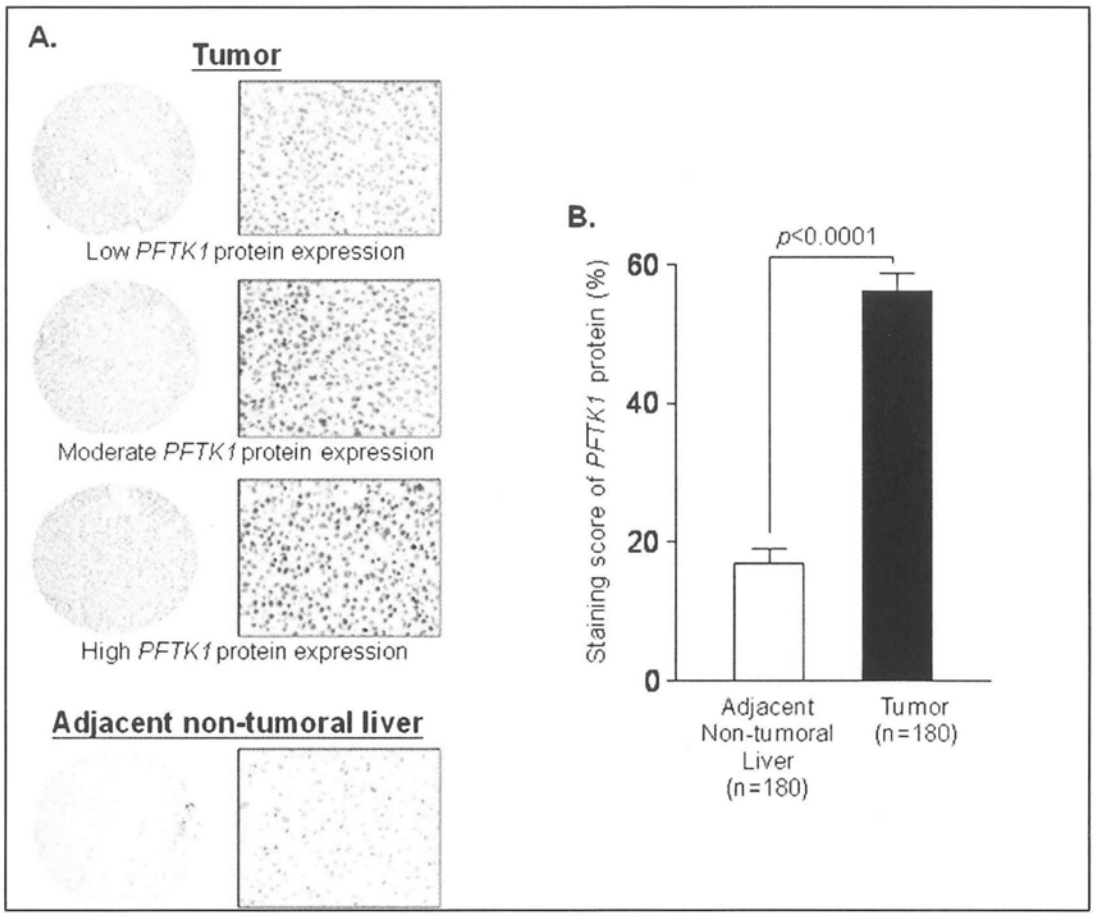

Figure 3-1 Tissue microarray analysis of *PFTK1* expression in human HCC and paired adjacent non-tumorous liver.

(A) Immunohistochemical staining of *PFTK1* protein at original magnification of X100 (*left panel*) and X400 (*right panel*). Representative images of *PFTK1* expressions in HCC tissues ranging from low, moderate to high staining intensities were illustrated. Negative staining is often observed in adjacent non-tumoral liver.

(B) TMA demonstrated increased *PFTK1* expression in HCC tumors is common as compared with the matched non-malignant counterpart ($P<0.0001$).

Table 3.1 Tissue microarray analysis of *PFTK1* expression in primary HCC cohort

	Immunohistochemical Scoring of PFTK1 Expression			
	Low	***Moderate***	***High***	**P-*value***
Gender				0.885
Male	30 (20.2%)	23 (15.4%)	96 (64.4%)	
Female	8 (25.8%)	2 (6.5%)	21 (67.7%)	
Age				0.021*
≤40	3 (10.3%)	1 (3.4%)	25 (86.3%)	
>40	35 (23.2%)	24 (15.9%)	92 (60.9%)	
HBsAg[a]				0.867
Positive	25 (18.7%)	19 (14.2%)	90 (67.1%)	
Negative	2 (15.4%)	0 (0.0%)	11 (84.6%)	
Cirrhosis				0.444
Present	25 (19.4%)	19 (14.7%)	85 (65.9%)	
Absent	13 (26.0%)	6 (12.0%)	31 (62.0%)	
Histology Grade				<0.0001***
Well differentiated	21 (51.2%)	8 (19.5%)	12 (29.3%)	
Moderately differentiated	17 (13.8%)	15 (12.2%)	91 (74.0%)	
Poorly differentiated	0 (0.0%)	2 (12.5%)	14 (87.5%)	
Stage[b]				0.139
I	25 (24.3%)	17 (16.5%)	61 (59.2%)	
II	6 (14.3%)	5 (11.9%)	31 (73.8%)	
III	5 (19.2%)	2 (7.7%)	19 (73.1%)	
No. of lesions[a]				0.850
Multiple	9 (25.7%)	2 (5.7%)	24 (68.6%)	
Solitary	27 (19.0%)	23 (16.2%)	92 (64.8%)	
Macrovascular Invasion				0.961
Present	3 (21.4%)	2 (14.3%)	9 (64.3%)	
Absent	35 (21.1%)	23 (13.9%)	108 (65.1%)	
Microvascular Invasion				0.050*
Present	8 (13.6%)	7 (11.9%)	44 (74.5%)	
Absent	30 (24.8%)	18 (14.9%)	73 (60.3%)	

*$P \leq 0.05$, ***$P < 0.0001$; a: Statistical analysis carried out on available data; b: Recurrent cases not included

3.2.2 Characterization of phosphorylated targets of PFTK1 *kinase in HCC*

3.2.2a Comparative 2D-PAGE mass spectrometric analysis for PFTK1*-phosphorylated candidates*

To underline the biological targets of *PFTK1*, 2D-PAGE proteomics was carried out to compare the phosphoproteins in Hep3B cells with or without *PFTK1* suppression. The usage of Hep3B cells was based on the fact that this cell line presents *PFTK1* up-regulation and possesses highly invasive phenotypes (Pang *et al.*, 2007). Nearly 2,000 spots were resolved by 2D-PAGE gel and more than 95% of the total spots resolved could be matched across the 2 gel images. By comparing the phospho-proteomes acquired from *PFTK1* knockdown and mock experiment, spot intensities were prioritized in accordance with their degree of signal differences. In particular, those spots that exhibited mark reduction ($\geq$2-fold) in spot intensities following the knockdown of *PFTK1* were selected. These spots plausibly signified downstream phosphorylated substrates of the *PFTK1* kinase. According to the scoring of signal intensities, five top ranked differential spots were excised from the 2D gel and further subjected to protein identification. Following tryptic digestion, mass spectrometry on the peptides indicated top ranked spots, including β-actin (ACTB), TAGLN2, heat shock protein 70, aldehyde dehydrogenase and 14-3-3 gamma protein accordingly (Figure 3-2).

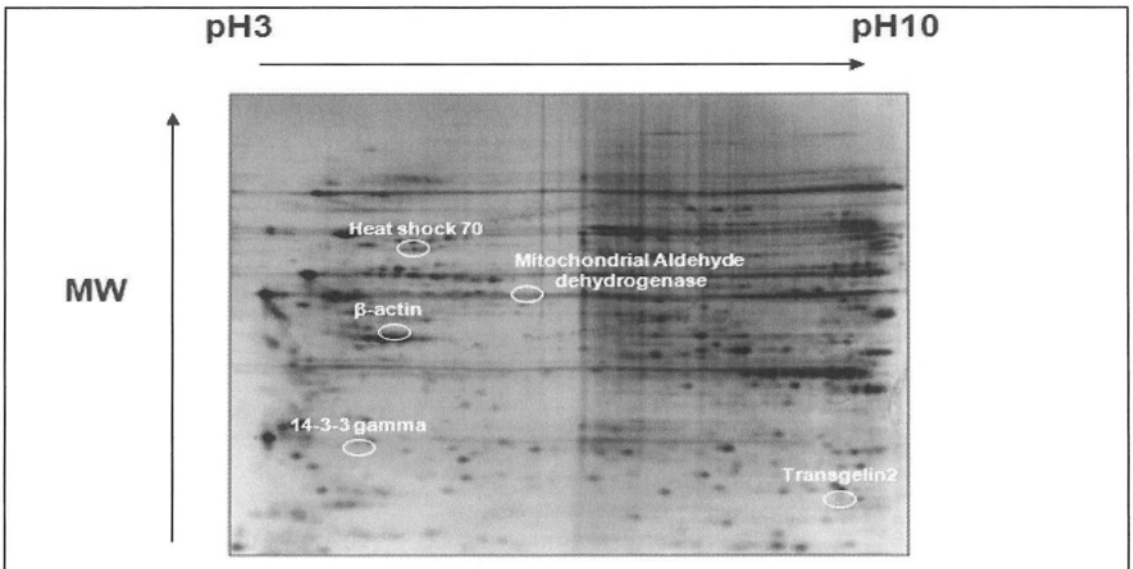

Rank	2D-PAGE Spots: Mock	2D-PAGE Spots: *PFTK1-kd*	Normalized Intensity: Mock	Normalized Intensity: *PFTK1-kd*	Fold change	Protein ID
1	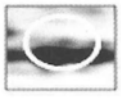		2904.5	869.9	3.34	β-actin (ACTB)
2	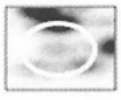		426.8	130.1	3.28	Transgelin2 (TAGLN2)
3			330.9	106.0	3.12	Aldehyde Dehydrogenase (ALDH)
4	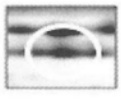	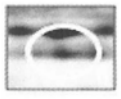	918.5	407.9	2.25	Heat shock protein 70 (HSP70)
5	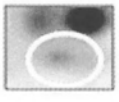	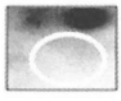	370.1	181.8	2.04	14-3-3 gamma (YWHAG)

Figure 3-2 Comparative 2D-PAGE proteomics analysis for *PFTK1*-phosphorylated proteins.

Enriched phosphoproteins derived from *PFTK1*-knockdown (*PFTK1*-kd) Hep3B and mock experiments were subjected to 2D-PAGE. After resolved by pI range and molecular weight, gel spots were matched across the 2D-PAGE images of *PFTK1*-kd and mock. Spots with reduction in quantities following *PFTK1* suppression are defined as differentially expressed subsequent to Mass Spectrometric protein identification. The spots were ranked according to fold induction. The top five phosphorylated proteins were highlighted.

3.2.2b PFTK1 *governs intracellular cytoskeletal dynamics*

To determine the biological pathway(s) modulated by *PFTK1*, an mRNA expression array was performed on Hep3B cells with or without *PFTK1* knockdown. As shown in Figure 3-3, functional annotation study by DAVID highlighted 5 ontology networks, namely neuroactive ligand-receptor interaction, regulation of actin cytoskeleton, gap junction, adherens junction and cell adhesion molecules. Except the neuroactive ligand-receptor interaction, 4 out of the 5 determined networks are related to cellular movement. This finding significantly underscores the importance of *PFTK1* in governing HCC cell migratory phenotype. Among these four pathways, regulation of actin cytoskeleton rates the largest proportion (23%), implying its significance under the *PFTK1* kinase activity.

As highlighted in both 2D-PAGE mass spectrometric and microarray analyses, ACTB was identified as the highest ranked downstream protein. This observation underpins a potent role for *PFTK1* in the cytoskeletal dynamics. Subsequent Western blot and immunofluorescence analyses on ACTB were performed to examine its involvement in the filamentous actin abundance and organizational changes. Vimentin (VIM) for intermediate filaments and β-tubulin (TUBB) for the microtubules, which are the other two major components of the intracellular cytoskeleton, were also included in these studies. Stably *PFTK1*-suppressed Hep3B cells were employed in the following investigations. Short hairpin (sh)-RNA suppressed sh-*PFTK1*-c1 and sh-*PFTK1*-c2 elicited evident inhibition on cell migration and invasion compared with sh-Mock control, while no apparent effect on cell viability was suggested (Figure 3-4).

Western blot analysis on sh-*PFTK1*-c1 and sh-*PFTK1*-c2 for ACTB, VIM and TUBB did not illustrate any change in ACTB and TUBB expression levels, but

profound diminution on VIM total protein was shown (Figure 3-5A). I further explored the influence of *PFTK1* on the intracellular structure of these cytoskeletal constituents. Immunofluorescence staining also revealed a consistent reduction of VIM in both sh-*PFTK1*-c1 and sh-*PFTK1*-c2 compared to sh-Mock. Interestingly, considerable depolymerization of actin stress fibers was readily observed in *PFTK1*-suppressed cells despite no apparent changes found in the total ACTB protein level (Figure 3-5B). Structural differences on TUBB organization were not indicated. Taken together, the findings suggested that *PFTK1* confers HCC cell motility conceivably through actin polymerization and VIM up-regulation.

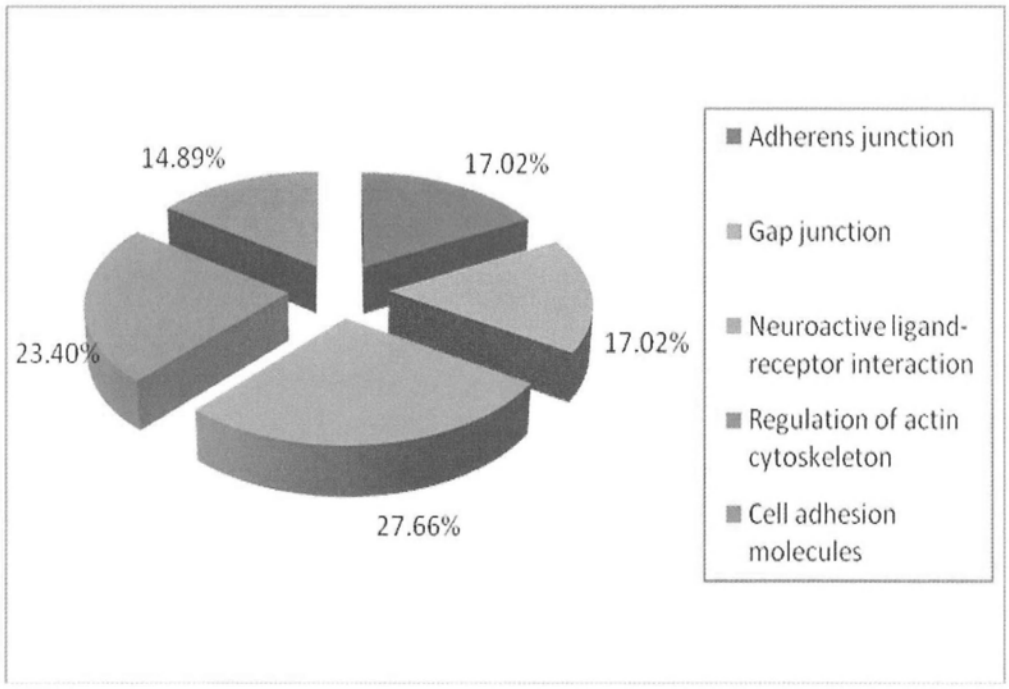

Figure 3-3 Expression array analysis on *PFTK1*-suppressed cells.
Functinal annotation suggested that *PFTK1* was highly associated with regulation of actin cytoskeleton.

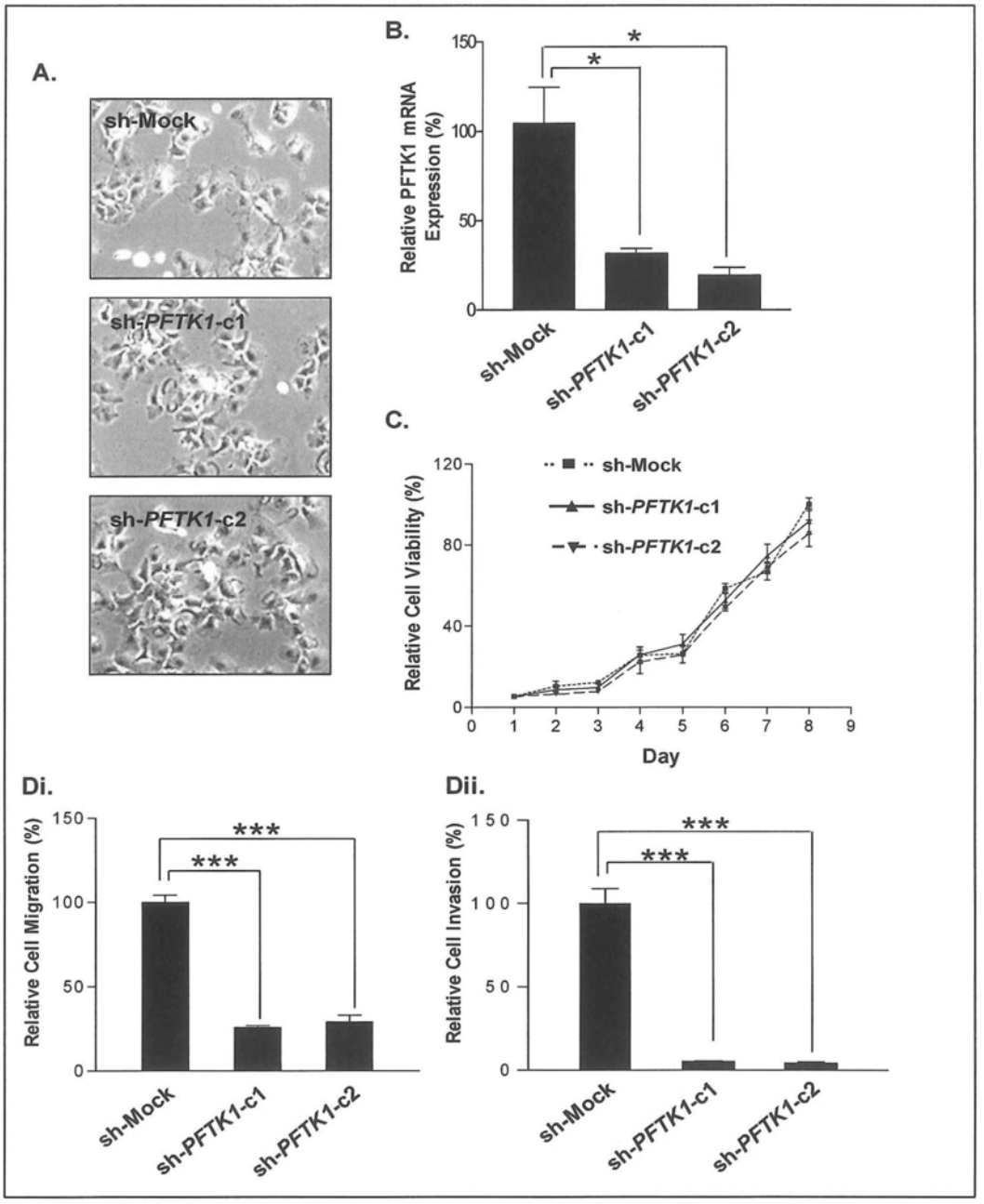

Figure 3-4 Knockdown of *PFTK1* impaired cell migratory and invasive properties of Hep3B cells.

(A) Stably *PFTK1*-suppressed Hep3B cells (sh-*PFTK1*-c1 and sh-*PFTK1*-c2) did not suggest any gross morphological changes as compared with *PFTK1*-expressing control cells (sh-Mock).

(B) Quantitative PCR confirmed a significant *PFTK1* suppression in the knockdown clones (*$P \leq 0.02$).

(C, Di & ii) Both sh-*PFTK1*-c1 and sh-*PFTK1*-c2 showed retarded cell motile and invasive phenotypes (***$P<0.0001$), although an effect on cell viability was not apparent.

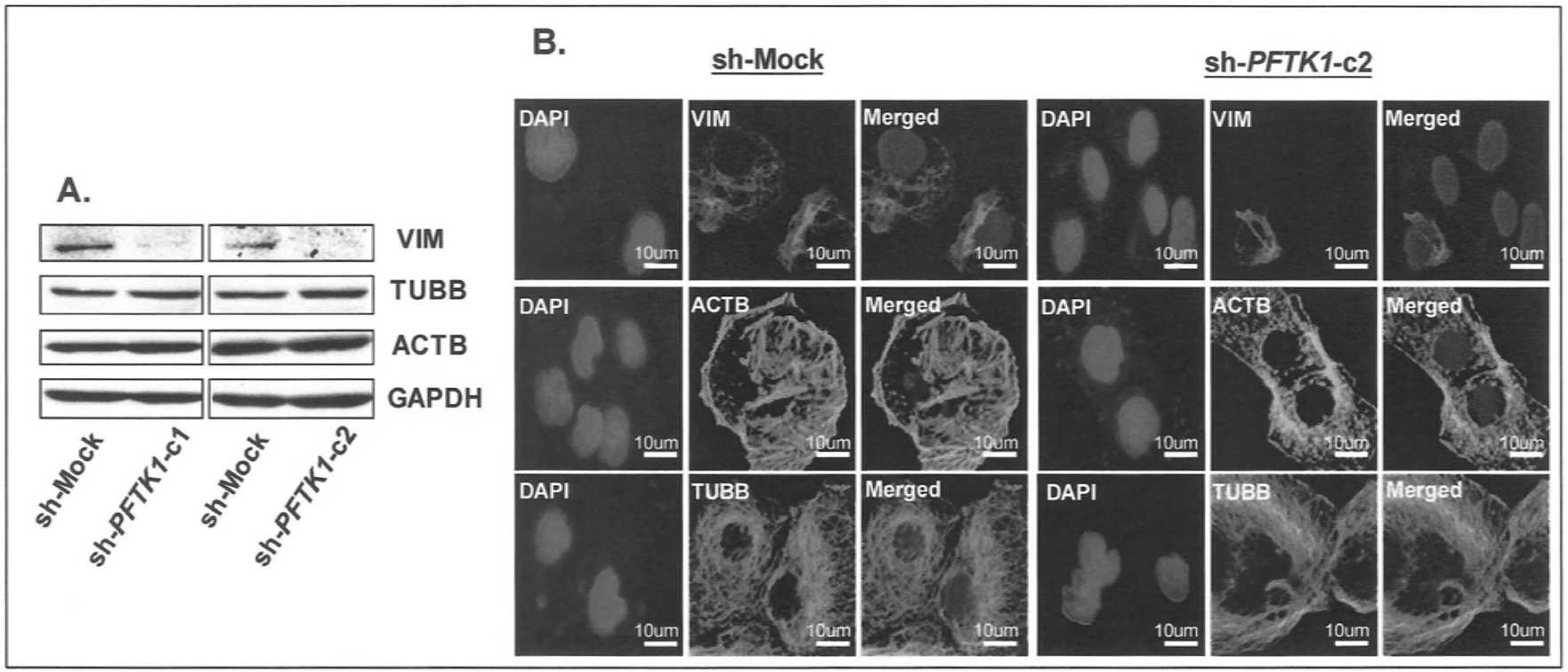

Figure 3-5 *PFTK1* affects intracellular cytoskeletal components.

(A) Western blot analysis indicated a reduction of VIM expression in *PFTK1*-suppressed cells.

(B) Immunofluorescence microscopy revealed a diminution in VIM expression in *PFTK1*-abrogated cells. Despite no change in ACTB protein being suggested in Western blotting, distinct actin remodelling with much profound reduction of actin stress fiber was evidently observed in sh-*PFTK1*-c1 and sh-*PFTK1*-c2. Changes in TUBB at both the total level and intracellular organization were not observed. Representative diagrams from sh-Mock and sh-*PFTK1*-c2 were shown.

3.2.2c TAGLN2 and ACTB phosphorylations

Based on the 2D-PAGE results, the phosphorylations of the two highest scored proteins, namely TAGLN2 and ACTB, were validated by immunoprecipitation assay. Reduced serine-phosphorylated TAGLN2 and tyrosine-phosphorylated ACTB in the two stably *PFTK1*-repressed clones were observed (Fig. 3-6Bi, ii). To further verify an effect of *PFTK1* on the serine phosphorylation of TAGLN2, exogenous *flag-TAGLN2* into *PFTK1*-suppressed Hep3B and HKCI-4 cells was expressed, and a concomitant diminution in serine-phosphorylated form of TAGLN2 was ascertained (Fig. 3-6Ci, ii). Similar to Hep3B, the HCC cell line HKCI-4 also manifested up-regulation of *PFTK1* as compared with normal livers. Conversely, ectopic *PFTK1*expression in immortalized hepatocyte cell line L02 that displayed negligible endogenous *PFTK1* expression evidently showed the presence of serine phosphorylation on the TAGLN2 protein (Figure 3-6Ciii). Intriguingly, it was also found that *PFTK1* suppression not only influenced the phospho-serine status of TAGLN2, but also resulted in an accumulation of TAGLN2 total protein (Figure 3-6A).

Studies on TAGLN have shown that it is an actin fibre-interacting protein and readily modulates actin cytoskeletal remodeling (Assinder *et al.*, 2009). However, serine phosphorylation on TAGLN highly weakens this actin-binding capability (Assinder *et al.*, 2009). To confirm if TAGLN2 serine phosphorylation plays a role on its actin-binding assay in HCC, a pull-down assay was carried out. Immunoprecipitation analysis showed binding of TAGLN2 to actin in both Hep3B and HKCI-4 cells, whereas enhanced physical interaction between these two proteins was readily found in the *PFTK1*-suppressed cells (Figure 3-6Ci, ii). On the other hand, serine-phosphorylation on TAGLN2 abrogated binding between

TAGLN2 and actin in *PFTK1*-expressing L02 cells (Figure 3-6Ciii). In summary, the findings proposed serine phosphorylation on TAGLN2 by *PFTK1* kinase inhibited physical interaction of TAGLN2 to actin in HCC.

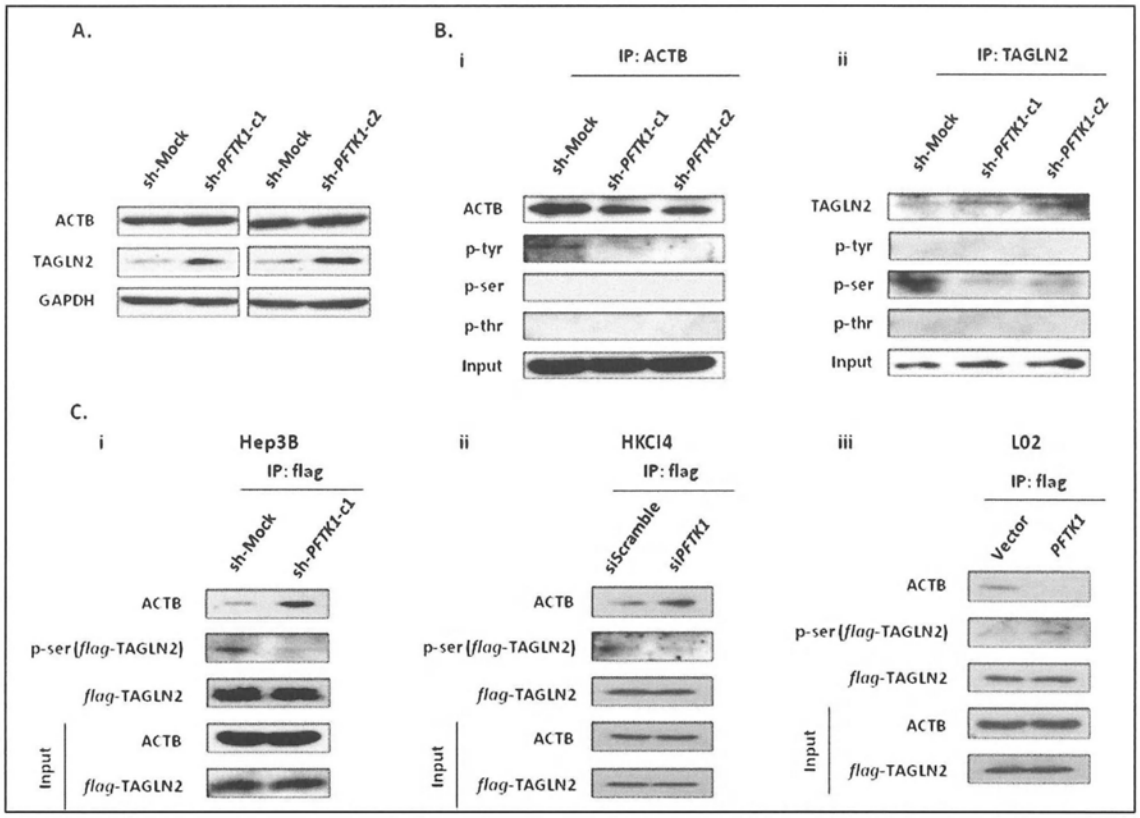

Figure 3-6 *PFTK1* kinase controls ACTB and TAGLN2 phosphorylations.

A) Western blot revealed an accumulation of TAGLN2 total protein in sh-*PFTK1*-c1 and sh-*PFTK1*-c2, whereas the ACTB expression level remained unchanged.

(Bi, ii) Immunoprecipitation experiments in Hep3B invariably showed a reduction in ACTB tyrosine phosphorylation in both sh-*PFTK1*-c1 and sh-*PFTK1*-c2 as compared with Mock control experiment. Decreased TAGLN2 serine phosphorylation was indicated in both sh-*PFTK1*-c1 and sh-*PFTK1*-c2 in proportion to sh-Mock.

(Ci, ii, iii) Immunoprecipitation assays against ectopically expressed *flag-TAGLN2* confirmed a concomitant decline in phospho-serine levels of TAGLN2 in *PFTK1*-suppressed Hep3B amd HKCI-4, whereas exogenous expression of GFP-tagged *PFTK1* in L02 showed an increase in serine-phosphorylated form of TAGLN2.

(Ci, ii, iii) Co-immunoprecipitation assays demonstrated a decrease in the actin-interacting capability of TAGLN2 in *PFTK1*-expressing cells, whereas in *PFTK1*-knockdown cells the physical interaction between TAGLN2 and ACTB was readily indicated.

3.2.3 Functional effects of TAGLN2 on HCC cell lines

3.2.3a Knockdown of TAGLN2 *restores migratory phenotype in* PFTK1*-supressed cells*

To examine whether TAGLN2 is a functional downstream target of *PFTK1*, knockdown experiment of *TAGLN2* was conducted in *PFTK1*-knockdown cells. In both sh-*PFTK1*-c1 and sh-*PFTK1*-c2, siRNA targeting *TAGLN2* promoted rescue of Hep3B cell motility and invasion ($P<0.05$), albeit the magnitude of restoration was not to the level of sh-Mock control (Figure 3-7Bi, ii). On the other hand, *TAGLN2* knockdown seemed to neither exert an influence on cell viability nor cell morphology (Figure 3-7A, C). Consistent with Hep3B, siRNA *TAGLN2* targeting in *PFTK1*-suppressed HKCI-4 cells rescued both cell motile ($P<0.01$) and invasive properties ($P<0.05$) without affecting cell viability (Figure 3-7Di, ii, E). Immunofluorescence analysis for filamentous actin organization in the *PFTK1*-suppressed Hep3B and HKCI-4 demonstrated marked recovery of actin stress fiber polymerizations following si*TAGLN2* treatment (Figure 3-8). To further verify the effect of *TAGLN2* suppression on actin polymerization, *flag-TAGLN2* was transfected into native Hep3B cells, and it was found that ectopically TAGLN2-expressing cells showed impaired actin stress fiber formation (Figure 3-9). These findings strongly suggested that TAGLN2 is a pivotal intermediate component in the biological cascade of *PFTK1*, and underscore a tumor suppressive role for TAGLN2 in the regulation of HCC cell dissemination. A novel interplay between *PFTK1* and TAGLN2 in the control of actin fiber polymerization is proposed in Figure 3-11B.

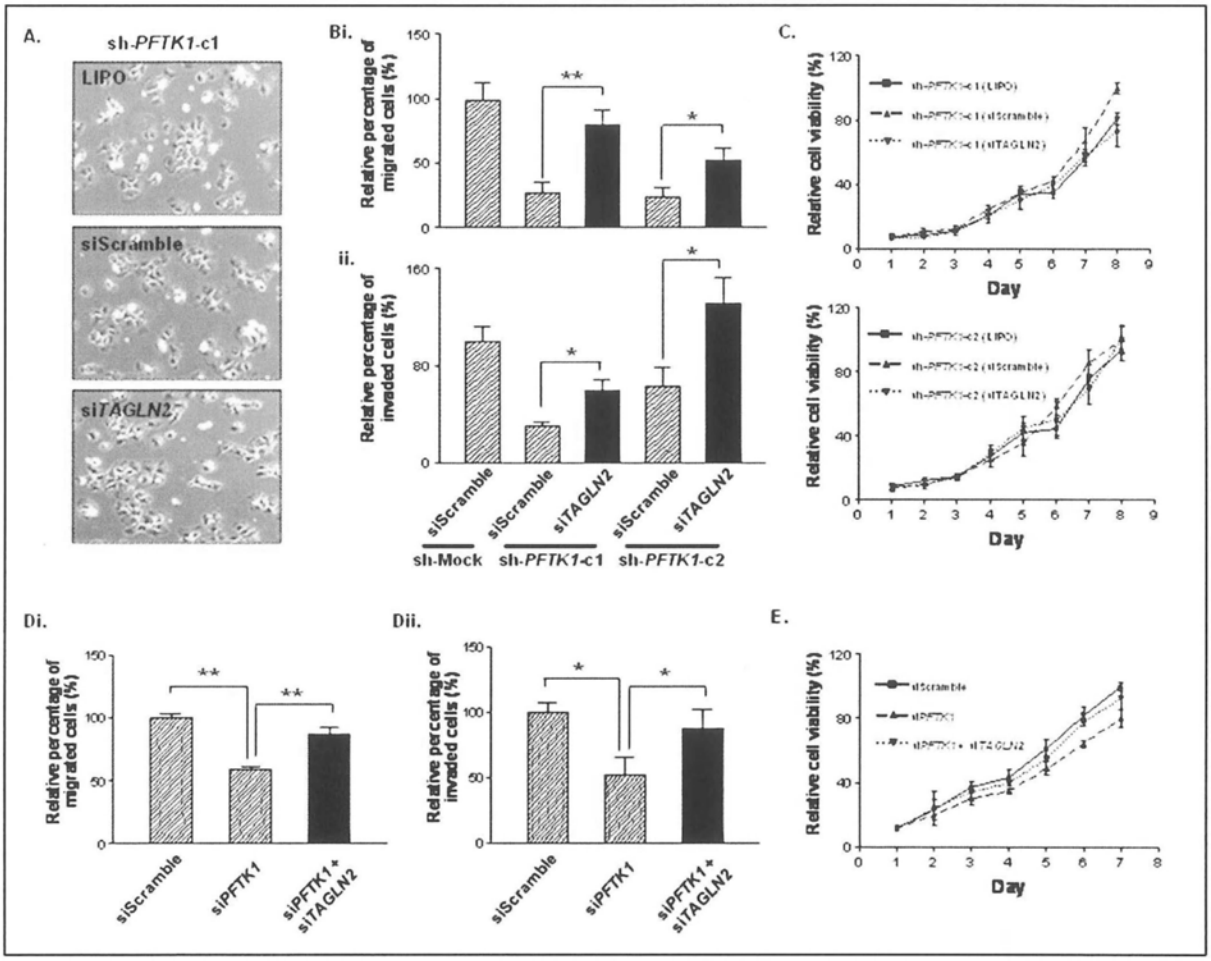

Figure 3-7 *TAGLN2* knockdown in *PFTK1*-suppressed cells counteracted inhibitory effects on cell migration.

(A, C) siRNA-mediated knockdown of *TAGLN2* in *PFTK1*-suppressed Hep3B did not indicate gross morphological changes and an effect on cell viability.

(Bi, ii) Suppression of *TAGLN2* in sh-*PFTK1*-c1 and sh-*PFTK1*-c2 evidently enhanced cell motile and invasive properties of cells.

(Di, ii, E) siRNA targeting *TAGLN2* in *PFTK1*-suppressed HKCI-4 cells promoted cell migration and invasion without exerting any effect on the cell viability. Nevertheless, only a partical recovery was demonstrated, as the degree of cell motility and invasion, except for sh-*PFTK1*-c2 invasion, did not reach to the extent of lipofectamine control (LIPO) and siScramble-treated sh-Mock cells (**P*<0.05; ***P*<0.01).

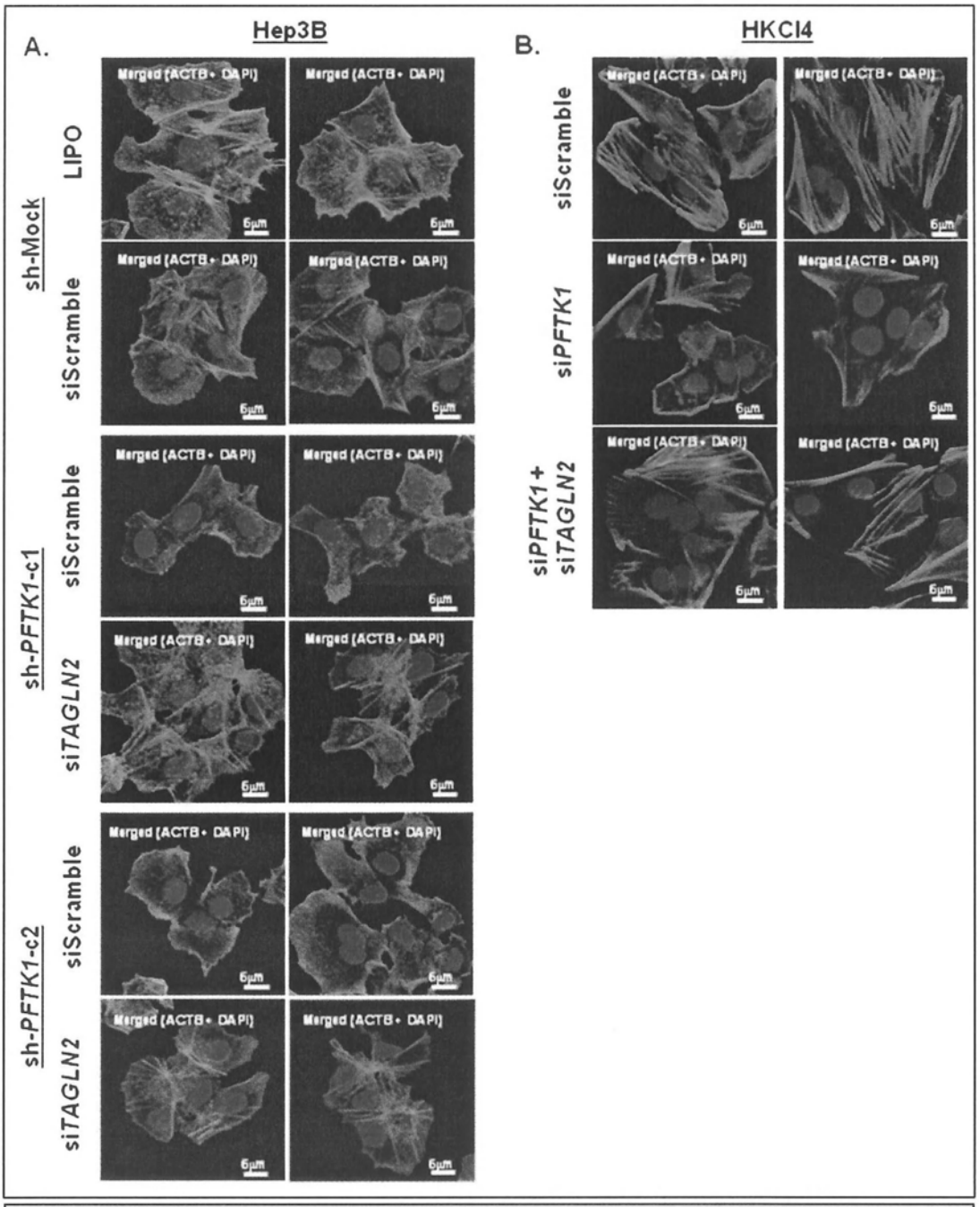

Figure 3-8 *TAGLN2* knockdown in *PFTK1*-abrogated cells restored actin stress fiber formation.

(A) Immunofluorescence analysis revealed si*TAGLN2*-transfected Hep3B cells (sh-*PFTK1*-c1 and sh-*PFTK1*-c2) showed recovery of actin fiber formation as compared with siScramble experiments.

(B) A similar circumstance was also suggested in HKCI-4, where si*TAGLN2* knockdown manifested the actin stress fiber formation. However, the extent of actin polymerization in both Hep3B and HKCI4 *PFTK1*-abrogated cells did not seem to revert to the level of siScramble transfected shMock cells.

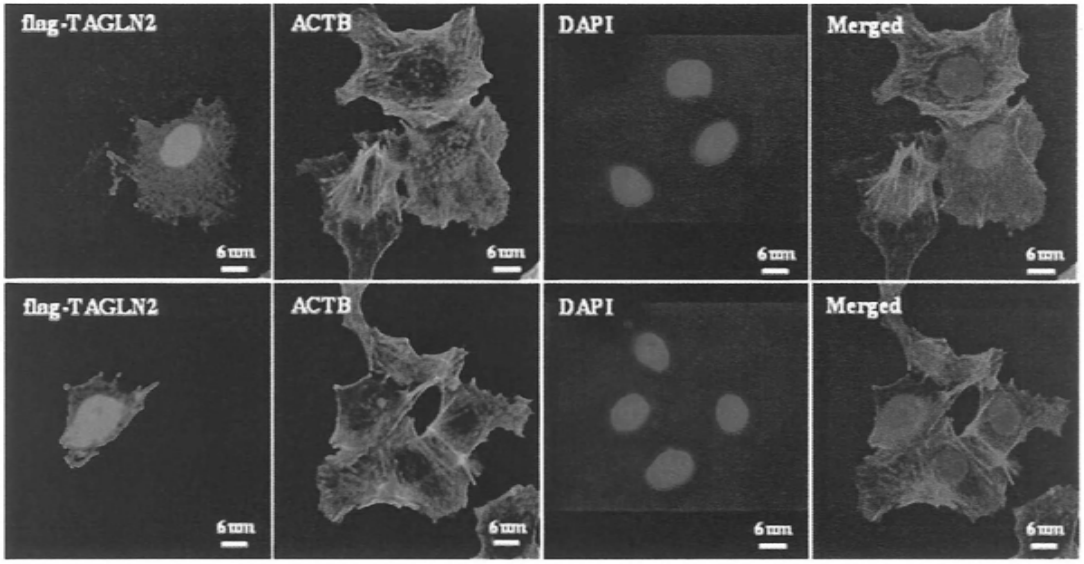

Figure 3-9 TAGLN2 inhibited the formation of actin stress fiber formation.

Co-immunofluorescence analysis showed that retardation in polymerized actin fiber was suggested in native Hep3B cells with ectopic TAGLN2 expression.

3.2.3b PFTK1 *kinase regulates actin binding ability of TAGLN2 through S83 and S163 residues*

To identify *PFTK1*-targeted sites on TAGLN2, a panel of phospho-defective mutants (S11A, S83A, S94A, S145A, S155A, S163A, S185A) was constructed with all serine (S) residues on TAGLN2 substituted with alanine (A), and the functional effect of these single-mutated constructs on actin-interacting affinity was explored. In *PFTK1*-expressing Hep3B control cells (sh-Mock), immunoprecipitation against *flag*-labeled wild-type *TAGLN2* and phospho-defective constructs demonstrated the presence of immune complexes with ACTB in cells transfected with S83A and S163A mutants, but not in other mutants, suggesting that these constructs abrogated the suppressive effect of *PFTK1* on the magnitude of physical interaction between TAGLN2 and ACTB (Figure 3-10Ai). To corroborate S83 and S163 residues are important for actin binding capability, phospho-mimetic mutants (S83D and S163D) with a substitution of aspartic acid (D) on S83 and S163, respectively, were created. The *PFTK*-suppressed Hep3B cells (sh-*PFTK1*) transfected with the phospho-mimetic mutants showed actin binding hinderance in the presence of S83D and S163D mutants when compared to wild-type *TAGLN2* (Figure 3-10Bi). These findings therefore highlight much importance for S83 and S163 residues on TAGLN2 in its actin-binding ability.

3.2.3c PFTK1 *regulates HCC cell motile phenotypes via S83 and S163 of TAGLN2*

To affirm functionality of serine residues identified in regulating HCC cell motility, phospho-defective *TAGLN2* mutants (S83A and S163A) were transfected into Hep3B sh-Mock cells. In line with their actin-binding ability as indicated in

Figure 3-10Ai, a profound reduction in cell migratory property was found ($P<0.05$) (Figure 3-10Aii). A reciprocal manner was suggested when phospho-mimetic mutants (S83D and S163D) were transfected into *PFTK1*-suppressed Hep3B cells, where enhanced motile phenotype was observed ($P<0.05$) (Figure 3-10Bii). Taken together, the data supported residues S83 and S163 on TAGLN2 are indeed functional candidates of *PFTK1* in the control of HCC cell migration.

3.2.3d PFTK1 *regulates TAGLN2 and VIM independently*

As down-regulation of VIM was evidently observed in *PFTK1*-supressed cells, I also examined if *PFTK1* exerted the effect on VIM expression through TAGLN2. A time-course experiment of TAGLN2 knockdown at 48h, 60h and 72h post-transfection in *PFTK1*-suppresed cells (sh-*PFTK1*-c2) was performed. Western blot analysis did not suggest an effect on the VIM protein expression (Figure 3-11A). This finding would suggest that *PFTK1* regulated the migratory phenotype of Hep3B cell through controlling VIM expression and TAGLN2-actin biological cascade independently.

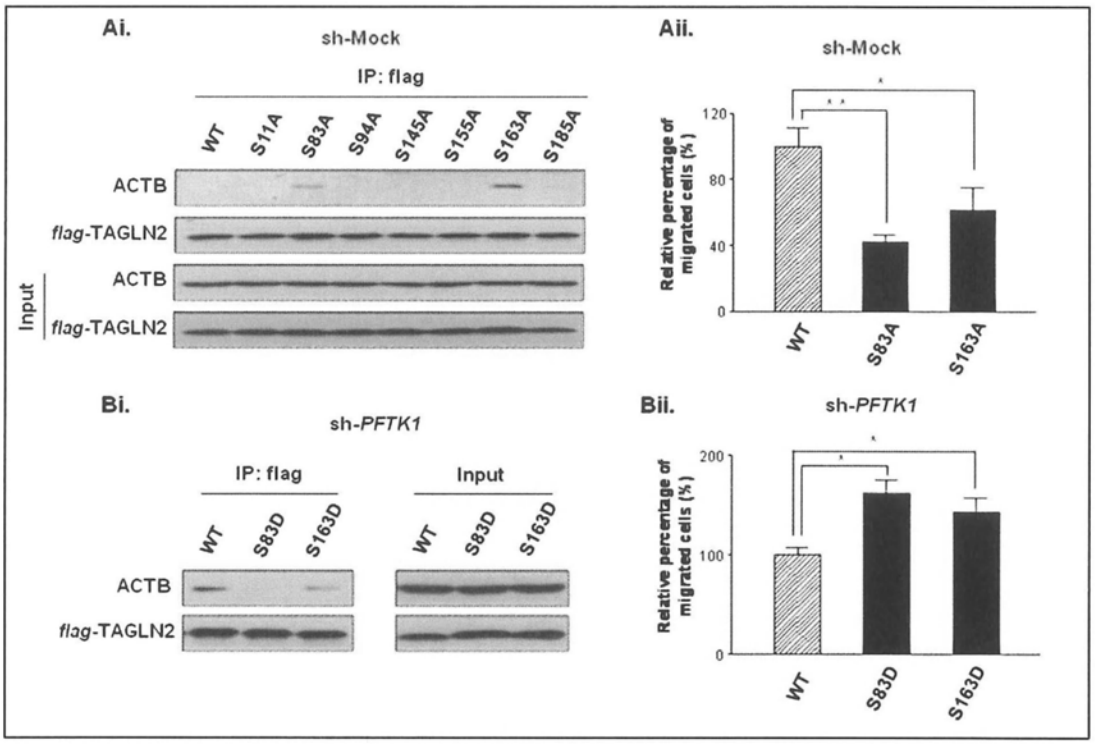

Figure 3-10 *PFTK1* regulates HCC cell migration through S83 and S163 residues of TAGLN2.

(Ai, ii) Phospho-defective mutants of *TAGLN2* transfected in Hep3B sh-Mock were immunoprecipitated by *flag* antibody and detected by ACTB antibody. Physical binding to actin was only suggested in the *PFTK1*-expressing sh-Mock with phospho-defective constructs S83A and S163A as compared with wild-type (WT) *TAGLN2* transfection. Impaired cell migratory phenotypes were also shown in sh-Mock expressing S83A and S163A (**P*<0.05; ***P*<0.01).

(Bi, ii) Phospho-mimetic assays illustrated the loss or reduced actin binding of TAGLN2 in *PFTK1*-suppressed Hep3B transfected with S83D and S163D. Besides, S83D and S163D expression in *PFTK1*-suppressed cells promoted cell motile properties (**P*<0.05).

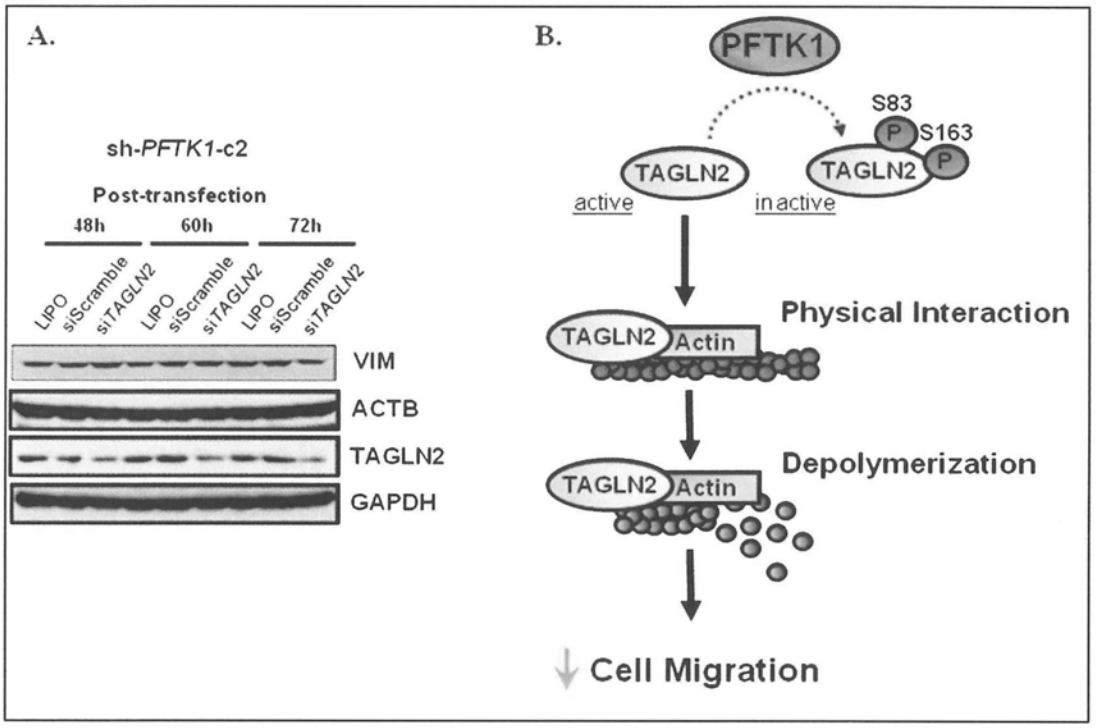

Figure 3-11 (A) *PFTK1* regulates VIM expression independent of TAGLN2. In time-course experiment, TAGLN2 knockdown in *PFTK1*-suppressed cells indicated no effect on VIM expressions. (B) A schematic diagram of the interplay among *PFTK1*, TAGLN2 and actin polymerization in the control of HCC cell migration was represented.

3.3 Discussion

In the present study, a prognostic value for *PFTK1* in primary HCC tumors was suggested, where frequent *PFTK1* up-regulations significantly correlated with advanced tumor grading, the presence of histologic micro-vascular invasion and the likely induction of an early age onset. Since vascular invasion commonly occurs in HCC and predicts tumor invasion and metastasis (Poon *et al.,* 1999), the finding from this chapter may be suggestive of *PFTK1* over-expressions in association with a more aggressive malignant phenotype. Functional informations illustrated the biological insight of *PFTK1* protein kinase through TAGLN2 as an intermediate substrate. It is therefore conceivable that in human HCC over-expression of oncogenic *PFTK1* actively phosphorylates TAGLN2, a process by which it inactivates the inhibitory effect of TAGLN2 on actin polymerization, leading to enhanced cellular motility and invasiveness. Interestingly, an observable accumulation of TAGLN2 total protein was found subsequent to the *PFTK1* knockdown. Although this may have been due to a delay in protease cleavage or a positive feedback mechanism on the endogenous expression of TAGLN2 from the serine unphosphorylated status, the actual fact is an accumulation of TAGLN2 protein may well have manifested its tumor suppressive function on the cell motile phenotypes via an increased extent of actin binding ability. In this regard, the serine-unphosphorylated form of TAGLN2 was postulated as the active tumor suppressing status with the actin-interacting function. Meanwhile, I was able to further show the biological significance of serine residues S83 and S163 on TAGLN2 in its actin-interacting magnitude as well as their influence on HCC cell migration. *PFTK1*-expressing cells transfected with abrogating phospho-defective

mutants S83A and S163A showed enhanced physical binding of TAGLN2 to actin and an inhibitory effect on cell motility. A reverse was shown from phospho-mimetic experiment that transfection of *TAGLN2* S83D and S163D mutants enhanced HCC cell migration, despite the cells were deprived of *PFTK1* expression. The findings provided supportive evidence that S83 and S163 residues on TAGLN2 were the crucial components in the *PFTK1*-TAGLN2 biological cascade. In line with my findings, *in-vitro* co-sedimentation assays have demonstrated that TAGLN2 could bind to actin and/or cause actin gelation via specific interaction sites, which if serine phosphorylation could substantially reduce its actin binding ability (Fu *et al.*, 2000). Given the biological significance of actin cytoskeletal dynamics on cell migration and tumorigenesis, understanding molecules involved in the physical interaction and regulation of actin organization could provide potential tumor markers and molecular targets for therapeutic regimens.

TAGLN, also known as the smooth muscle protein 22-alpha (*SM22-alpha*), is an actin stress fibre-associated protein ubiquitously found in vascular and visceral smooth muscle (Assinder *et al.*, 2009). It is commonly repressed in breast, colon (Shields *et al.*, 2002; Wulfkuhle *et al.*, 2002) and prostate carcinomas (Yang *et al.*, 2007), where a tumor suppressor role has been proposed. In colorectal cancer, low TAGLN expression has further been reported as an independent prognostic marker for shorter patients' survival (Zhao *et al.*, 2009), whereas an inhibitory role in metastasis was highly suggested in breast cancer (Xu *et al.*, 2010). TAGLN also acts to suppress the expression of metallo-matrix proteinase (MMP9), which is a central molecule involved in the extracellular matrix remodeling during cancer cells dissemination into surrounding tissues (Nair *et al.*, 2006). In this thesis, I support a tumor suppressor role of TAGLN2, of which presence could inhibit HCC cell

motility through actin depolymerization. RNAi silencing of *TAGLN2* was found to circumvent the suppressive action of *PFTK1* knockdown on the motile phenotypes of HCC cells. However, although knockdown of *TAGLN2* was able to recover HCC cell migration and invasion along with obvious re-emergence of actin stress fiber polymerization, the extent of recovery was only partial compared with sh-Mock control. These observations would invariably suggest other downstream candidates of *PFTK1* are likely involved in the control of HCC cell migration. Using 2D-PAGE mass spectrometry, a few phosphorylation targets of *PFTK1*, including ACTB tyrosine phosphorylation, were shortlisted. Since *PFTK1* is a serine/threonine protein kinase, it is plausible that ACTB tyrosine phosphorylation would be caused by indirect influence of the *PFTK1* pathway, while serine phosphorylation on TAGLN2 is likely resulted from a direct kinase activity of *PFTK1*. Nonetheless, it is worthwhile to note that extensive studies have established a close relation between actin phosphorylation and cytoskeletal reorganization (Baek *et al.*, 2008; Rush *et al.*, 2005). Specifically, tyrosine phosphorylation on ACTB has been shown to induce considerable actin remodelling and cytoskeletal rearrangement (Rush *et al.*, 2005). Tyrosine phosphorylation of actin in fact can protect its D-loop structure from proteasomal degradation, resulting in a more stable D-loop conformation as compared with the unphosphorylated form (Baek *et al.*, 2008). Conformational stability of the D-loop possesses much importance in conferring cell migratory phenotypes, which if unstable can result in a weakened contractile force and hence much reduced gliding velocity (Kubota *et al.*, 2009). My findings on reduced ACTB tyrosine phosphorylation in the *PFTK1*-suppressed cells would seem to be in line with the development of a less stable actin structure, which could have suppressed HCC cell migration. In the meantime, *PFTK1* knockdown could also abolish the

expression of VIM, a well-known marker for cellular mesenchymal feature as well as a structural protein constituting the intermediate filaments of the intracellular cytoskeleton. The process of epithelial-to-mesenchymal transition (EMT) attributes to the trans-differentiation of epithelial cells into fibroblastic, migratory cells characterized by mesenchymal cell morphology (Vincent-Salomon and Thiery, 2003). This mesenchymal phenotype is a hallmark of tumour cells acquiring migratory and aggressively metastatic properties. Thus, loss of VIM expression shown from the *PFTK1* knockdown could be suggestive of a regression on mesenchymal features and a retarded cell migratory potential. The precise underlying mechanism of *PFTK1* in the process of EMT however deserves further investigations.

The acquisitions of cell migratory and invasive capabilities are pre-requisite for cancer cells to invade and metastasize. This process consists of multiple intracellular cytoskeletal components and intricate orchestration of biological cascades, often arising from complex interplay between molecules. In this study, my work outlined the value of 2D-PAGE Mass Spectrometric proteomics in short-listing downstream phosphorylated candidates of a protein kinase. I also showed that suppressed *PFTK1* expression can significantly impede HCC cell migration and invasion; meanwhile, siRNA targeting of *TAGLN2*, a phosphorylated substrate of *PFTK1* kinase, can considerably rescue HCC cell migration through actin stress fiber polymerization. A schematic representation highlighting the relationship among *PFTK1* kinase, TAGLN2 and actin is illustrated in Figure 3-10B. This newly defined oncogene–tumor suppressor biological cascade, in which oncogenic *PFTK1* inactivates a tumor suppressor gene TAGLN2 via phosphorylation, offers a novel avenue for better understanding of liver carcinogenesis, especially on tumor cell

dissemination and metastasis, and thus may facilitate the development of potential curative options for individuals being diagnosed with HCC.

Chapter 4

Phosphorylation on Caldesmon by *PFTK1* kinase promotes actin binding and formation of stress fibers

4.1 Introduction

Caldesmon (CaD), encoded by *CALD1* gene, is an actin-regulatory protein that is able to stabilize and protect the filamentous actin against actin-severing molecules. First identified in chicken gizzard (Sobue *et al.,* 1981), CaD protein has been long known to be associated with cytoskeletal organization such as membrane ruffles and actin stress fibers, and seems to play a role in processes, including cell division, migration, adhesion, and apoptosis (Haxhinasto *et al.,* 2002; Deng *et al.,* 2007; Numaguchi *et al.,* 2003; Yamashiro *et al.,* 1991; Yamboliev and Gerthoffer, 2001). In addition, phosphorylation of CaD has been well demonstrated in the control of cell motile phenotypes. Previous reports on protein kinases phosphorylating CaD have demonstrated that CaD can be readily phosphorylated by Cdc2 kinase in regulating cell motility and progression of G2/M checkpoint during mitosis (Manes *et al.,* 2003; Juliano, 2003; Yamashiro *et al.,* 2001). The *PFTK1* protein kinase is a novel Cdc2-related gene that was initially discovered in the mouse nervous system (Lazzaro and Julien, 1997). Human *PFTK1* is highly expressed in brain, heart, kidney, ovary, pancreas and testis, but minimally detected in other tissues such as liver, prostate and skeletal muscle (Yang and Chen, 2001). Studies on mouse *PFTK1* have related its function in the process of meiotic division and neuron differentiation (Besset *et al.,* 1998), yet the underlying biological basis of human *PFTK1* remains largely undefined. Our earlier studies showed that *PFTK1* plays an oncogenic role in human HCC, where over-expression of *PFTK1* enhanced cellular chemotactic motility and invasiveness through promoting the actin stress fiber assembly (Pang *et al.,* 2007).

In this study, I investigated in HCC cells whether or not CaD is a

downstream phosphorylation target of the *PFTK1* kinase. The *PFTK1*-triggered phosphorylation enabled physical interaction between CaD and filamentous actin, and promoted an actin-stabilizing effect that manifested formation of actin stress fibers.

4.2 Results

4.2.1 PFTK1 *kinase phosphorylates CaD and controls CaD cellular localization.*

To determine whether CaD is a downstream phosphorylation target of the *PFTK1* kinase, 2 stably *PFTK1*-suppressed (sh-*PFTK1*-c1 and sh-*PFTK1*-c2) and one control Hep3B cells (sh-Mock) as described in Chapter 3 were employed for investigations. Pull-down assay on CaD phosphorylation demonstrated a reduction on threonine- and tyrosine-phosphorylation levels in sh-*PFTK1*-c1 and sh-*PFTK1*-c2 compared with sh-Mock, but no observable changes were suggested in the serine-phosphorylation (Figure 4-1A). As *PFTK1* exerts its kinase activity on threonine phosphorylations, our finding would imply CaD could be a downstream substrate of *PFTK1*. Immunofluorescence microscopy against cellular CaD on the *PFTK1*-knockdown cells illustrated a re-localization of CaD protein from the membrane ruffles and stress fibers in sh-Mock to a diffused and blurred appearance in sh-*PFTK1*-c1 and sh-*PFTK1*-c2 (Figure 4-1B). The findings underscored the cellular distribution of CaD protein can be readily affected by *PFTK1* expression.

I next examined actin cytoskeletal organization under the influence of *PFTK1*, reasoning that enhanced cellular migratory phenotype was evidently regulated by the filamentous actin (F-actin) dynamics as mentioned in Chapter 3. Stained by TRITC-conjugated phalloidin on F-actin, immunofluorescence analysis suggested marked reductions in actin polymerizations and stress fiber formation in *PFTK1*-abrogated cells (Figure 4-2).

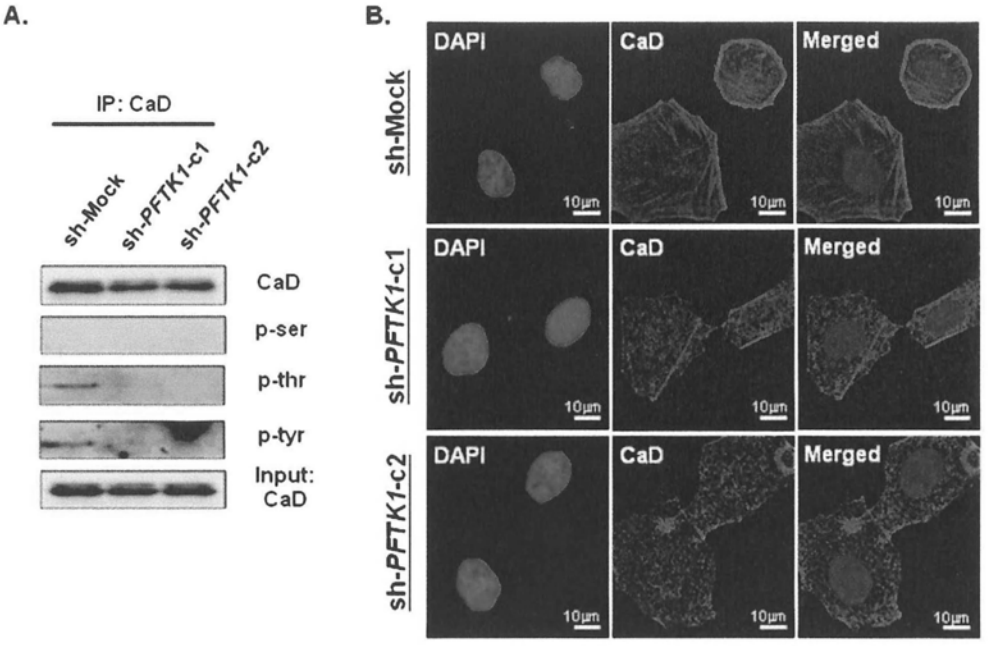

Figure 4-1 Effects of *PFTK1* on CaD phosphorylations and cellular localizations.

(A) Immunocomplexes precipitated from sh-Mock, sh-*PFTK1*-c1 and sh-*PFTK1*-c2 cell lysates using anti-CaD antibody showed a considerable diminution in phospho-threonine and phospho-tyrosine levels in sh-*PFTK1*-c1 and sh-*PFTK1*-c2 as compared with sh-Mock. Input reference represents the endogenous CaD total protein expression in corresponding samples.

(B) In the *PFTK1*-expressing control cells (sh-Mock), CaD was shown to localize at the membrane ruffles and actin stress fibers. In the *PFTK1*-knockdown cells (sh-*PFTK1*), cellular distribution of CaD protein demonstrated a diffused and blurred appearance.

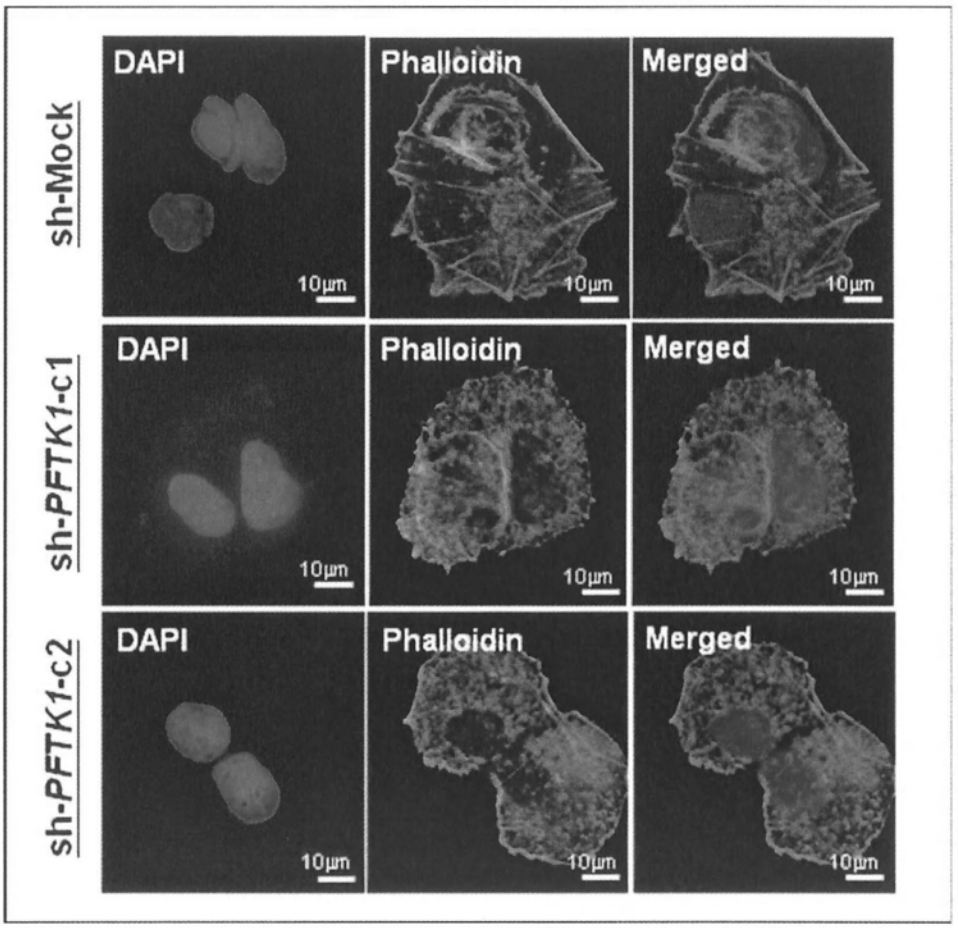

Figure 4-2 *PFTK1* directs the process of actin stress fiber formation.
Immunofluorescence analysis revealed that *PFTK1*-suppressed cells (sh-*PFTK1*-c1 and sh-*PFTK1*-c2) demonstrated marked reduction of actin stress fibers formation in proportion to *PFTK1*-expressing control cells (sh-Mock), which showed a considerable presence of actin stress fibers.

4.2.2 PFTK1 *phosphorylation on CaD enhances physical binding between CaD and ACTB.*

Previous studies have shown phosphorylation on CaD protein influenced its interacting magnitude to actin (ACTB) (Bogatcheva *et al.,* 2006; Borbiev *et al.,* 2003; Lin *et al.,* 2009). Co-immunoprecipitation assay was carried out to determine if *PFTK1* suppression played a role for the CaD-ACTB interaction. Data showed the presence of endogenous complex of CaD with ACTB protein in mock controls, but not detected in sh-*PFTK1*-c1 and sh-*PFTK1*-c2 (Figure 4-3A, *Upper panel*). A reciprocal co-immunoprecipitation using anti-ACTB antibody also detected endogenous protein complexes of CaD and ACTB proteins in sh-Mock, while no apparent CaD complexes were observed in cells with *PFTK1* suppression (Figure 4-3A, *Lower panel*). Further immunofluorescence analysis on CaD protein revealed cellular co-localization of phosphorylated CaD protein with actin stress fibers in the control cells, whereas this observation was no longer shown in *PFTK1*-knockdown cells (Figure 4-3B). Taken together, the data suggested phosphorylation on CaD protein by *PFTK1* kinase could strengthen CaD actin-binding and -stabilizing capabilities. The schematic diagram of the interaction between *PFTK1* and CaD was illustrated in Figure 4-5.

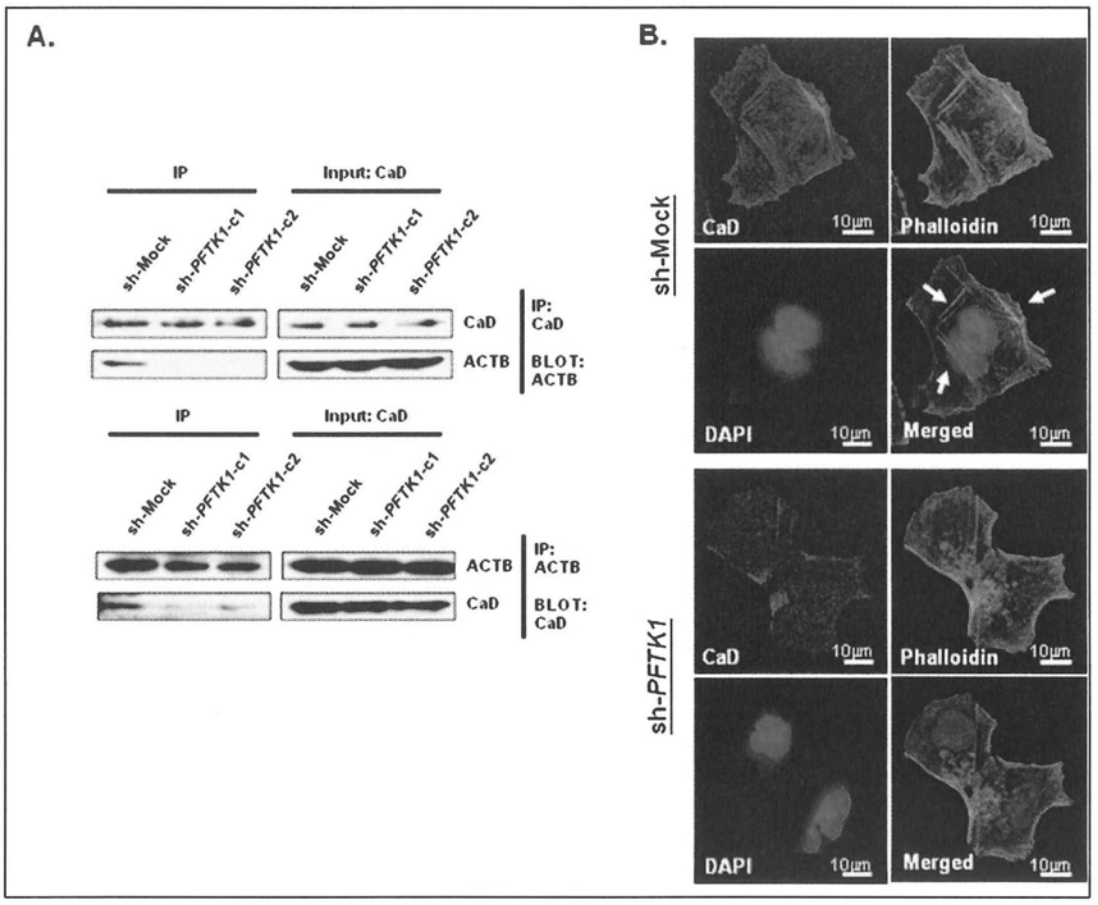

Figure 4-3 *PFTK1* modulates the magnitude of CaD actin-binding affinity.

(A) Protein complexes immunoprecipitated using anti-CaD antibody detected the positive staining of actin in *PFTK1*-expressing sh-Mock, but not in *PFTK1*-suppressed sh-*PFTK1*-c1 and sh-*PFTK1*-c2 cells (*Upper panel*). Reciprocal immunoprecipitation assay was performed by anti-ACTB showing the presence of CaD protein in sh-Mock, whereas no observable bands were shown in sh-*PFTK1*-c1 and sh-*PFTK1*-c2 (*Lower panel*).

(B) Dual-immunofluorescence microscopy presented co-localization of CaD with actin stress fibers as arrowed indicated in sh-Mock. This observation was not found when *PFTK1* was suppressed (sh-*PFTK1*).

4.2.3 Common overexpression of CALD1 *mRNA in human HCC primary.*

To define the clinical significance of caldesmon in human HCC, expression of *CALD1* mRNA was examined in a cohort of 25 primary HCC tumors compared with their paired non-malignant counterparts using qRT-PCR analysis. A significant up-regulation of *CALD1* in HCC tumors was suggested compared to their adjacent non-tumorous livers ($P<0.05$; Figure 4-4A).

Further immunoprecipitation assay was performed on 6 primary HCC tumors in order to examine the phosphorylation status of CaD protein. Of the 6 HCC tumors, two present multiple lesions and four cases are solitary tumors. Western blot did not suggest any apparent differences in CaD total protein among these human HCC tumors (Figure 4-4B). Nevertheless, the pull-down assay evidently demonstrated the presence of CaD phospho-tyrosine and phospho-threonine in the two HCC cases presented with multiple lesions, but not detected in the four cases of solitary HCC tumors (Figure 4-4C). I thus postulated that *CALD1* was closely related to hepatic tumorigenesis, and metastatic potential of HCC.

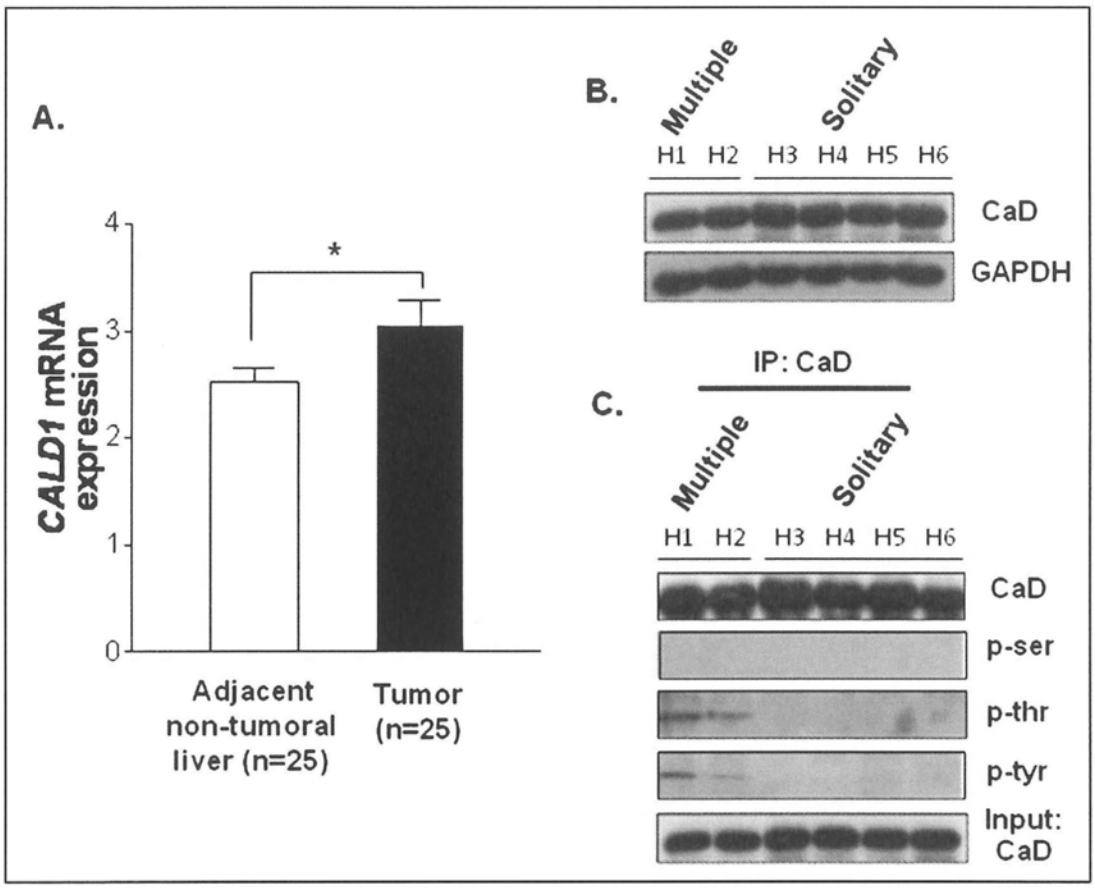

Figure 4-4 Expression and phosphorylation status of Caldesmon in human HCC tumors.

(A) Expressions of *CALD1* mRNA were analyzed by qRT-PCR in a cohort of 25 paired primary HCC. Data indicated that *CALD1* is significantly up-regulated in tumors compared with their matched non-malignant counterparts ($P \leq 0.05$).

(B) Western blot analysis showed similar CaD protein expressions in primary HCC presented with multiple lesions (H1 & H2) and solitary tumors (H3-6).

(C) Immunoprecipitation experiments showed an increase in the threonine and tyrosine phosphorylations of CaD protein in HCC with multiple lesion presentation but absent in solitary tumors.

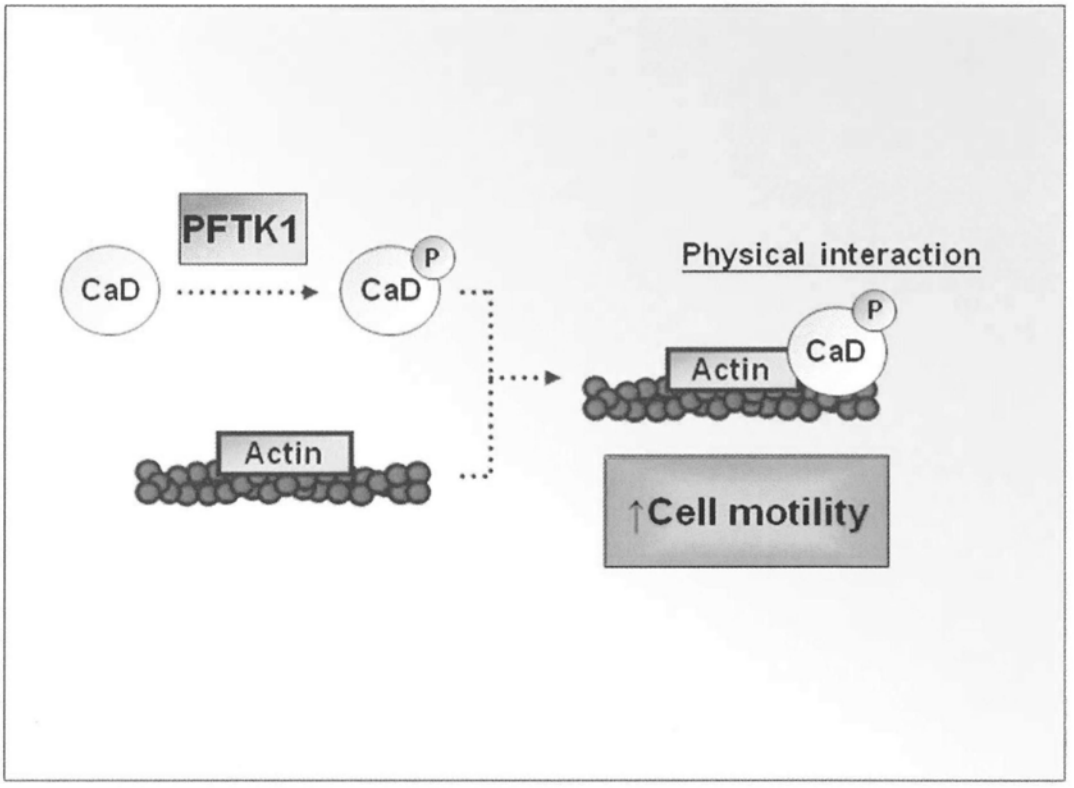

Figure 4-5 Schematic representation of the *PFTK1*-CaD biological cascade.
Phosphorylation on CaD by *PFTK1* protein kinase promotes the physical interaction between caldesmon and actin stress fibers.

4.3 Discussion

In the present study, *PFTK1* kinase was highlighted as a newly identified contributor in the CaD-ACTB biological cascade. The actin-binding and –stabilizing effect of CaD was shown to be under the influence of *PFTK1* kinase activity, which altered the phosphorylation status of CaD protein. Concordant with my study, reposts on CaD have illustrated that phosphorylated CaD colocalizes with thrombin-induced actin stress fibers, and an increase in CaD ser/thr phosphorylations from prolonged PMA exposure could enhance the physical interaction of CaD to actin (Bogatcheva *et al.,* 2006; Borbiev *et al.,* 2003). In addition, phosphorylations on CaD, in general, can confer cell migratory properties (Goncharova *et al.,* 2002; Han [2] *et al.,* 2007). Specifically, it was shown in prostate cancer that CaD phosphorylation by Cdc2 kinase could enhance cancer cell motile and invasive properties (Juliano, 2003; Manes *et al.,* 2003). Although *PFTK1* encodes a highly conserved ser/thr kinase signature with Cdc2 kinase, limited has been known about its physiological functions and regulatory cyclin subunits. Recently, it was demonstrated that *PFTK1* showed physical binding to cyclin Y (Jiang *et al.,* 2009). However, the phosphorylation target(s) of *PFTK1* kinase, especially in the control of cancer cell migration remains largely elusive. Based on the findings, I therefore postulated that CaD could represent a downstream substrate in the *PFTK1*-modulated HCC cell motility through regulation on actin remodeling, which our group has previously described (Pang *et al.,* 2007).

The data here showed the fact that *PFTK1* phosphorylation on CaD controlled its cellular re-distribution, and markedly enhanced its extent of actin-interacting affinity. I demonstrated that suppressed *PFTK1* expression caused

concomitant reduction in phospho-threonine and phospho-tyrosine levels on CaD protein. The reduced phosphorylations led to the CaD protein to displace from actin, and hence a disassembly of the actin stress fibers. The results would suggest phosphorylation on CaD by *PFTK1* kinase not only promoted the CaD actin-binding ability, but also could enhance the process of actin polymerizations, which are both important events in the control of cell migratory phenotypes. Moreover, *CALD1* mRNA was shown to commonly up-regulate in HCC tumors compared with their adjacent non-tumoral liver, and, more interestingly, CaD hyperphosphorylations can be readily observed in primary HCC cases presenting multiple lesions. This may well suggest the participation of CaD in liver carcinogenesis through the effect of *PFTK1* kinase activity, where its expression was also frequently over-expressed in HCC primary (Pang *et al.,* 2007). In conclusion, the findings here underscored the *PFTK1* function in conferring selective advantages towards cell motility through CaD-ACTB biological cascade.

Chapter 5

Role of miR-183/96/182 overexpression in HCC

5.1 Introduction

Despite the growing knowledge on HCC tumor biology, the transcriptional regulation of many causal tumor suppressors or oncogenes remains largely unknown. Recently, microRNAs (miRNAs) have emerged as key posttranscriptional regulators of gene expression. It belongs to a class of endogenous and noncoding small RNA that primarily regulates gene expression through perfect or imperfect complementaries to the 3' untranslated region (UTR) of their target messenger RNAs (mRNAs) (Peters and Meister, 2007). The base pairing process leads to mRNA degradation and/or translational repression, subsequently leading to the suppression of protein expression. Through the actions on their target mRNAs, miRNAs can direct a vast number of physiological functions such as apoptosis, cell proliferation and differentiation, and cell migration. The concept of miRNA deregulations has been recognized as an important event in cancer development, where their influence on a multitude of tumor suppressors and oncogenes has been illustrated (Spizzo *et al.,* 2009). Specifically in HCC, evidences supported miRNA deregulations in correlation with tumor progression, clinicopathlogic features and patient prognosis (Budhu *et al.,* 2008; Xiong *et al.,* 2010; Ura *et al.,* 2009).

Our earlier studies using miRNA expression profiling reported a concordant up-regulation of three miRNAs, namely miR-183/96/182 cluster (Wong *et al.,* 2010); the biological role(s) of miR-183, -96 and -182 in HCC remains largely unclear. In this study, it was found that these miRNAs hold prognostic values in patients with HCC. Similar to *PFTK1*, it was also determined that each of these miRNAs holds metastatic potentials in regulating HCC cell migratory and invasive phenotypes. In-silico predictions and Western blot analysis further suggested miR-183, -96 and

-182 converged in targeting Forkhead BoxO1 (FOXO1). In the investigation of upstream regulation of the miR-183/96/182 cluster, β-catenin (CTNNB1) was shown to be a regulator in enhancing the concordant up-regulation of these three miRNAs in HCC.

5.2 Results

5.2.1 Prognostic value of miR-183, -96 & -182 expressions.

To verify the role of miR-183/96/182 cluster in HCC, qRT-PCR analyses of miR-183, -96 and -182 expressions were performed on a cohort of 81 paired HCC primary and adjacent non-tumoral liver. Of the cases studied, 48 HCC tumors (59.3%) showed concordant up-regulations of miR-183, -96 and -182 (≥2-fold) compared with their matched non-malignant counterparts ($P<0.05$) (Figure 5-1 & -2). Correlative analyses of miR-183/96/182 expression with clinicopathological features including age onset, gender, hepatitis B infection, liver cirrhosis, tumor grading, clinical staging, tumor multiplicity or vascular invasion were conducted. Increased expression of miR-183/96/182 was shown to significantly associate with features of metastatic potential including advanced tumor grading to poorly differentiated state ($P<0.01$) and the presence of microvascular invasion ($P<0.05$) (Table 5.1).

To further establish the prognostic value of miR-183/96/182, HCC cases were divided into three subgroups (A, B & C) using median as cutoff. A total of 33 cases showing concordant up-regulations of miR-183, -96 and -182 were subcategorized into A, whereas 19 cases with either one or two of the miRNA up-regulations were included into subgroup B. The remaining 29 cases that illustrated concomitant down-regulations of miR-183, -96 and -183 were classified as subgroup C.

The characteristics of HCC patients related to the survival status are shown in Table 5.2. As expected, clinical staging ($P=0.0089$) and tumor multiplicity ($P=0.0101$) that had been previously regarded as prognostic factors for HCC patients were shown to significantly associate with disease-free survival. This association was also suggested when concordantly increased miR-183, -96 and -182 expressions (subgroup

A) were detected in tumor tissues (P=0.0461).

In univariate Cox regression analysis, concordant up-regulations of miR-183, -96 and -182 in HCC primary tissues (subgroup A) was associated with a significantly increased risk of cancer-related death (RR: 1.8255; 95% confidence interval (CI): 1.0303-3.2342; P=0.0402) (Table 5.3). Advanced tumor staging (P=0.0038), multiple intrahepatic nodules (P=0.0003), the presence of macro- (P=0.0372) and micro-vascular invasions (P=0.0025) were also suggested as significant prognostic predictors.

After the adjustment of the potential confounding factors, multivariate model indicated concomitantly increased expression of miR-183, -96 and -182 (subgroup A) was found to be the only independent predictor for disease-free survival (RR: 2.0471; 95% CI: 1.0799-3.8806; P=0.0289) (Table 5.4).

As indicated in the Kaplan-Meier analysis, the HCC patients in subgroup A were shown to have a significantly shorter disease-free survival when compared with the others in either subgroups B or C (P=0.0370) (Figure 5-3).

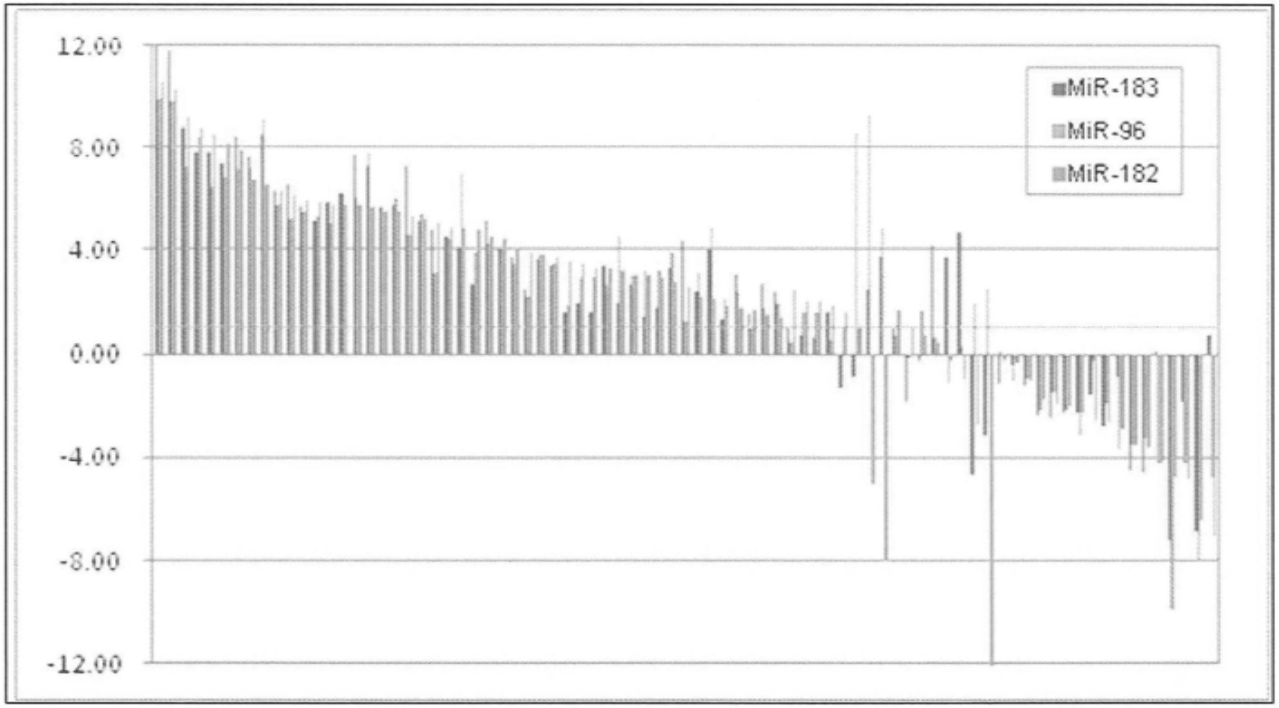

Figure 5-1 Expressions of miR-183, -96 and -182 in a cohort of 87 HCC tumors.

Expressions of miR-183, -96 and -182 in primary HCCs compared with their corresponding nontumorous livers (TN). A total of 59.3% (48 of 81) HCC cases demonstrated concordantly ≥2-fold over-expressions of the three miRNAs compared to their paired non-malignant counterparts (*dotted lines*).

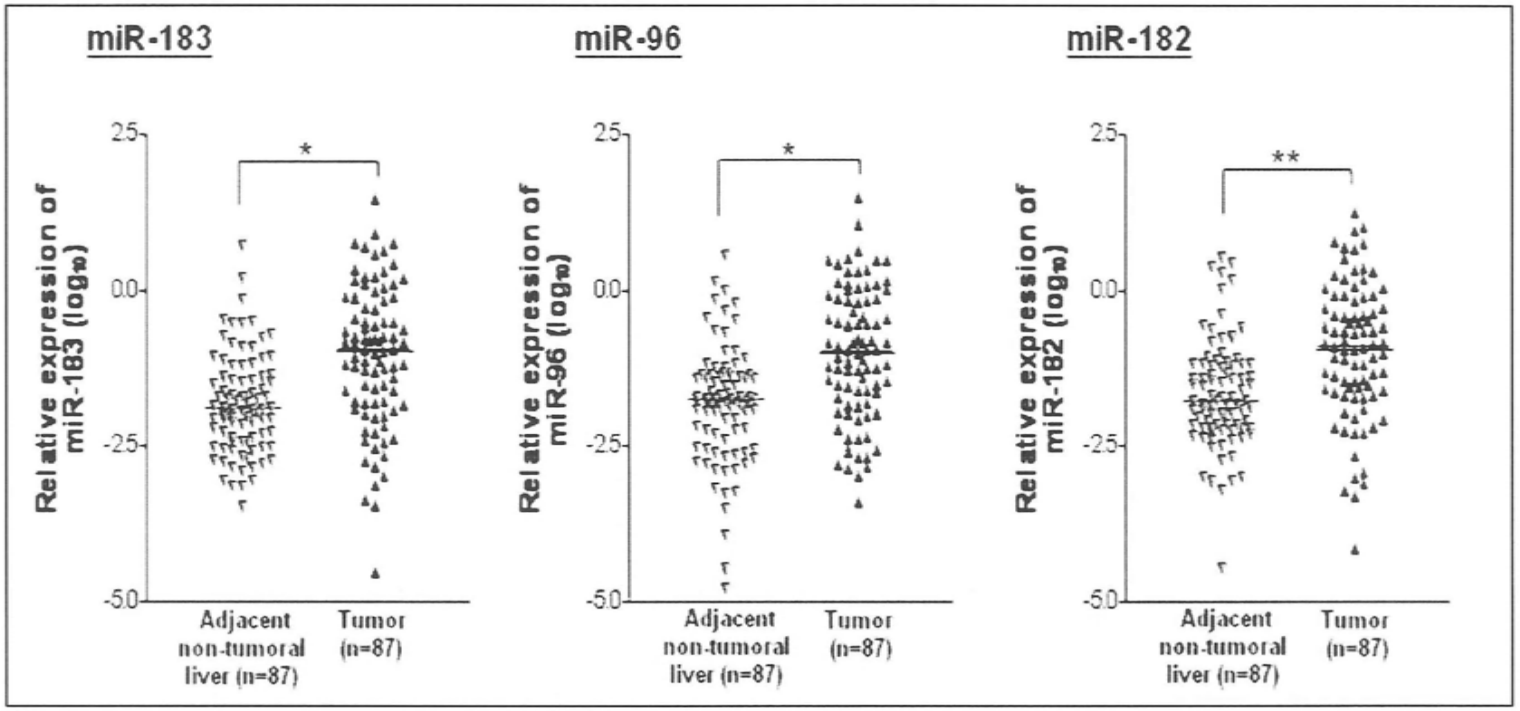

Figure 5-2 Expressions of miR-183, -96 and -182 in HCC tumors compared with their adjacent nontumoral livers.
Expressions of miR-183, -96 and -182 were significantly higher in HCC tumors as compared with adjacent non-malignant counterpart (*P<0.05; **P<0.01).

Table 5.1 Clinicopathologic correlations of miR-183, -96 and -182 expressions in HCC tumors

	MiR-183/96/182 Expression	P-*value*
Gender		0.362
Male	25.20 (7.490 – 160.7)	
Female	10.37 (0.5550 - 144.5)	
Age		0.994
≤40	17.68 (3.715 - 697.0)	
>40	25.20 (5.750 – 151.5)	
HBsAg		0.194
Present	22.64 (4.890 – 138.1)	
Absent	34.61 (15.93 – 1010)	
Cirrhosis		0.620
Present	28.11 (6.355 – 138.1)	
Absent	18.43 (2.300 – 206.6)	
Histology Grade		0.010**
Well to moderately differentiated	20.50 (3.715 – 130.3)	
Poorly differentiated	199.8 (92.61 – 703.1)	
Stage		0.153
Early (Stage I & II)	20.50 (3.715 – 145.5)	
Advanced (Stage III)	49.00 (16.41 – 385.8)	
No. of lesions		0.826
Multiple	31.55 (7.235 – 165.3)	
Solitary	21.66 (4.415 – 160.7)	
Macrovascular Invasion		0.214
Present	45.41 (23.30 – 385.8)	
Absent	20.83 (4.890 – 145.5)	
Microvascular Invasion		0.021*
Present	49.00 (24.98 – 620.7)	
Absent	20.50 (2.800 – 122.9)	

*$P<0.05$; miR-183/96/182 value expressed as Median (25%-75% percentiles)

Table 5.2 Distribution of patient characteristics by survival status

Variable	Alive (n=34)	%	Death (n=47)	%	*P*-value
MiR-183/96/182					0.0461
Subgroup A	9	27.3	24	72.7	
Subgroup B & C	25	52.1	23	47.9	
Mean age, y ± SD	55.6 ± 11.2		57.0 ± 12.2		0.6065
Gender					0.1151
Male	27	38.0	44	62.0	
Female	7	70.0	3	30.0	
HBsAg					0.8423
Positive	31	43.1	41	56.9	
Negative	3	33.3	6	66.7	
Cirrhosis					0.3282
Present	21	37.5	35	62.5	
Absent	13	52.0	12	48.0	
Histology grading					0.2501
Well differentiated	7	63.6	4	36.4	
Moderately differentiated	25	39.7	38	60.3	
Poorly differentiated	2	28.6	5	71.4	
AJCC staging					0.0089
I	28	54.9	23	45.1	
II	3	20.0	12	80.0	
III	3	20.0	12	80.0	
Tumoral lesions					0.0101
Multiple	4	17.4	19	82.6	
Solitary	30	51.7	28	48.3	
Macrovascular invasion					0.1609
Present	1	12.5	7	87.5	
Absent	33	45.2	40	54.8	
Microvascular invasion					0.1051
Present	3	20.0	12	80.0	
Absent	31	47.0	35	53.0	

Table 5.3 Univariate cox regression analysis of potential poor prognostic factors for HCC patients

	Disease-free survival	
Variable	**RR (95% CI)**	***P*-value**
MiR-183/96/182 expression		
Subgroup A	1.8255 (1.0303-3.2342)	0.0402
Subgroup B&C	1.0000	
Age, y	1.0186 (0.9916-1.0463)	0.1813
Gender		
Male	1.0000	
Female	0.3954 (0.1232-1.2692)	0.1208
HBsAg		
Positive	1.0000	
Negative	1.5991 (0.6785-3.7687)	0.2857
Cirrhosis		
Present	1.0000	
Absent	0.7375 (0.3826-1.4215)	0.3655
Histology grading		
Well differentiated	0.6152 (0.2202-1.7184)	0.3564
Moderately differentiated	1.0000	
Poorly differentiated	1.4843 (0.5848-3.7675)	0.4083
AJCC staging		
I	1.0000	
II	3.0001 (1.4762-6.0969)	0.0025
III	2.8452 (1.4073-5.7523)	0.0038
Tumoral lesions		
Multiple	2.9843 (1.6502-5.3970)	0.0003
Solitary	1.0000	
Macrovascular invasion		
Present	2.3726 (1.0569-5.3259)	0.0372
Absent	1.0000	
Microvascular invasion		
Present	2.8299 (1.4474-5.5330)	0.0025
Absent	1.0000	

Table 5.4 Multivariate cox regression analysis of potential poor prognostic factors for HCC patients

Variable	Disease-free survival	
	RR (95% CI)	*P*-value
MiR-183/96/182 expression		
Subgroup A	2.0471 (1.0799-3.8806)	0.0289
Subgroup B&C	1.0000	
Age, y	1.0218 (0.9921-1.0523)	0.1539
Gender		
Male	1.0000	
Female	0.6349 (0.1877-2.1477)	0.4673
AJCC staging		
I	1.0000	
II	1.7829 (0.5166-6.1536)	0.3627
III	0.8222 (0.2215-3.0523)	0.7710
Tumoral lesions		
Multiple	2.2323 (0.8754-5.6929)	0.0944
Solitary	1.0000	
Macrovascular invasion		
Present	3.1553 (0.6256-15.9141)	0.1661
Absent	1.0000	
Microvascular invasion		
Present	1.1089 (0.3548-3.4654)	0.8596
Absent	1.0000	

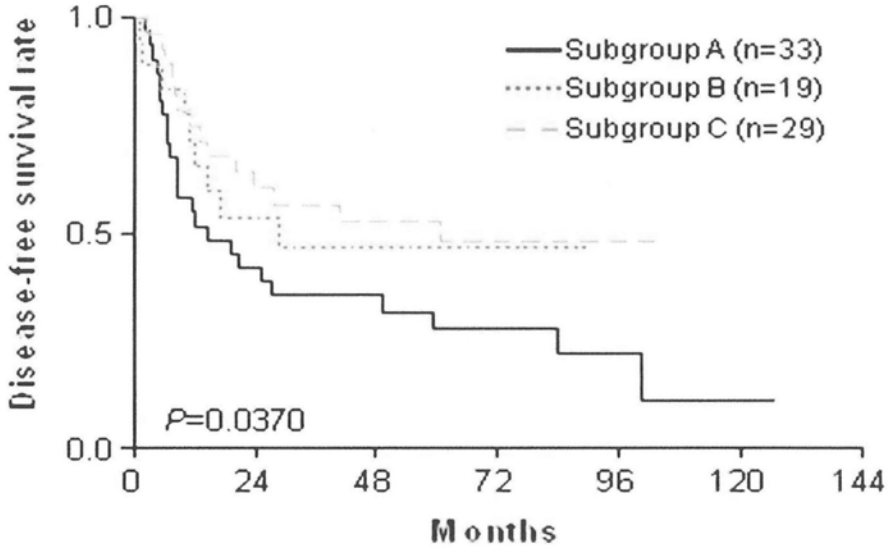

Figure 5-3 Concomitant up-regulations of miR-183, -96 and -182 in HCC were associated with poorer prognosis.

The disease-free survival rate in patients with concordantly high expression of miR-183, -96 and -182 (subgroup A; *solid line*) was significantly lower than those in either subgroups B or C (*dotted and dashed lines* respectively) (P=0.0370).

5.2.2 Expressions of miR-183, -96 and -182 in HCC cells

qRT-PCR analyses were performed on a panel of 20 HCC cell lines, of which 18 (90%) showed concordant up-regulations of miR-183, -96 and -182 from 7- to 300-fold as compared to a reference pool of 3 normal livers ($P<0.05$; Figure 5-4). This suggested the potential use of cell line models in the study on the role(s) of miR-183, -96 and -182 in HCC tumorigenesis.

5.2.3 MiR-183/96/182 knockdown subdued HCC cell invasiveness

Two invasive HCC cells (Hep3B and HKCI-1) showing up-regulation of miR-183, -96 and -182 by at least 70- to 300-fold respectively were selected. The knockdown efficiency of ~70% was suggested for miR-183, -96 and -182 from quantitative RT-PCR analyses. Knockdown of individual miR-183, -96 and -182 by antisense oligos in Hep3B and HKCI-1 cells did not suggest an apparent effect on cell viability (Figure 5-5). However, the knockdown experiment demonstrated retarded cell motile and invasive properties in both cell lines ($P<0.01$; Figure 5-6 & -7).

Combined knockdown of miR-183, -96 and -182 in Hep3B and HKCI-1 also revealed reduced cell motility and invasiveness ($P<0.01$; Figure 5-6 & -7), but the magnitude of retardation on the cell invasiveness was similar to individual miRNA suppression.

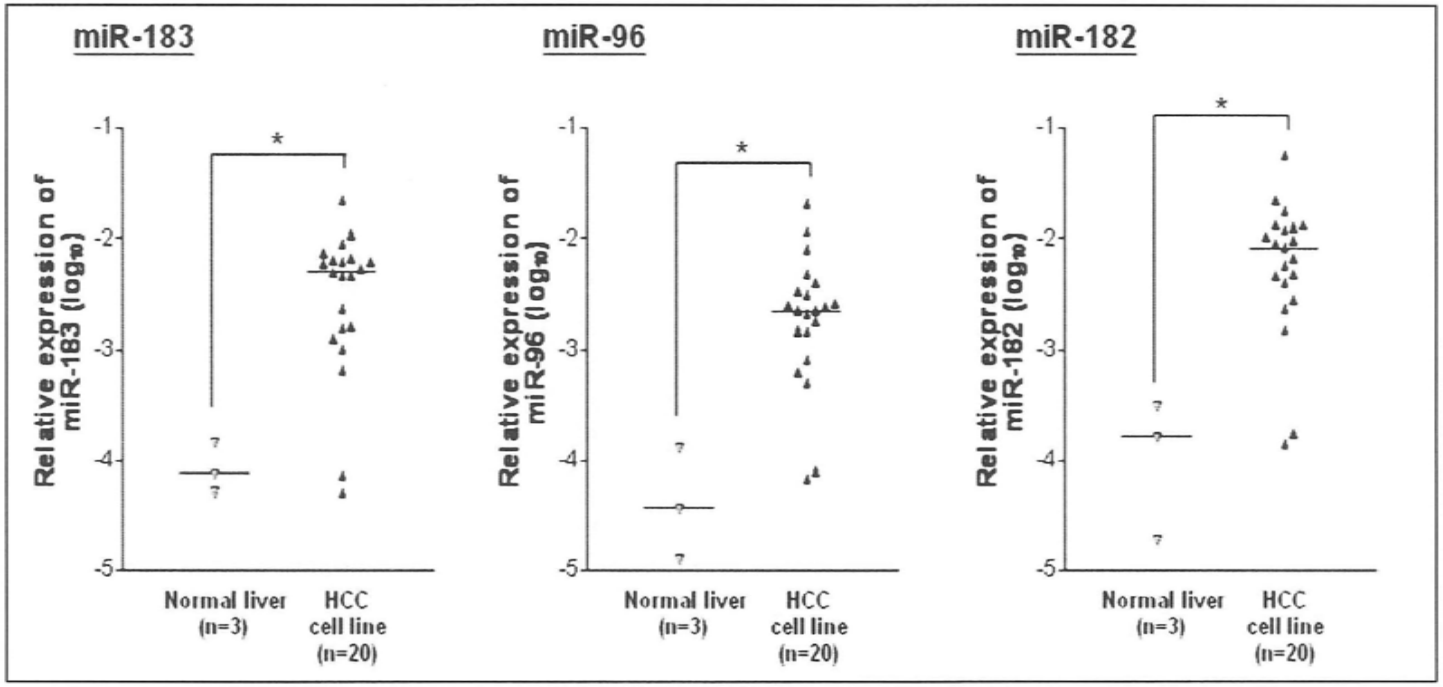

Figure 5-4 Expressions of miR-183, -96 and -182 in HCC cell lines.

qRT-PCR analysis was performed on 20 HCC cell lines and 3 normal liver samples. A significant up-regulation of miR-183, -96 and -182 was suggested in HCC cells as compared to normal liver (*P<0.05).

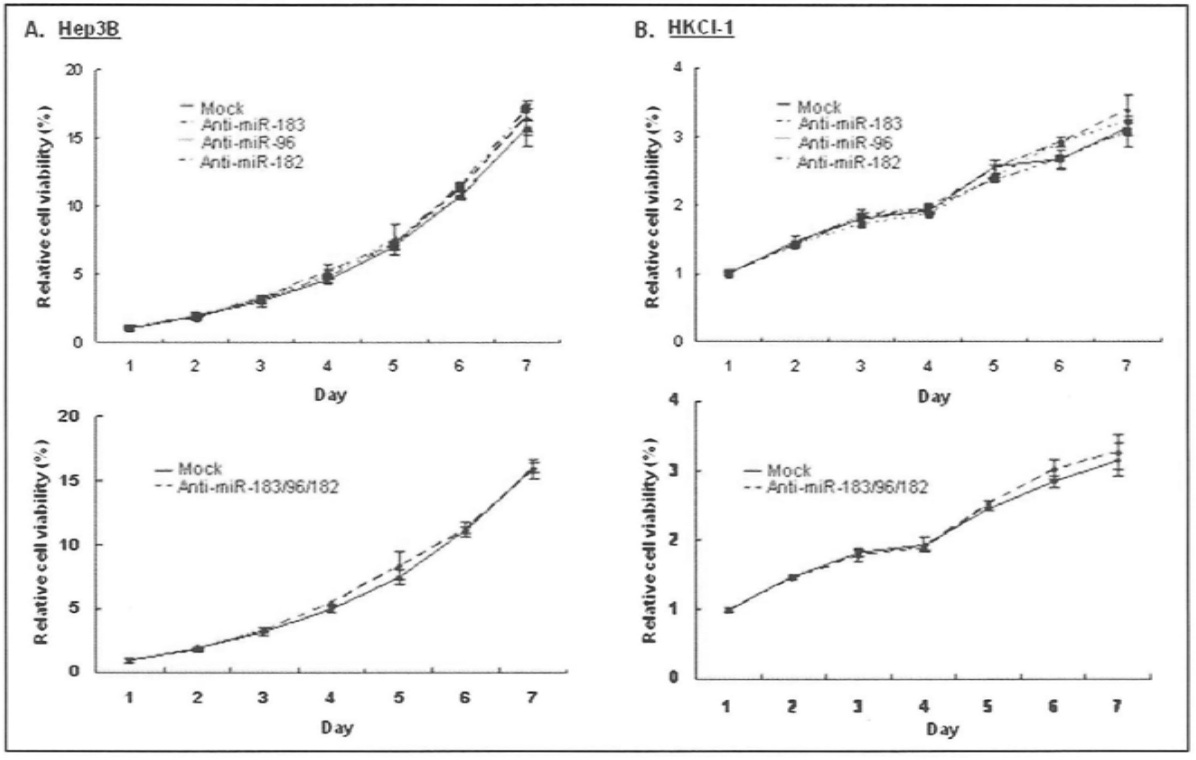

Figure 5-5 Effects of miR-183, -96 and -182 knockdown on HCC cell viability.

Suppression of miR-183, -96 and -182 showed no effect on cell viability of Hep3B and HKCI-1 cells.

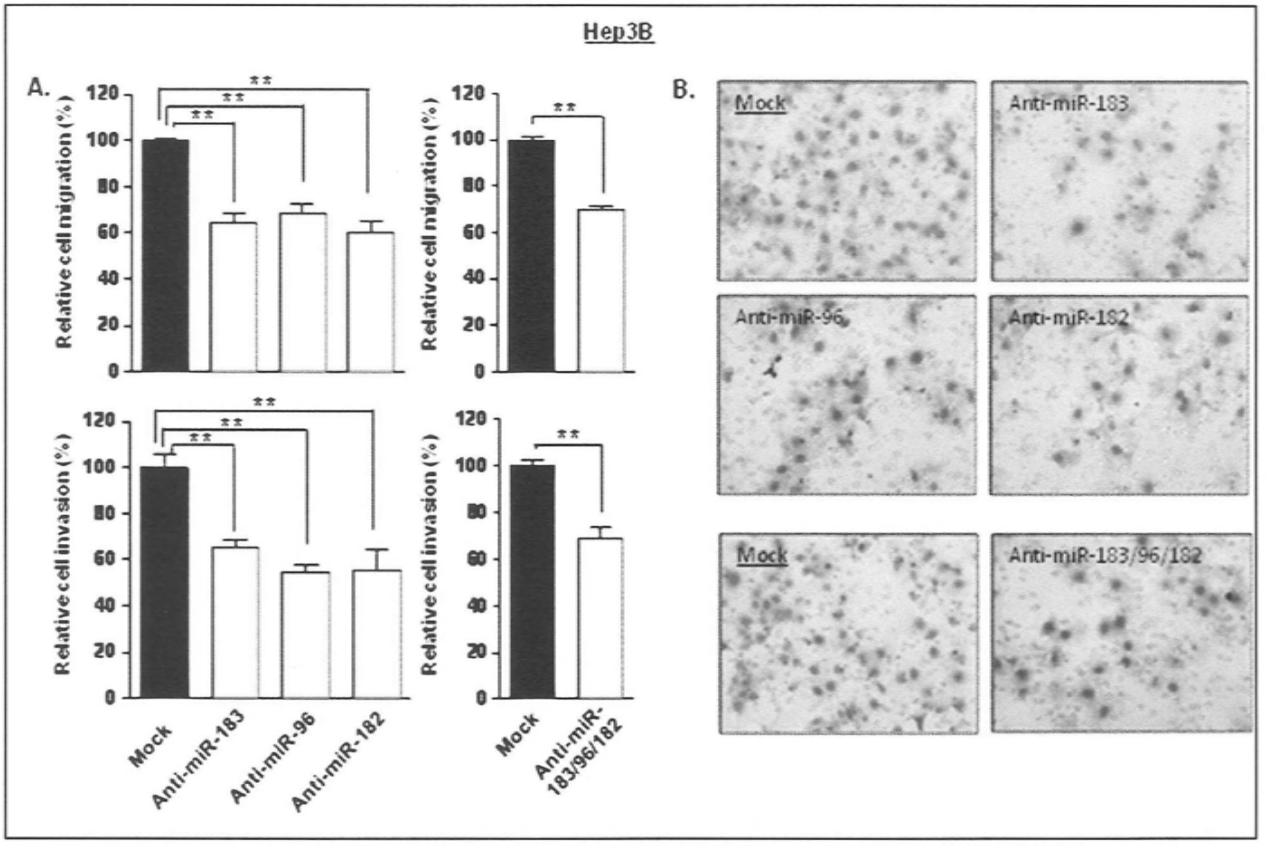

Figure 5-6 Knockdown of miR-183, -96 and -182 abrogated cell motility and invasiveness of Hep3B.

Suppression of miR-183, -96 and -182 expressions significantly retarded cell migratory and invasive properties of Hep3B cells (**P<0.01).

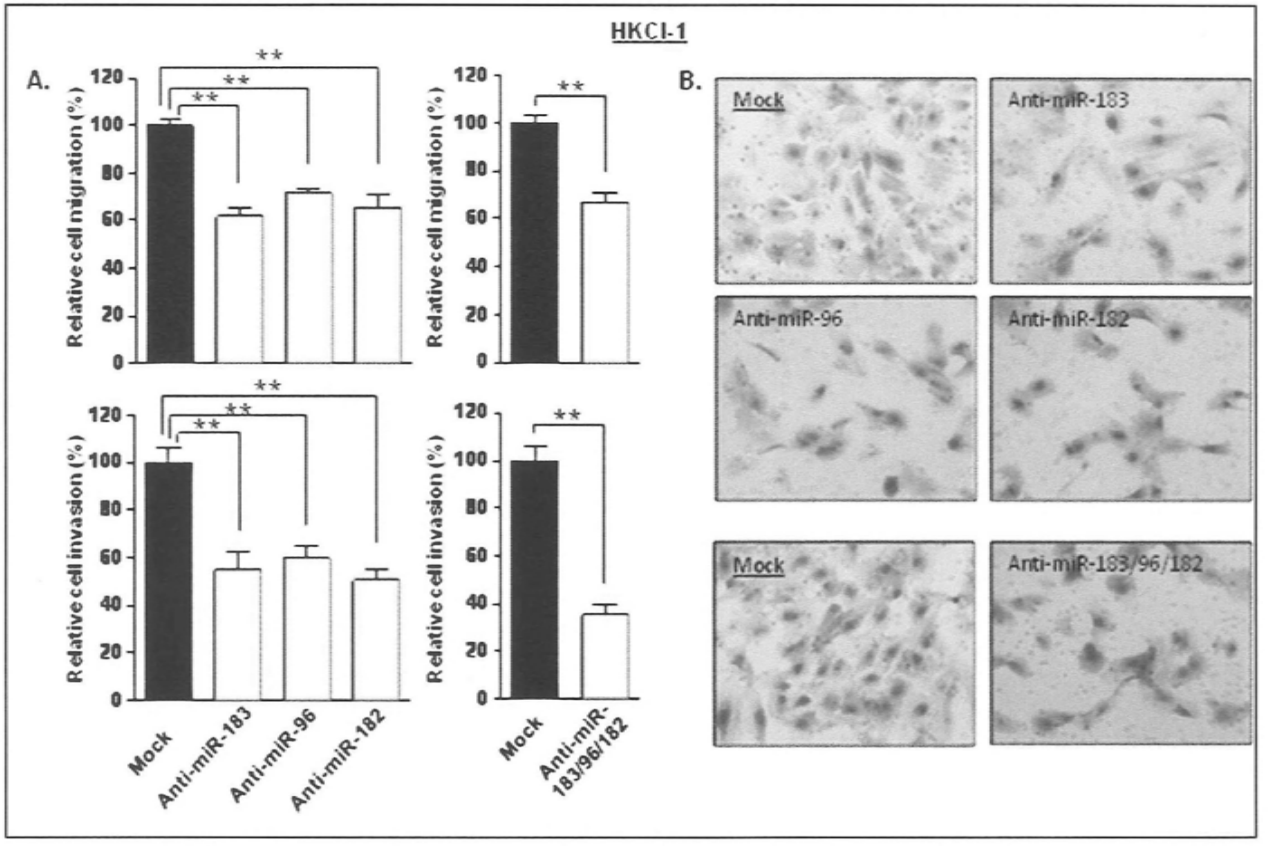

Figure 5-7 Knockdown of miR-183, -96 and -182 suppressed cell motility and invasiveness of HKCI-1.

Abrogation of miR-183, -96 and -182 expressions significantly circumvented cell migratory and invasive phenotypes in HKCI-1 cells (**P<0.01).

5.2.4 MiR-183/96/182 potentially targeted FOXO1

Since the functional effect of the combined knockdown showed similar extent to that of individual knockdown, it was postulated that convergent pathways were targeted by these three miRNAs. Given that FOXO1 was a well recognized tumor suppressor gene and reported to be the only target concordantly regulated by miR-183, -96 and -182 in various cancers, except HCC (Guttilla and White, 2009; Myatt *et al.,* 2010; Stittrich *et al.,* 2010), we next examined if FOXO1 was a convergent target of miR-183, -96 and -182. In silico analysis (TargetScan 5.1; http://www.targetscan.org) on the FOXO1 3'UTR showed putative target seed sequences of miR-183, -96 and -182 (Figure 5-8B). To verify this interaction between miR-183/96/182 and FOXO1 in HCC, Western blot analysis suggested that knockdown of miR-183, -96 and -182 concomitantly enhanced FOXO1 protein expression (Figure 5-8A). Subsequent luciferase reporter assay indicated knockdown of miR-183/96/182 in HKCI-1 cell significantly augmented the signal from the wild-type (WT) construct of FOXO1 3'UTR by ~80% ($P<0.01$) (Figure 5-8C), whereas the increase in luciferase signal was not suggested with mutant construct (MUT).

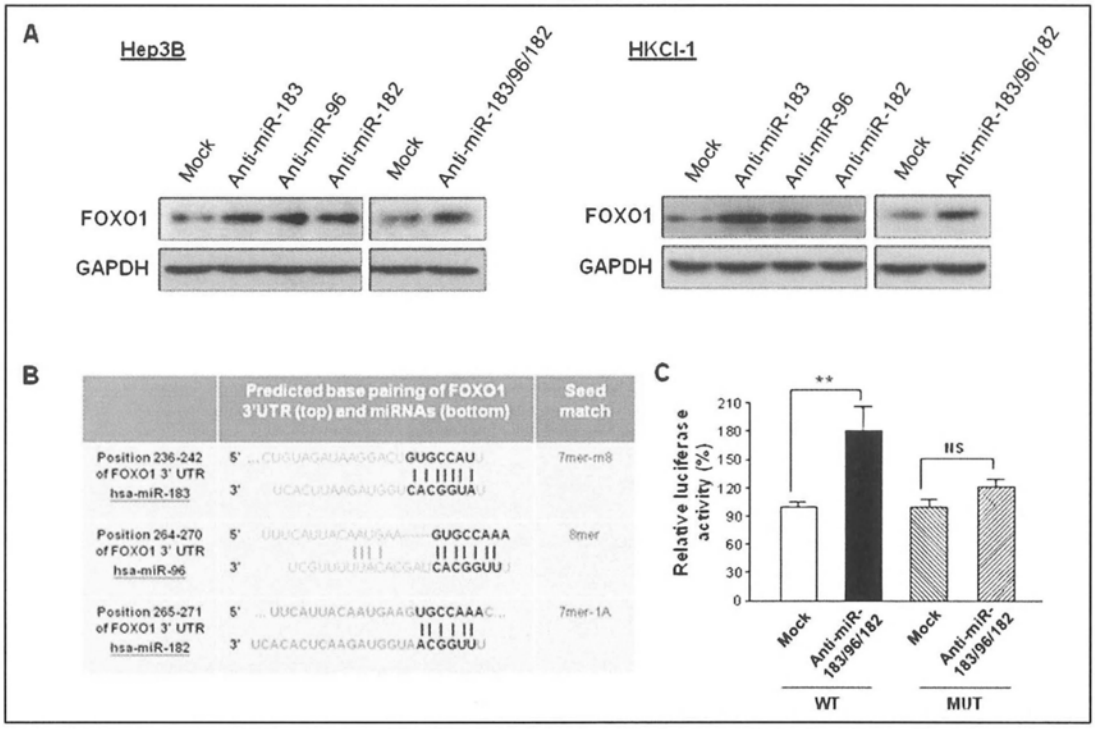

Figure 5-8 FOXO1 is a potential target of miR-183/96/182.

(A) Suppression of miR-183, -96 and -182 in Hep3B and HKCI-1 cells increased the protein expression of FOXO1.

(B) Insilico prediction indicated the putative miR-183, -96 and -182 target sequences on FOXO1 3'UTR.

(C) A significant increase in luciferase activity was detected in HKCI-1 cell transfected with anti-miR-183/96/182 compared with mock experiment (**P<0.01), whereas no significant difference was suggested in cells transfected with mutant construct (MUT) as compared with wild-type (WT) construct.

5.2.5 CTNNB1 regulated the expressions of miR-183/96/182.

Recent data from our laboratory using ChIP (Chromatin Immunoprecipitation)-chip assay found that the promoter region of miR-183/96/182 transcription start was significantly bound by CTNNB1 in Hep3B cell (data not shown). Searching from computational algorithm (Transcription Element Search System) on the specific promoter binding region, further led to the identification of a putative consensus binding sequence of transcription factor (TCF)-3 at ~700bp from the transcription start of miR-183/96/182. Since activation of CTNNB1 signaling is commonly observed in many types of cancers, especially in liver carcinoma (El-Serag and Rudolph, 2007), I further determined if CTNNB1 activation could regulate miR-183/96/182 expression. In Hep3B and HKCI-1, knockdown of CTNNB1 was ensured by Western blot (Figure 5-9B). RNA interference targeting *CTNNB1* revealed significant reduction in activated and total CTNNB1. As activated CTNNB1 will bind TCF family factors and subsequently control target gene expression, the reduced active CTNNB1 could result in targeting gene/miRNA repression. In the two HCC cell lines studied, a concordant down-regulation of miR-183, -96 and -182 in si*CTNNB1* experiment by ~40% was detected ($P<0.01$; Figure 5-9A). On the other hand, FOXO1, a proposed target of miR-183/96/182, was shown to be up-regulated in *CTNNB1*-suppressed cells (Figure 5-9B). These results proposed a potential activation mechanism of FOXO1 elicited by *CTNNB1* down-regulation intermediately through miR-183/96/182.

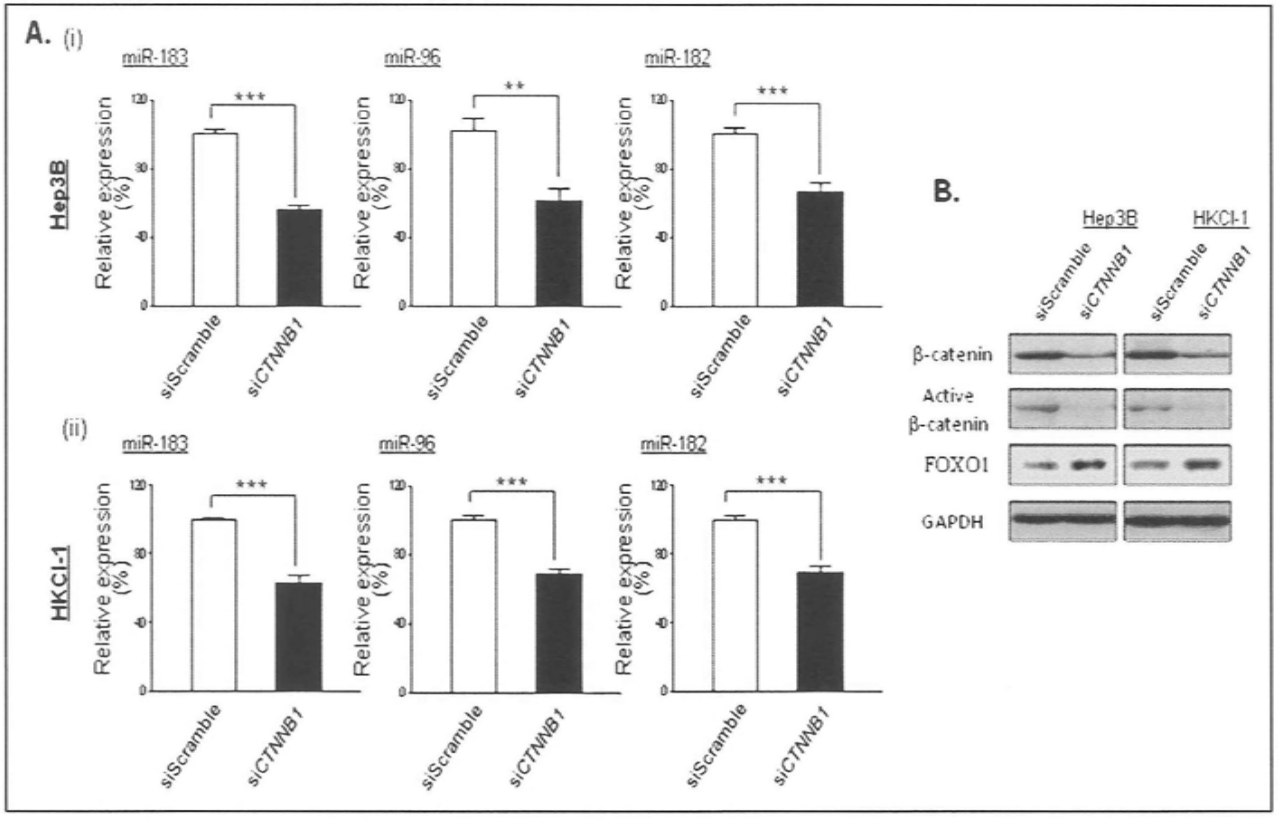

Figure 5-9 CTNNB1 modulated FOXO1 expression via miR-183/96/182 regulation.

(A) *CTNNB1* suppression indicated reduction of miR-183, -96 and -182 expressions in Hep3B and HKCI-1 cells (***P*<0.01; ****P*<0.001).

(B) Knockdown of CTNNB1 was confirmed by Western blot analysis. Meanwhile, FOXO1 was suggested to up-regulate in *CTNNB1*-suppressed HCC cells.

5.3 Discussion

Since the initial discovery on the functional roles of let-7 miRNA by targeting RAS 3'UTR (Johnson *et al.,* 2005), significant effort has been devoted for curative therapies in cancers that utilize this pathway. As previous findings suggested common up-regulations of miR-183, -96 and -182 in various types of cancers (Bandrés *et al.,* 2006; Guttilla *et al.,* 2009; Lin *et al.,* 2010; Myatt *et al.,* 2010; Schaefer *et al.,* 2010; Segura *et al.,* 2009), in this chapter the clinico-pathologic significance of these three miRNAs in a cohort of primary HCC cases was investigated. Correlative analysis suggested increased miR-183/96/182 expression was significantly associated with cases in the histologic presence of microvascular invasion. Since the presence of venous invasion has been widely ascribed as a prognostic indicator for aggressive behavior (Vauthey *et al.,* 2002), this finding may have biological implication for miR-183/96/182 in association with metastatic potentials of HCC. In support of this interpretation, functional investigations shown here indicated individual miR-183, -96 and -182 play an oncogenic role in directly regulating liver cancer cell motility and invasiveness. In addition, Kaplan-Meier analysis affirmed the prognostic value of miR-183/96/182 that increased miR-183/96/182 expression in HCC patients correlated with a shorter post-operative survival. These findings further illustrate the importance of miR-183/96/182 as a predictive prognostic biomarker for HCC patients.

Although functionally individual miR-183, -96 and -182 promoted HCC cell motility, no additive or synergistic effect of combined miR-183/96/182 knockdown could be observed. This observation might be suggestive of convergent pathways targeted by these three miRNAs. Bioinformatic algorithm (TargetScan) showed the seed sequences among these three miRNAs are closely conserved given they varied in

one to two nucleotides (seed regions: CACGGUA (miR-183); CACGGUU (miR-96); _ACGGUU (miR-182)), indicating their potential competitiveness for the same target pairing. It is found in this work miR-183, -96 and -182 converge in targeting *FOXO1* at the 3'UTR. In addition, the database also predicted miR-96 and miR-182 to compete for the same target site on *FOXO1* 3'UTR (Figure 5-8A).

FOXO1 belongs to the FOXO (*F*orkhead b*OX*-containing protein, *O* sub-family) family of transcription factors that have been implicated in a variety of processes including cellular differentiation, cell death, protection from oxidative stress and tumor suppression (Arden, 2007). Recent studies have suggested the inhibitory effect of human epidermal growth factor receptor 2 (HER2) on FOXO1 expression in breast cancer cells (Wu *et al.,* 2010), where increased HER2 level in breast cancer closely represents the aggressive malignant behaviors of tumors (Pellikainen *et al.,* 2004; Pugliese *et al.,* 2010). In addition, FOXO1 was demonstrated to inhibit prostate cancer cell migration in a Runx2-dependent manner (Zhang *et al.,* 2011), further supporting FOXO1 as a critical suppressor in the process of advanced tumor progression. In line with these studies, the data from this thesis suggested miR-183/96/182 as a regulatory repressor of FOXO1 expression, which in turn might promote cell migratory properties of HCC cells.

More intriguingly, it was highlighted miR-183/96/182 cluster is a potential downstream effector of Wnt signaling pathway, where activation is commonly associated with the development of HCC and other human cancers (Moon *et al.,* 2004). CTNNB1 plays a key role in this signaling pathway, and its activation commonly occurs in mouse and human HCC involving somatic mutations (de La Coste *et al.,* 1998). CTNNB1 was also reported as a nuclear regulator of Wnt-dependent gene expression through its interacting with TCF family members

(Städeli *et al.,* 2006). In this study, it was found that *CTNNB1* knockdown concomitantly suppressed miR-183, -96 and -182 expressions. Based on the preliminary findings from ChIP-chip assay and bioinformatic searching of the miR-183/96/182 promoter region, several consensus TCF-binding sites were found. These observations postulated that binding of CTNNB1 to these TCF-binding regions potentially allows a direct influence on miR-183/96/182 trasnscription. This is also in line with previous report suggesting that miR-183/96/182 cluster is over-expressed in the Wnt signaling activated medulloblastomas (Gokhale *et al.,* 2010). Given that CTNNB1 is an important player in the process of HCC metastasis (Lai *et al.,* 2011), this study showed much importance for miR-183/96/182 in HCC cell dissemination, and highlighted metastatic link between CTNNB1 activation on miR-183/96/182 expression. While FOXO1 was suggested to be concomitantly down-regulated by miR-183/96/182, it was also demonstrated that knockdown of *CTNNB1* could re-express FOXO1, possibly through down-regulation of miR-183/96/182.

In summary, the work carried out in this chapter outlined the prognostic value of miR-183/96/182, where their up-regulation correlated significantly with features of metastatic potentials, including presence of venous invasion and advanced tumor differentiation. The data also showed a metastatic regulatory basis of miR-183/96/182 targeting on FOXO1 expression. In investigating the upstream control of miR-183/96/182 cluster expression, it was found CTNNB1 activation could induce up-regulation of all 3 miRNAs. Since hepatic metastases are the major causes of high morbidity and mortality of the patients with HCC, further investigations on miR-183/96/182 dysregulation may aid molecular underpinning of HCC metastasis, and may enhance the development of novel therapeutic regimens for individuals.

Chapter 6

Conclusion and proposed future studies

6. Conclusion and proposed future studies

Since the importance of 7q21-32 amplification has been widely ascribed in advanced stage HCC tumors (Poon *et al.,* 2006; Sy *et al.,* 2005), positional mapping analysis of this region is an important strategy in defining candidate genes. In this thesis, two proto-oncogenes *PFTK1* and miR-183/96/182 on 7q21-32 were highlighted. Up-regulations of *PFTK1* or miR-183/96/182 were shown to be more profound in primary HCC tumors with metastatic features, including advanced tumor grading and presence of microvascular invasion. Functional investigations also suggested both *PFTK1* and miR-183/96/182 played an important role in HCC cell migratory phenotypes.

Knockdown of *PFTK1* suppressed the migratory and invasive properties of HCC cells through TAGLN2-ACTB pathway; meanwhile, *PFTK1* suppression was also suggested to reduce expression of VIM, a well recognized cellular hallmark for mesenchymal feature in the process of EMT (Vincent-Salomon and Thiery, 2003). It is plausible that *PFTK1* not only phosphorylates TAGLN2 protein, but also elicits influence on EMT process in the control of HCC cell motility. Therefore, I propose to examine the effect of *PFTK1* on a panel of EMT cellular markers. Recent studies have demonstrated cancer cells can acquire stem-like characteristics following passage through the EMT process (Singh and Settleman, 2010). In the future lines of investigations, it will also be worth examining other biological functions of *PFTK1*, such as the EMT-induced stem-like features.

Based on in-house ChIP-chip assay, miR-183/96/182 expression was found to be regulated by CTNNB1. To affirm this finding, ChIP-PCR validation should be performed. Moreover, luciferase reporter assays with deletion mutants will also need

to be conducted to determine the effect of TCF binding region deletions on reporter gene activity.

In conclusion, this thesis sought to characterize the underlying molecular mechanism of chromosomal 7q21-32 over-representation in HCC. Within this region, corresponding up-regulations of *PFTK1* and miR-183/96/182 were identified as key contributors to liver cancer cell motility. Thus, elucidating causal genomic alterations for affected genes, such as 7q21-32, holds much importance in understanding the molecular basis of HCC development and progression.

References

References

Ahn JY, Jung EY, Kwun HJ, Lee CW, Sung YC, Jang KL. (2002). Dual effects of hepatitis B virus X protein on the regulation of cell-cycle control depending on the status of cellular p53. *J Gen Virol.* 83(Pt 11), 2765-72.

Altekruse SF, McGlynn KA, Reichman ME. (2009). Hepatocellular carcinoma incidence, mortality, and survival trends in the United States from 1975 to 2005. *J Clin Oncol.* 27(9), 1485-1491.

Ambros V. (2001). microRNAs: tiny regulators with great potential. *Cell.* 107(7), 823-6.

Arden KC. (2007). FoxOs in tumor suppression and stem cell maintenance. *Cell.* 128(2), 235-7.

Asangani IA, Rasheed SA, Nikolova DA, Leupold JH, Colburn NH, Post S, Allgayer H. (2008). MicroRNA-21 (miR-21) post-transcriptionally downregulates tumor suppressor Pdcd4 and stimulates invasion, intravasation and metastasis in colorectal cancer. *Oncogene.* 27(15), 2128-2136.

Assinder SJ, Stanton JA, Prasad PD. (2009). Transgelin: an actin-binding protein and tumour suppressor. *Int J Biochem Cell Biol.* 41, 482-486.

Baek K, Liu X, Ferron F, Shu S, Korn ED, Dominguez R. (2008). Modulation of actin structure and function by phosphorylation of Tyr-53 and profilin binding. *Proc Natl Acad Sci U S A.* 105, 11748-11753.

Bandrés E, Cubedo E, Agirre X, Malumbres R, Zárate R, Ramirez N, Abajo A, Navarro A, Moreno I, Monzó M, García-Foncillas J. (2006). Identification by Real-time PCR of 13 mature microRNAs differentially expressed in colorectal cancer and non-tumoral tissues. *Mol Cancer.* 19, 5-29.

Bedogni G, Miglioli L, Masutti F, Tiribelli C, Marchesini G, Bellentani S. (2005). Prevalence of and risk factors for nonalcoholic fatty liver disease: the Dionysos nutrition and liver study. *Hepatology.* 42(1), 44-52.

Besset V, Rhee K, Wolgemuth DJ. (1998). The identification and characterization of expression of Pftaire-1, a novel Cdk family member, suggest its function in the mouse testis and nervous system. *Mol Reprod Dev.* 50, 18-29.

Bogatcheva NV, Birukova A, Borbiev T, Kolosova I, Liu F, Garcia JG, Verin AD. (2006). Caldesmon is a cytoskeletal target for PKC in endothelium. *J Cell Biochem.* 99, 1593-1605.

Borbiev T, Verin AD, Birukova A, Liu F, Crow MT, Garcia JG. (2003). Role of CaM

kinase II and ERK activation in thrombin-induced endothelial cell barrier dysfunction. *Am J Physiol Lung Cell Mol Physiol.* 285, L43-54.

Bosch FX, Ribes J, Díaz M, Cléries R. (2004). Primary liver cancer: worldwide incidence and trends. *Gastroenterology.* 127(5 Suppl 1), S5-S16.

Bosetti C, Levi F, Boffetta P, Lucchini F, Negri E, La-Vecchia C. (2008). Trends in mortality from hepatocellular carcinoma in Europe, 1980-2004. *Hepatology.* 48(1), 137-145.

Bouchard MJ, Schneider RJ. (2004). The enigmatic X gene of hepatitis B virus. *J Virol.* 78(23), 12725-34.

Bressac B, Kew M, Wands J, Ozturk M. (1991). Selective G to T mutations of p53 gene in hepatocellular carcinoma from southern Africa. *Nature.* 350(6317), 429-31.

Budhu A, Jia HL, Forgues M, Liu CG, Goldstein D, Lam A, Zanetti KA, Ye QH, Qin LX, Croce CM, Tang ZY, Wang XW. (2008). Identification of metastasis-related microRNAs in hepatocellular carcinoma. *Hepatology.* 47(3), 897-907.

Bugianesi E, Leone N, Vanni E, Marchesini G, Brunello F, Carucci P, Musso A, De Paolis P, Capussotti L, Salizzoni M, Rizzetto M. (2002). Expanding the natural history of nonalcoholic steatohepatitis: from cryptogenic cirrhosis to hepatocellular carcinoma. *Gastroenterology.* 123(1), 134-40.

Caldwell SH, Crespo DM, Kang HS, Al-Osaimi AM. (2004). Obesity and hepatocellular carcinoma. *Gastroenterology.* 127(5 Suppl 1), S97-103.

Calle EE, Rodriguez C, Walker-Thurmond K, Thun MJ. (2003). Overweight, obesity, and mortality from cancer in a prospectively studied cohort of U.S. adults. *N Engl J Med.* 348(17), 1625-38.

Chayama K, Hayes CN. (2011). Hepatitis C virus: How genetic variability affects pathobiology of disease. *J Gastroenterol Hepatol.* 26(Suppl 1), 83-95.

Chen CL, Yang HI, Yang WS, Liu CJ, Chen PJ, You SL, Wang LY, Sun CA, Lu SN, Chen DS, Chen CJ. (2008). Metabolic factors and risk of hepatocellular carcinoma by chronic hepatitis B/C infection: a follow-up study in Taiwan. *Gastroenterology.* 135(1), 111-21.

Chigrinova E, Mian M, Shen Y, Greiner TC, Chan WC, Vose JM, Inghirami G, Chiappella A, Baldini L, Ponzoni M, Ferreri AJ, Franceschetti S, Gaidano G, Tucci A, Facchetti F, Lazure T, Lambotte O, Montes-Moreno S, Piris MA, Zucca E, Kwee I, Bertoni F. (2011). Integrated profiling of diffuse large B-cell

lymphoma with 7q gain. *Br J Haematol.* 153(4), 499-503.

Chiu CM, Yeh SH, Chen PJ, Kuo TJ, Chang CJ, Chen PJ, Yang WJ, Chen DS. (2007). Hepatitis B virus X protein enhances androgen receptor-responsive gene expression depending on androgen level. *Proc Natl Acad Sci U S A.* 104(8), 2571-8.

Chung KY, Cheng IK, Ching AK, Chu JH, Lai PB, Wong N. (2011). Block of Proliferation 1 (BOP1) plays an oncogenic role in hepatocellular carcinoma by promoting epithelial-to-mesenchymal transition. *Hepatology.* (in press).

Collonge-Rame MA, Bresson-Hadni S, Koch S, Carbillet JP, Blagosklonova O, Mantion G, Miguet JP, Heyd B, Bresson JL. (2001). Pattern of chromosomal imbalances in non-B virus related hepatocellular carcinoma detected by comparative genomic hybridization. *Cancer Genet Cytogenet.* 127(1), 49-52.

Craig JR. (1997). Cirrhosis, hepatocellular carcinoma, and survival. *Hepatology.* 26(3), 798-9.

Cross JC, Wen P, Rutter WJ. (1993). Transactivation by hepatitis B virus X protein is promiscuous and dependent on mitogen-activated cellular serine/threonine kinases. *Proc Natl Acad Sci U S A.* 90(17), 8078-82.

de La Coste A, Romagnolo B, Billuart P, Renard CA, Buendia MA, Soubrane O, Fabre M, Chelly J, Beldjord C, Kahn A, Perret C. (1997). Somatic mutations of the beta-catenin gene are frequent in mouse and human hepatocellular carcinomas. *Proc Natl Acad Sci U S A.* 95(15), 8847-51.

Deng M, Mohanan S, Polyak E, Chacko S. (2007). Caldesmon is necessary for maintaining the actin and intermediate filaments in cultured bladder smooth muscle cells. *Cell Motil Cytoskeleton.* 64, 951-965.

Di Bisceglie AM. (1997). Hepatitis C and hepatocellular carcinoma. *Hepatology.* 26(3 Suppl 1), 34S-38S.

El-Serag HB, Mason AC. (1999). Rising incidence of hepatocellular carcinoma in the United States. *N Engl J Med.* 340(10), 745-50.

El-Serag HB, Rudolph KL. (2007). Hepatocellular carcinoma: epidemiology and molecular carcinogenesis. *Gastroenterology.* 132(7), 2557-76.

Fabbri M, Garzon R, Cimmino A, Liu Z, Zanesi N, Callegari E, Liu S, Alder H, Costinean S, Fernandez-Cymering C, Volinia S, Guler G, Morrison CD, Chan KK, Marcucci G, Calin GA, Huebner K, Croce CM. (2007). MicroRNA-29 family reverts aberrant methylation in lung cancer by targeting DNA

methyltransferases 3A and 3B. *Proc Natl Acad Sci U S A.* 104(40), 15805-15810.

Ferber MJ, Montoya DP, Yu C, Aderca I, McGee A, Thorland EC, Nagorney DM, Gostout BS, Burgart LJ, Boix L, Bruix J, McMahon BJ, Cheung TH, Chung TK, Wong YF, Smith DI, Roberts LR. (2003). Integrations of the hepatitis B virus (HBV) and human papillomavirus (HPV) into the human telomerase reverse transcriptase (hTERT) gene in liver and cervical cancers. *Oncogene.* 22(24), 3813-20.

Ferlay J, Shin HR, Bray F, Forman D, Mathers C and Parkin DM. (2010). GLOBOCAN 2008, Cancer Incidence and Mortality Worldwide: IARC CancerBase No. 10 [Internet].

Fornari F, Gramantieri L, Giovannini C, Veronese A, Ferracin M, Sabbioni S, Calin GA, Grazi GL, Croce CM, Tavolari S, Chieco P, Negrini M, Bolondi L. (2009). MiR-122/cyclin G1 interaction modulates p53 activity and affects doxorubicin sensitivity of human hepatocarcinoma cells. *Cancer Res.* 69(14), 5761-7.

Frezza M, di Padova C, Pozzato G, Terpin M, Baraona E, Lieber CS. (1990). High blood alcohol levels in women. The role of decreased gastric alcohol dehydrogenase activity and first-pass metabolism. *N Engl J Med.* 322(2), 95-9.

Fu Y, Liu HW, Forsythe SM, Kogut P, McConville JF, Halayko AJ, Camoretti-Mercado B, Solway J. (2000). Mutagenesis analysis of human SM22: characterization of actin binding. *J Appl Physiol.* 89, 1985-1990.

García JL, Hernandez JM, Gutiérrez NC, Flores T, González D, Calasanz MJ, Martínez-Climent JA, Piris MA, Lopéz-Capitán C, González MB, Odero MD, San Miguel JF. (2003). Abnormalities on 1q and 7q are associated with poor outcome in sporadic Burkitt's lymphoma. A cytogenetic and comparative genomic hybridization study. *Leukemia.* 17, 2016-2024.

Garner RC, Miller EC, Miller JA. (1972). Liver microsomal metabolism of aflatoxin B 1 to a reactive derivative toxic to Salmonella typhimurium TA 1530. *Cancer Res.* 32(10), 2058-66.

Ghosh AK, Majumder M, Steele R, Meyer K, Ray R, Ray RB. (2000). Hepatitis C virus NS5A protein protects against TNF-alpha mediated apoptotic cell death. *Virus Res.* 67(2), 173-8.

Ghosh AK, Steele R, Meyer K, Ray R, Ray RB. (1999). Hepatitis C virus NS5A protein modulates cell cycle regulatory genes and promotes cell growth. *J Gen Virol.* 80 (Pt 5), 1179-83.

Girard M, Jacquemin E, Munnich A, Lyonnet S, Henrion-Caude A. (2008). miR-122, a paradigm for the role of microRNAs in the liver. *J Hepatol.* 48(4), 648-56.

Gokhale A, Kunder R, Goel A, Sarin R, Moiyadi A, Shenoy A, Mamidipally C, Noronha S, Kannan S, Shirsat NV. (2010). Distinctive microRNA signature of medulloblastomas associated with the WNT signaling pathway. *J Cancer Res Ther.* 6(4), 521-9.

Goncharova EA, Vorotnikov AV, Gracheva EO, Wang CL, Panettieri RA Jr, Stepanova VV, Tkachuk VA. (2002). Activation of p38 MAP-kinase and caldesmon phosphorylation are essential for urokinase-induced human smooth muscle cell migration. *Biol Chem.* 383, 115-126.

Ground KE. (1982). Liver pathology in aircrew. *Aviat Space Environ Med.* 53(1), 14-8.

Guttilla IK, White BA. (2009). Coordinate regulation of FOXO1 by miR-27a, miR-96, and miR-182 in breast cancer cells. *J Biol Chem.* 284(35), 23204-16.

[1] Han HK, Han CY, Cheon EP, Lee J, Kang KW. (2007). Role of hypoxia-inducible factor-alpha in hepatitis-B-virus X protein-mediated MDR1 activation. *Biochem Biophys Res Commun.* 357(2), 567-73.

[2] Han IS, Seo TB, Kim KH, Yoon JH, Yoon SJ, Namgung U. (2007). Cdc2-mediated Schwann cell migration during peripheral nerve regeneration. *J Cell Sci.* 120, 246-255.

Haxhinasto KB, Kamath AM, Blackwell K, Zabner J, Lin J, Moy AB. (2002). The effects of caldesmon on fibroblast cell adhesion and motility. *Mol Biol Cell.* 13, 314a.

Herath NI, Leggett BA, MacDonald GA. (2006). Review of genetic and epigenetic alterations in hepatocarcinogenesis. *J Gastroenterol Hepatol.* 21: 15-21.

Hilden M, Christoffersen P, Juhl E, Dalgaard JB. (1977). Liver histology in a 'normal' population--examinations of 503 consecutive fatal traffic casualties. *Scand J Gastroenterol.* 12(5), 593-7.

Hoek JB, Pastorino JG. (2002). Ethanol, oxidative stress, and cytokine-induced liver cell injury. *Alcohol.* 27(1), 63-8.

Horikawa I, Barrett JC. (2001). cis-Activation of the human telomerase gene (hTERT) by the hepatitis B virus genome. *J Natl Cancer Inst.* 93(15), 1171-3.

Hu N, Wang C, Ng D, Clifford R, Yang HH, Tang ZZ, Wang QH, Han XY, Giffen C, Goldstein AM, Taylor PR, Lee MP. (2009). Genomic characterization of

esophageal squamous cell carcinoma from a high-risk population in China. *Cancer Res.* 69(14), 5908-17.

Hu Z, Zhang Z, Kim JW, Huang Y, Liang TJ. (2006). Altered proteolysis and global gene expression in hepatitis B virus X transgenic mouse liver. *J Virol.* 80(3), 1405-13.

Hsu IC, Metcalf RA, Sun T, Welsh JA, Wang NJ, Harris CC. (1991). Mutational hotspot in the p53 gene in human hepatocellular carcinomas. *Nature.* 350(6317), 427-8.

Jiang J, Gusev Y, Aderca I, Mettler TA, Nagorney DM, Brackett DJ, Roberts LR, Schmittgen TD. (2008). Association of MicroRNA expression in hepatocellular carcinomas with hepatitis infection, cirrhosis, and patient survival. *Clin Cancer Res.* 14(2), 419-27.

Jiang M, Gao Y, Yang T, Zhu X, Chen J. (2009). Cyclin Y, a novel membrane-associated cyclin, interacts with PFTK1. *FEBS letters.* 583, 2171-2178.

Johnson SM, Grosshans H, Shingara J, Byrom M, Jarvis R, Cheng A, Labourier E, Reinert KL, Brown D, Slack FJ. (2005). *RAS* is regulated by the *let-7* microRNA family. *Cell.* 120(5), 635-647.

Jopling CL, Yi M, Lancaster AM, Lemon SM, Sarnow P. (2005). Modulation of hepatitis C virus RNA abundance by a liver-specific MicroRNA. *Science.* 309(5740), 1577-81.

Juliano R. (2003). Movin' on through with Cdc2. *Nat Cell Biol.* 5(7), 589-90.

Katoh H, Ojima H, Kokubu A, Saito S, Kondo T, Kosuge T, Hosoda F, Imoto I, Inazawa J, Hirohashi S, Shibata T. (2007). Genetically distinct and clinically relevant classification of hepatocellular carcinoma: putative therapeutic targets. *Gastroenterology.* 133(5), 1475-86.

Kirschner M. (1992). The cell cycle then and now. *Trends Biochem Sci.* 17, 281-285.

Knuutila S, Björkqvist AM, Autio K, Tarkkanen M, Wolf M, Monni O, Szymanska J, Larramendy ML, Tapper J, Pere H, El-Rifai W, Hemmer S, Wasenius VM, Vidgren V, Zhu Y. (1998). DNA copy number amplifications in human neoplasms: review of comparative genomic hybridization studies. *Am J Pathol.* 152, 1107-1123.

Kota J, Chivukula RR, O'Donnell KA, Wentzel EA, Montgomery CL, Hwang HW, Chang TC, Vivekanandan P, Torbenson M, Clark KR, Mendell JR, Mendell JT.

(2009). Therapeutic microRNA delivery suppresses tumorigenesis in a murine liver cancer model. *Cell.* 137(6), 1005-17.

Krek A, Grün D, Poy MN, Wolf R, Rosenberg L, Epstein EJ, MacMenamin P, da Piedade I, Gunsalus KC, Stoffel M, Rajewsky N. (2005). Combinatorial microRNA target predictions. *Nat Genet.* 37(5), 495-500.

Kubota H, Mikhailenko SV, Okabe H, Taguchi H, Ishiwata S. (2009). D-loop of actin differently regulates the motor function of myosins II and V. *J Biol Chem.* 284, 35251-35258.

Kwun HJ, Jung EY, Ahn JY, Lee MN, Jang KL. (2001). p53-dependent transcriptional repression of p21(waf1) by hepatitis C virus NS3. *J Gen Virol.* 82(Pt 9), 2235-41.

Lai SW, Tan CK, Ng KC. (2002). Epidemiology of fatty liver in a hospital-based study in Taiwan. *South Med J.* 95(11), 1288-92.

Lai TY, Su CC, Kuo WW, Yeh YL, Kuo WH, Tsai FJ, Tsai CH, Weng YJ, Huang CY, Chen LM. (2011). β-catenin plays a key role in metastasis of human hepatocellular carcinoma. *Oncol Rep.* 26(2), 415-22.

Lamba JK, Chen X, Lan LB, Kim JW, Wei Wang X, Relling MV, Kazuto Y, Watkins PB, Strom S, Sun D, Schuetz JD, Schuetz EG. (2006). Increased CYP3A4 copy number in TONG/HCC cells but not in DNA from other humans. *Pharmacogenet Genomics.* 16(6), 415-27.

Lavanchy D. (2005). Worldwide epidemiology of HBV infection, disease burden, and vaccine prevention. *J Clin Virol.* 34 (Suppl 1), S1-3.

Lavanchy D. (2011). Evolving epidemiology of hepatitis C virus. *Clin Microbiol Infect.* 17(2), 107-15.

Lazzaro MA, Julien JP. (1997). Chromosomal mapping of the PFTAIRE gene, *Pftk1*, a Cdc-related kinase expressed predominantly in the mouse nervous system. *Genomics* 42, 536-537.

Lee AT, Ren J, Wong ET, Ban KH, Lee LA, Lee CG. (2005). The hepatitis B virus X protein sensitizes HepG2 cells to UV light-induced DNA damage. *J Biol Chem.* 280(39), 33525-35.

Lee MN, Jung EY, Kwun HJ, Jun HK, Yu DY, Choi YH, Jang KL. (2002). Hepatitis C virus core protein represses the p21 promoter through inhibition of a TGF-beta pathway. *J Gen Virol.* 83(Pt 9), 2145-51.

Leung WK, Wong N. (2011). Liang Q (ed). *Molecular Aspects of Hepatocellular*

carcinoma: MicroRNA in Human Hepatocellular Carcinoma (Chapter 6). Betham Science Publisher: Australia pp 56-66.

Lew EA, Garfinkel L. (1979). Variations in mortality by weight among 750,000 men and women. *J Chronic Dis.* 32(8), 563-76.

Lewis BP, Burge CB, Bartel DP. (2005). Conserved seed pairing, often flanked by adenosines, indicates that thousands of human genes are microRNA targets. *Cell.* 120(1), 15-20.

Lin H, Dai T, Xiong H, Zhao X, Chen X, Yu C, Li J, Wang X, Song L. (2010). Unregulated miR-96 induces cell proliferation in human breast cancer by downregulating transcriptional factor FOXO3a. *PLoS One.* 5(12), e15797.

Lin JJ, Li Y, Eppinga RD, Wang Q, Jin JP. (2009). Chapter 1: roles of caldesmon in cell motility and actin cytoskeleton remodeling. *Int Rev Cell Mol Biol.* 274, 1-68.

Liu WH, Yeh SH, Lu CC, Yu SL, Chen HY, Lin CY, Chen DS, Chen PJ. (2009). MicroRNA-18a prevents estrogen receptor-alpha expression, promoting proliferation of hepatocellular carcinoma cells. *Gastroenterology.* 136(2), 683-93.

Longerich T, Mueller MM, Breuhahn K, Schirmacher P, Benner A, Heiss C. (2011). Oncogenetic tree modeling of human hepatocarcinogenesis. *Int J Cancer.* doi, 10.1002/ijc.26063.

Ma L, Teruya-Feldstein J, Weinberg RA. (2007). Tumour invasion and metastasis initiated by microRNA-10b in breast cancer. *Nature*. 449(7163), 682-688.

Ma WL, Hsu CL, Wu MH, Wu CT, Wu CC, Lai JJ, Jou YS, Chen CW, Yeh S, Chang C. (2008). Androgen receptor is a new potential therapeutic target for the treatment of hepatocellular carcinoma. *Gastroenterology.* 135(3), 947-55.

Maeda S, Kamata H, Luo JL, Leffert H, Karin M. (2005). IKKbeta couples hepatocyte death to cytokine-driven compensatory proliferation that promotes chemical hepatocarcinogenesis. *Cell.* 121(7), 977-90.

Manes T, Zheng DQ, Tognin S, Woodard AS, Marchisio PC, Languino LR. (2003). Alpha(v)beta3 integrin expression up-regulates cdc2, which modulates cell migration. *J Cell Biol.* 161(4), 817-26.

Martínez-López N, Varela-Rey M, Fernández-Ramos D, Woodhoo A, Vázquez-Chantada M, Embade N, Espinosa-Hevia L, Bustamante FJ, Parada LA, Rodriguez MS, Lu SC, Mato JM, Martínez-Chantar ML. (2010). Activation of LKB1-Akt pathway independent of phosphoinositide 3-kinase plays a critical role

in the proliferation of hepatocellular carcinoma from nonalcoholic steatohepatitis. *Hepatology.* 52(5), 1621-31.

Mathonnet G, Lachance S, Alaoui-Jamali M, Drobetsky EA. (2004). Expression of hepatitis B virus X oncoprotein inhibits transcription-coupled nucleotide excision repair in human cells. *Mutat Res.* 554(1-2), 305-18.

McGlynn KA, London WT. (2005). Epidemiology and natural history of hepatocellular carcinoma. *Best Pract Res Clin Gastroenterol.* 19(1), 3-23.

Méndez-Sánchez N, Villa AR, Vázquez-Elizondo G, Ponciano-Rodríguez G, Uribe M. (2008). Mortality trends for liver cancer in Mexico from 2000 to 2006. *Ann Hepatol.* 7(3), 226-229.

Midorikawa Y, Yamamoto S, Ishikawa S, Kamimura N, Igarashi H, Sugimura H, Makuuchi M, Aburatani H. (2006). Molecular karyotyping of human hepatocellular carcinoma using single-nucleotide polymorphism arrays. *Oncogene.* 25(40), 5581-90.

Moon RT, Kohn AD, De Ferrari GV, Kaykas A. (2004). WNT and beta-catenin signalling: diseases and therapies. *Nat Rev Genet.* 5(9), 691-701.

Morgan TR, Mandayam S, Jamal MM. (2004). Alcohol and hepatocellular carcinoma. *Gastroenterology.* 127(5 Suppl 1), S87-96.

Murakami Y, Saigo K, Takashima H, Minami M, Okanoue T, Bréchot C, Paterlini-Bréchot P. (2005). Large scaled analysis of hepatitis B virus (HBV) DNA integration in HBV related hepatocellular carcinomas. *Gut.* 54(8), 1162-8.

Myatt SS, Wang J, Monteiro LJ, Christian M, Ho KK, Fusi L, Dina RE, Brosens JJ, Ghaem-Maghami S, Lam EW. (2010). Definition of microRNAs that repress expression of the tumor suppressor gene FOXO1 in endometrial cancer. *Cancer Res.* 70(1), 367-77.

Nair RR, Solway J, Boyd DD. (2006). Expression cloning identifies transgelin (SM22) as a novel repressor of 92-kDa type IV collagenase (MMP-9) expression. *J Biol Chem.* 281, 26424-26436.

Nakao K, Shibusawa M, Ishihara A, Yoshizawa H, Tsunoda A, Kusano M, Kurose A, Makita T, Sasaki K. (2001). Genetic changes in colorectal carcinoma tumors with liver metastases analyzed by comparative genomic hybridization and DNA ploidy. *Cancer.* 91, 721-726.

Naugler WE, Sakurai T, Kim S, Maeda S, Kim K, Elsharkawy AM, Karin M. (2007). Gender disparity in liver cancer due to sex differences in MyD88-dependent IL-6

production. *Science.* 317(5834), 121-4.

Neumeister P, Pixley FJ, Xiong Y, Xie H, Wu K, Ashton A, Cammer M, Chan A, Symons M, Stanley ER, Pestell RG. (2003). Cyclin D1 Governs Adhesion and Motility of Macrophages. *Mol Biol Cell.* 14, 2005-2015.

Nomura H, Kashiwagi S, Hayashi J, Kajiyama W, Tani S, Goto M. (1988). Prevalence of fatty liver in a general population of Okinawa, Japan. *Jpn J Med.* 27(2), 142-9.

Nonomura A, Mizukami Y, Unoura M, Kobayashi K, Takeda Y, Takeda R. (1992). Clinicopathologic study of alcohol-like liver disease in non-alcoholics; non-alcoholic steatohepatitis and fibrosis. *Gastroenterol Jpn.* 27(4), 521-8.

Norder H, Couroucé AM, Coursaget P, Echevarria JM, Lee SD, Mushahwar IK, Robertson BH, Locarnini S, Magnius LO. (2004). Genetic diversity of hepatitis B virus strains derived worldwide: genotypes, subgenotypes, and HBsAg subtypes. *Intervirology.* 47(6), 289-309.

Numaguchi Y, Huang S, Polte TR, Eichler GS, Wang N, Ingber DE. (2003). Caldesmon-dependent switching between capillary endothelial cell growth and apoptosis through modulation of cell shape and contractility. *Angiogenesis* 6, 55-64.

Omagari K, Kadokawa Y, Masuda J, Egawa I, Sawa T, Hazama H, Ohba K, Isomoto H, Mizuta Y, Hayashida K, Murase K, Kadota T, Murata I, Kohno S. (2002). Fatty liver in non-alcoholic non-overweight Japanese adults: incidence and clinical characteristics. *J Gastroenterol Hepatol.* 17(10), 1098-105.

Pang E, Wong N, Lai PB, To KF, Lau JW, Johnson PJ. (2000). A comprehensive karyotypic analysis on a newly developed hepatocellular carcinoma cell line, HKCI-1, by spectral karyotyping and comparative genomic hybridization. *Cancer Genet Cytogenet.* 121(1), 9-16.

Pang EY, Bai AH, To KF, Sy SM, Wong NL, Lai PB, Squire JA, Wong N. (2007). Identification of PFTAIRE protein kinase 1, a novel cell division cycle-2 related gene, in the motile phenotype of hepatocellular carcinoma cells. *Hepatology.* 46(2), 436-45.

Paterlini-Bréchot P, Saigo K, Murakami Y, Chami M, Gozuacik D, Mugnier C, Lagorce D, Bréchot C. (2003). Hepatitis B virus-related insertional mutagenesis occurs frequently in human liver cancers and recurrently targets human telomerase gene. *Oncogene.* 22(25), 3911-6.

Pellikainen JM, Ropponen KM, Kataja V.V, Kellokoski JK, Eskelinen MJ, Kosma VM. (2004). Expression of matrix metalloproteinase (MMP)-2 and MMP-9 in breast cancer with a special reference to activator protein-2, HER2, and prognosis. *Clin Cancer Res.* 10(22), 7621-8.

Peters L, Meister G. (2007). Argonaute proteins: mediators of RNA silencing. *Mol Cell.* 26(5), 611-23.

Pines J. (1992). Cell proliferation and control. *Curr Opin Cell Biol.* 4, 144-148.

Pinto AE, Roque L, Rodrigues R, André S, Soares J. (2006). Frequent 7q gains in flow cytometric multiploid/hypertetraploid breast carcinomas: a study of chromosome imbalances by comparative genomic hybridisation. *J Clin Pathol.* 59(4), 367-72.

Polesel J, Zucchetto A, Montella M, Dal Maso L, Crispo A, La Vecchia C, Serraino D, Franceschi S, Talamini R. (2009). The impact of obesity and diabetes mellitus on the risk of hepatocellular carcinoma. *Ann Oncol.* 20(2), 353-7.

Ponchel F, Puisieux A, Tabone E, Michot JP, Fröschl G, Morel AP, Frébourg T, Fontanière B, Oberhammer F, Ozturk M. (1994). Hepatocarcinoma-specific mutant p53-249ser induces mitotic activity but has no effect on transforming times. *Cancer Res.* 54(8), 2064-8.

Poon RT, Fan ST, Lo CM, Liu CL, Wong J. (1999). Intrahepatic recurrence after curative resection of hepatocellular carcinoma: long-term results of treatment and prognostic factors. *Ann Surg.* 229(2), 216-22.

Poon TC, Wong N, Lai PB, Rattray M, Johnson PJ, Sung JJ. (2006). A tumor progression model for hepatocellular carcinoma: bioinformatic analysis of genomic data. *Gastroenterology.* 131(4), 1262-70.

Pugliese M, Stempel M, Patil S, Hsu M, Ho A, Traina T, Morrow M, Cody H 3rd, Gemignani ML. (2010). The clinical impact and outcomes of immunohistochemistry-only metastasis in breast cancer. *Am J Surg.* 200(3), 368-73.

Qian GS, Ross RK, Yu MC, Yuan JM, Gao YT, Henderson BE, Wogan GN, Groopman JD. (1994). A follow-up study of urinary markers of aflatoxin exposure and liver cancer risk in Shanghai, People's Republic of China. *Cancer Epidemiol Biomarkers Prev.* 3(1), 3-10.

Ray RB, Lagging LM, Meyer K, Ray R. (1996). Hepatitis C virus core protein cooperates with ras and transforms primary rat embryo fibroblasts to

tumorigenic phenotype. *J Virol.* 70(7), 4438-43.

Ray RB, Lagging LM, Meyer K, Steele R, Ray R. (1995). Transcriptional regulation of cellular and viral promoters by the hepatitis C virus core protein. *Virus Res.* 37(3), 209-20.

Rush J, Moritz A, Lee KA, Guo A, Goss VL, Spek EJ, Zhang H, Zha XM, Polakiewicz RD, Comb MJ. (2005). Immunoaffinity profiling of tyrosine phosphorylation in cancer cells. *Nat Biotechnol.* 23, 94-101.

Schaefer A, Jung M, Mollenkopf HJ, Wagner I, Stephan C, Jentzmik F, Miller K, Lein M, Kristiansen G, Jung K. (2010). Diagnostic and prognostic implications of microRNA profiling in prostate carcinoma. *Int J Cancer.* 126(5), 1166-76.

Segura MF, Hanniford D, Menendez S, Reavie L, Zou X, Alvarez-Diaz S, Zakrzewski J, Blochin E, Rose A, Bogunovic D, Polsky D, Wei J, Lee P, Belitskaya-Levy I, Bhardwaj N, Osman I, Hernando E. (2009). Aberrant miR-182 expression promotes melanoma metastasis by repressing FOXO3 and microphthalmia-associated transcription factor. *Proc Natl Acad Sci U S A.* 106(6), 1814-9.

Shen L, Fan JG, Shao Y, Zeng MD, Wang JR, Luo GH, Li JQ, Chen SY. (2003). Prevalence of nonalcoholic fatty liver among administrative officers in Shanghai: an epidemiological survey. *World J Gastroenterol.* 9(5), 1106-10.

Shields JM, Rogers-Graham K, Der CJ. (2002). Loss of transgelin in breast and colon tumors and in RIE-1 cells by Ras deregulation of gene expression through Raf-independent pathways. *J Biol Chem.* 277, 9790-9799.

Shiratori Y, Shiina S, Imamura M, Kato N, Kanai F, Okudaira T, Teratani T, Tohgo G, Toda N, Ohashi M, et al. (1995). Characteristic difference of hepatocellular carcinoma between hepatitis B and C- viral infection in Japan. *Hepatology.* 22(4 Pt 1), 1027-1033.

Singh A, Settleman J. (2010). EMT, cancer stem cells and drug resistance: an emerging axis of evil in the war on cancer. *Oncogene.* 29(34), 4741-51.

Sobue K, Muramoto Y, Fujita M, Kakiuchi S. (1981). Purification of a calmodulin-binding protein from chicken gizzard that interacts with F-actin. *Proc Natl Acad Sci U S A.* 78, 5652-5655.

Solomon MJ. (1993). Activation of the various cyclin/cdc2 protein kinases. *Curr Opin Cell Biol.* 5, 180-186.

Spizzo R, Nicoloso MS, Croce CM, Calin GA. (2009). SnapShot: MicroRNAs in

Cancer. *Cell.* 137(3), 586-586.e1.

Städeli R, Hoffmans R, Basler K. (2006). Transcription under the control of nuclear Arm/beta-catenin. *Curr Biol.* 16(10), R378-85.

Stittrich AB, Haftmann C, Sgouroudis E, Kühl AA, Hegazy AN, Panse I, Riedel R, Flossdorf M, Dong J, Fuhrmann F, Heinz GA, Fang Z, Li N, Bissels U, Hatam F, Jahn A, Hammoud B, Matz M, Schulze FM, Baumgrass R, Bosio A, Mollenkopf HJ, Grün J, Thiel A, Chen W, Höfer T, Loddenkemper C, Löhning M, Chang HD, Rajewsky N, Radbruch A, Mashreghi MF. (2010). The microRNA miR-182 is induced by IL-2 and promotes clonal expansion of activated helper T lymphocytes. *Nat Immunol.* 11(11), 1057-62.

Strohmeyer DM, Berger AP, Moore DH 2nd, Bartsch G, Klocker H, Carroll PR, Loening SA, Jensen RH. (2004). Genetic aberrations in prostate carcinoma detected by comparative genomic hybridization and microsatellite analysis: association with progression and angiogenesis. *Prostate.* 59, 43-58.

Sy SM, Wong N, Lai PB, To KF, Johnson PJ. (2005). Regional over-representations on chromosomes 1q, 3q and 7q in the progression of hepatitis B virus-related hepatocellular carcinoma. *Mod Pathol.* 18(5), 686-92.

Tamori A, Nishiguchi S, Kubo S, Koh N, Moriyama Y, Fujimoto S, Takeda T, Shiomi S, Hirohashi K, Kinoshita H, Otani S, Kuroki T. (1999). Possible contribution to hepatocarcinogenesis of X transcript of hepatitis B virus in Japanese patients with hepatitis C virus. *Hepatology.* 29(5), 1429-34.

Tsai WC, Hsu PW, Lai TC, Chau GY, Lin CW, Chen CM, Lin CD, Liao YL, Wang JL, Chau YP, Hsu MT, Hsiao M, Huang HD, Tsou AP. (2009). MicroRNA-122, a tumor suppressor microRNA that regulates intrahepatic metastasis of hepatocellular carcinoma. *Hepatology.* 49(5), 1571-82.

Turner PC, Sylla A, Diallo MS, Castegnaro JJ, Hall AJ, Wild CP. (2002). The role of aflatoxins and hepatitis viruses in the etiopathogenesis of hepatocellular carcinoma: A basis for primary prevention in Guinea-Conakry, West Africa. *J Gastroenterol Hepatol.* 17 (Suppl), S441-8.

Umemura T, Ichijo T, Yoshizawa K, Tanaka E, Kiyosawa K. (2009). Epidemiology of hepatocellular carcinoma in Japan. *J Gastroenterol. 44*(Suppl 19), 102-107.

Ura S, Honda M, Yamashita T, Ueda T, Takatori H, Nishino R, Sunakozaka H, Sakai Y, Horimoto K, Kaneko S. (2009). Differential microRNA expression between hepatitis B and hepatitis C leading disease progression to hepatocellular

carcinoma. Differential microRNA expression between hepatitis B and hepatitis C leading disease progression to hepatocellular carcinoma. *Hepatology.* 49(4), 1098-112.

Vauthey JN, Lauwers GY, Esnaola NF, Do KA, Belghiti J, Mirza N, Curley SA, Ellis LM, Regimbeau JM, Rashid A, Cleary KR, Nagorney DM. (2002). Simplified staging for hepatocellular carcinoma. *J Clin Oncol.* 20(6), 1527-36.

Vincent-Salomon A, Thiery JP. (2003). Host microenvironment in breast cancer development: epithelial-mesenchymal transition in breast cancer development. *Breast Cancer Res.* 5, 101–106.

Wang J, Zindy F, Chenivesse X, Lamas E, Henglein B, Bréchot C. (1992). Modification of cyclin A expression by hepatitis B virus DNA integration in a hepatocellular carcinoma. *Oncogene.* 7(8), 1653-6.

Wang XW, Gibson MK, Vermeulen W, Yeh H, Forrester K, Stürzbecher HW, Hoeijmakers JH, Harris CC. (1995). Abrogation of p53-induced apoptosis by the hepatitis B virus X gene. *Cancer Res.* 55(24), 6012-6.

Wang Y, Lau SH, Sham JS, Wu MC, Wang T, Guan XY. (2004). Characterization of HBV integrants in 14 hepatocellular carcinomas: association of truncated X gene and hepatocellular carcinogenesis. *Oncogene.* 23(1), 142-8.

Williams CD, Stengel J, Asike MI, Torres DM, Shaw J, Contreras M, Landt CL, Harrison SA. (2011). Prevalence of nonalcoholic fatty liver disease and nonalcoholic steatohepatitis among a largely middle-aged population utilizing ultrasound and liver biopsy: a prospective study. *Gastroenterology.* 140(1), 124-31.

Wolk A, Gridley G, Svensson M, Nyrén O, McLaughlin JK, Fraumeni JF, Adam HO. (2001). A prospective study of obesity and cancer risk (Sweden). *Cancer Causes Control.* 12(1), 13-21.

Wong N, Lai P, Lee SW, Fan S, Pang E, Liew CT, Sheng Z, Lau JW, Johnson PJ. (1999). Assessment of genetic changes in hepatocellular carcinoma by comparative genomic hybridization analysis: relationship to disease stage, tumor size, and cirrhosis. *Am J Pathol.* 154(1), 37-43.

Wong N, Yeo W, Wong WL, Wong NL, Chan KY, Mo FK, Koh J, Chan SL, Chan AT, Lai PB, Ching AK, Tong JH, Ng HK, Johnson PJ, To KF. (2009). TOP2A overexpression in hepatocellular carcinoma correlates with early age onset, shorter patients survival and chemoresistance. *Int J Cancer.* 124(3), 644-52.

Wong QW, Ching AK, Chan AW, Choy KW, To KF, Lai PB, Wong N. (2010). MiR-222 overexpression confers cell migratory advantages in hepatocellular carcinoma through enhancing AKT signaling. *Clin. Cancer Res.* 16(3), 867-875.

Wong QW, Lung RW, Law PT, Lai PB, Chan KY, To KF, Wong N. (2008). MicroRNA-223 is commonly repressed in hepatocellular carcinoma and potentiates expression of Stathmin1. *Gastroenterology.* 135(1), 257-69.

World Health Organization. *World Health Report*, Geneva, Switzerland 1996.

Wu Y, Shang X, Sarkissyan M, Slamon D, Vadgama JV. (2010). FOXO1A is a target for HER2-overexpressing breast tumors. *Cancer Res.* 70(13), 5475-85.

Wulfkuhle JD, Sgroi DC, Krutzsch H, McLean K, McGarvey K, Knowlton M, Chen S, Shu H, Sahin A, Kurek R, Wallwiener D, Merino MJ, Petricoin EF 3rd, Zhao Y, Steeg PS. (2002). Proteomics of human breast ductal carcinoma in situ. *Cancer Res.* 62, 6740-6749.

Xiong Y, Fang JH, Yun JP, Yang J, Zhang Y, Jia WH, Zhuang SM. (2010). Effects of microRNA-29 on apoptosis, tumorigenicity, and prognosis of hepatocellular carcinoma. *Hepatology.* 51(3), 836-45.

Xu SG, Yan PJ, Shao ZM. (2010). Differential proteomic analysis of a highly metastatic variant of human breast cancer cells using two-dimensional differential gel electrophoresis. *J Cancer Res Clin Oncol.* 136, 1545-1556.

Yamashiro S, Yamakita Y, Hosoya H, Matsumura F. (1991). Phosphorylation of non-muscle caldesmon by p34Cdc2 kinase during mitosis. *Nature.* 349, 169-172.

Yamashiro S, Chern H, Yamakita Y, Matsumura F. (2001). Mutant Caldesmon lacking Cdc2 phosphorylation sites delays M-phase entry and inhibits cytokinesis. *Mol Biol Cell.* 12, 239-250.

Yamboliev IA, Gerthoffer WT. (2001). Modulatory role of ERK MAPK-caldesmon pathway in PDGF-stimulated migration of cultured pulmonary artery SMCs. *Am J Physiol Cell Physiol.* 280, C1680-1688.

Yang J, Qin LX, Ye SL, Liu YK, Li Y, Gao DM, Chen J, Tang ZY. (2003). The abnormalities of chromosome 8 in two hepatocellular carcinoma cell clones with the same genetic background and different metastatic potential. *J Cancer Res Clin Oncol.* 129(5), 303-8.

Yang T, Chen JY. (2001). Identification and cellular localization of human PFTAIRE1. *Gene.* 267(2), 165-72.

Yang Z, Chang YJ, Miyamoto H, Ni J, Niu Y, Chen Z, Chen YL, Yao JL, di

Sant'Agnese PA, Chang C. (2007). Transgelin functions as a suppressor via inhibition of ARA54-enhanced androgen receptor transactivation and prostate cancer cell growth. *Mol Endocrinol.* 21, 343-358.

Yen CC, Liang SC, Jong YJ, Chen YJ, Lin CH, Chen YM, Wu YC, Su WC, Huang CY, Tseng SW, Whang-Peng J. (2007). Chromosomal aberrations of malignant pleural effusions of lung adenocarcinoma: different cytogenetic changes are correlated with genders and smoking habits. *Lung Cancer.* 57(3), 292-301.

Yoo YG, Na TY, Seo HW, Seong JK, Park CK, Shin YK, Lee MO. (2008). Hepatitis B virus X protein induces the expression of MTA1 and HDAC1, which enhances hypoxia signaling in hepatocellular carcinoma cells. *Oncogene.* 27(24), 3405-13.

Zeisberg M, Yang C, Martino M, Duncan MB, Rieder F, Tanjore H, Kalluri R. (2007). Fibroblasts derive from hepatocytes in liver fibrosis via epithelial to mesenchymal transition. *J Biol Chem.* 282(32), 23337-47.

Zhang H, Pan Y, Zheng L, Choe C, Lindgren B, Jensen ED, Westendorf JJ, Cheng L, Huang H. (2011). FOXO1 Inhibits Runx2 Transcriptional Activity and Prostate Cancer Cell Migration and Invasion. *Cancer Res.* 71(9), 3257-67.

Zhang Z, Torii N, Hu Z, Jacob J, Liang TJ. (2001). X-deficient woodchuck hepatitis virus mutants behave like attenuated viruses and induce protective immunity in vivo. *J Clin Invest.* 108(10), 1523-31.

Zhao L, Wang H, Deng YJ, Wang S, Liu C, Jin H, Ding YQ. (2009). Transgelin as a suppressor is associated with poor prognosis in colorectal carcinoma patients. *Mod Pathol.* 22, 786-796.

Ziemer M, Garcia P, Shaul Y, Rutter WJ. (1985). Sequence of hepatitis B virus DNA incorporated into the genome of a human hepatoma cell line. *J Virol.* 53(3), 885-92.